STATISTICAL DESCRIPTION OF PACK ICE IN THE BEAUFORT SEA, LANCASTER SOUND AND THE LABRADOR SEA

EE-62

STATISTICAL DESCRIPTION OF PACK ICE IN THE BEAUFORT SEA, LANCASTER SOUND AND THE LABRADOR SEA

by

D. Dickins
A. Dickinson
B. Humphrey
DF Dickins Associates Ltd.
Vancouver, B.C.

This report has not undergone detailed technical review by the Environmental Protection Service and the content does not necessarily reflect the views and policies of Environment Canada. Mention of trade names or commercial products does not constitute endorsement for use.

This unedited version is undergoing a limited distribution to transfer the information to people working in related studies. This distribution is not intended to signify publication and, if the report is referenced, the author should cite it as an unpublished report of the Branch indicated below.

Any comments concerning its content should be directed to:

Environmental Emergencies Technology Division
Technical Services Branch
Environmental Protection Programs Directorate
Environmental Protection Service
Environment Canada
Ottawa, Ontario
K1A 1C8

EE-62

May, 1985

CONTENTS

		Page
ABSTRACT		i
1.0 INTRODUCTION		1
2.0 METHODOLOGY		4
2.1	Literature Review	4
2.2	Geographic Subdivisions	5
2.3	Ice Statistics: Definitions and Sources	9
2.3.1	Median Ice Cover	11
2.3.2	Ice Velocities	11
2.4	Wind Statistics	17
2.4.1	Wind Speed Dependence on Cloud Cover	17
2.4.2	Offshore Wind Statistics	18
2.5	Refreezing of Pack Ice Leads	19
3.0 RESULTS AND DISCUSSION		26
3.1	Pack Ice Concentrations	26
3.2	Leads	32
3.2.1	Distribution of Data	32
3.2.2	Lead Dimensions	37
3.2.3	Lead Orientation	40
3.2.4	Lead Opening and Closing Rates	42
3.3	Floes	45
3.3.1	Distribution of Data	50
3.3.2	Floe Velocities	54
3.3.3	Ice Floe Size	62
3.4	Ice Freeboard	64
3.5	Winds Effects on Ice Dynamics	67
3.5.1	Modification of Measured Ice Speeds to Reflect Cloud Cover Wind Speed Bias	67
3.5.2	Comparison of Average Winds and Ice Velocity	69
3.6	Refreezing of Pack Ice Leads	70

CONTENTS

		Page
4.0	CONCLUSIONS AND RECOMMENDATIONS	76
	ACKNOWLEDGEMENTS	
	REFERENCES	
	APPENDICES	
A	Remote Sensing Inventory	
B	Offshore Wind Statistics	
C	Monthly Distribution of Floe Speeds	
D	Representative Profiles of Labrador Sea Ice Cakes	

FIGURES

		Page
Figure 1.1	Location Map Showing Study Areas	1
Figure 2.1	Beaufort Sea Location Map	7
Figure 2.2	Lancaster Sound Location Map	7
Figure 2.3	Labrador Coast Location Map	8
Figure 2.4	March Landsat Image Showing Pack Ice North of Cape Bathurst	12
Figure 2.5	July SLAR Image Showing Pack Ice in Lancaster Sound	13
Figure 2.6	Example Data Format for Floes and Leads	15
Figure 2.7	March Aerial Photograph of Pack Ice in the Labrador Sea	16
Figure 2.8	Lead Refreezing Processes	20
Figure 3.1	Median Bi-Weekly Ice Concentration - Beaufort Sea	27
Figure 3.2	Median Bi-Weekly Ice Concentration - Lancaster Sound	28
Figure 3.3	Median Bi-Weekly Ice Concentration - Labrador Sea	29
Figure 3.4	Distribution of Beaufort Sea Lead Statistics by Region	33
Figure 3.5	Distribution of Lancaster Sound Lead Statistics by Month	33
Figure 3.6	Overlay of Satellite Image, March 10, 1975	34
Figure 3.7	Landsat Image of Same Area as Figure 3.6	35
Figure 3.8	Comparison of Lead Appearance in Lancaster Sound	36
Figure 3.9	Distribution of Lead Widths - Beaufort Sea	38
Figure 3.10	Distribution of Lead Widths - Lancaster Sound	38
Figure 3.11	Lead Width Distributions in the Polar Pack, April 1972	39
Figure 3.12	Cumulative Probability of Lead Density	40
Figure 3.13	Beaufort Sea Lead Orientation	41
Figure 3.14	Lancaster Sound Lead Orientation	41
Figure 3.15	Lead Opening and Closing Rates - Beaufort Sea	43
Figure 3.16	Lead Opening and Closing Rates - Lancaster Sound	43
Figure 3.17	Lancaster Sound Landsat Image, April 25, 1977	46

FIGURES

		Page
Figure 3.18	Landsat Images Showing 24 Hour Changes in Pack Ice Concentration in the Beaufort Sea	47
Figure 3.19	Landsat Image Showing Labrador Sea Pack Ice, February 22, 1979	48
Figure 3.20	Labrador Sea Pack Ice Conditions, April 1, 1979	49
Figure 3.21	Floe Data Distribution According to Month	51
Figure 3.22	Floe Data Distribution According to Ice Concentration	52
Figure 3.23	Floe Data Distribution According to Floe Area	53
Figure 3.24	Distribution of Floe Speeds - Beaufort Sea	56
Figure 3.25	Distribution of Floe Speeds - Lancaster Sound	56
Figure 3.26	Distribution of Floe Speeds - Labrador Sea	56
Figure 3.27	Direction of Floe Motion - Beaufort Sea	57
Figure 3.28	Direction of Floe Motion - Lancaster Sound	57
Figure 3.29	Direction of Floe Motion - Labrador Sea	57
Figure 3.30	Variation in Ice Speed with Concentration - Beaufort Sea	58
Figure 3.31	Variation in Ice Speed with Concentration - Lancaster Sound	58
Figure 3.32	Variation in Ice Speed with Floe Area - Lancaster Sound	59
Figure 3.33	Cumulative Probability of Ice Speed Comparison with Schwab (1978)	60
Figure 3.34	Comparison of Reported Floe Speeds for the Beaufort Sea	61
Figure 3.35	Comparison of Reported Floe Speeds for Lancaster Sound	61
Figure 3.36	Beaufort Sea Floe Size Distribution from SLAR	62
Figure 3.37	Labrador Sea Floe Size Distribution from 1:20,000 Scale Photography	63
Figure 3.38	Labrador Sea Floe Size Distribution from 1:2,600 Scale Photography	63
Figure 3.39	Percent of Time Cloud Cover Found for a Given Wind Speed - Tuktoyaktuk	68
Figure 3.40	Percent of Time Cloud Cover Found for a Given Wind Speed - Resolute	68
Figure 3.41	Percent of Time Cloud Cover Found for a Given Wind Speed - Hopedale	68

TABLES

		Page
Table 2.1	Data Collection and Entry Rules	10
Table 2.2	Data Base on Offshore Wind Statistics	18
Table 2.3	Annual Non-Uniformity of Wind Statistics	19
Table 3.1	Regional Comparison of Ice Regimes	30
Table 3.2	Regional Summary of Average Pack Ice Duration	31
Table 3.3	Icebreaker Track Closure Observations	44
Table 3.4	Representative Ice Freeboard	66
Table 3.5	Comparison of Relative Frequency of Wind Speeds in Cloud Cover <20% to all Cloud Covers	69
Table 3.6	Wind Speed/Ice Floe Speed Comparison	70
Table 3.7	Beaufort Sea Climate	71
Table 3.8	Lancaster Area Climate	72
Table 3.9	Labrador Area Climate	72
Table 3.10	Beaufort Sea Lead Refreezing	73
Table 3.11	Lancaster Sound Lead Refreezing	74
Table 3.12	Labrador Sea Refreezing Rates	74

ABSTRACT

Pack ice conditions were analyzed from remote sensing imagery in three Canadian offshore regions: the Beaufort Sea, Lancaster Sound and the Labrador Sea. The primary study objective was to provide statistics on lead and floe dimensions, ice concentrations, ice movements and new ice growth for future predictions and modelling of oil spill behaviour in pack ice. Data on 702 floes and 255 leads was collected from satellite and side looking airborne radar imagery, and stored on computer for analysis and plotting.

Results show distinct regional differences in pack ice characteristics. Leads are the dominant dynamic ice features in the Beaufort Sea and Lancaster Sound for over seven months of the year, while individual floes in significant ice concentrations (>4/10) are present for less than six weeks per year, on average. The Labrador Sea experiences a highly mobile and variable ice cover for half of the year. Floe interactions are a more common dynamic event than clearly defined leads in this region.

Detailed pack ice statistics are presented in the report for leads and floes in histogram form. These results are summarized as follows:

Over 50% of all leads observed off Landsat were less than 500 m in width. Previous research using aerial photography has indicated similar distributions, with a median value of only 30 m. There were no significant trends in lead orientation except in the Beaufort Sea nearshore areas, where leads tended to parallel the shoreline. Lead motion statistics showed that both the Beaufort Sea and Lancaster Sound can be characterized as expanding ice covers. Lead closures were observed in only 17% of the documented events. Maximum measured rates of expansion and contraction were 17 and 3 km day^{-1}, respectively. At the average recorded rates of less than 20 m h^{-1}, a typical 30 m lead would take over an hour to close fully.

A comparison of lead refreezing times with lead closure rates indicates at least half the leads present over 100 m wide will close before being covered by a stable young ice sheet. Oil in this case will become

incorporated in the pressure ridge created through deformation of the new ice within the lead during closure.

Floe movements showed distinct regional differences in speed and direction. In the Beaufort Sea, fewer than 30% of the floes moved at rates greater than 10 km day^{-1} compared to 45% in Lancaster Sound and 75% off Labrador. The most rapid floe movements were observed in Amundsen Gulf, at the entrance to Lancaster Sound and at the entrance to Hudson Strait. Measured floe directions agreed with known trends of large scale ice motion in the three regions, i.e. west in the Beaufort Sea, east in Lancaster Sound and south in the Labrador Sea. There was no significant dependence of floe speed on either surrounding ice concentration or floe size. Ice freeboard was evaluated as a separate parameter of interest for oil spill modelling work. A range of values are presented based on limited measurements of offshore pack ice thickness in the Beaufort Sea, theoretical ice growth in Lancaster Sound and field measurements of floe geometry in the Labrador Sea. Typical mid-winter values of ice freeboard are 15, 11 and 100 cm in the respective regions. The high freeboard of Labrador Sea ice reflects the dynamic nature of floe interactions.

A correlation of offshore wind records with cloud cover indicated that ice movements derived from Landsat imagery could be 20% lower than actual values. With this correction factor, the average ratio of ice floe speed to wind speed in this study was about 2% in the Beaufort Sea and Lancaster Sound, increasing to 3% in the Labrador Sea.

In conclusion, this study provides a valuable data set on lead and floe dynamics in three different pack ice regimes. This work also provides the only known statistical description of lead opening and closing rates. Recommendations are made for further investigations of relative short time period displacements of small scale ice features.

1.0 INTRODUCTION

This study was initiated to provide data on pack ice dynamics necessary to model the behaviour of oil spilled in a moving broken ice environment.

The term 'pack ice' describes any ice cover which is not fast to shore, and has the potential for movement in response to local winds and currents. There are significant temporal and spatial differences in pack ice environments encountered in Canadian offshore exploration areas (Figure 1.1). Major regional differences include the seasonal variation in ice concentration, areal distribution of leads, floe sizes, and rates of ice movement.

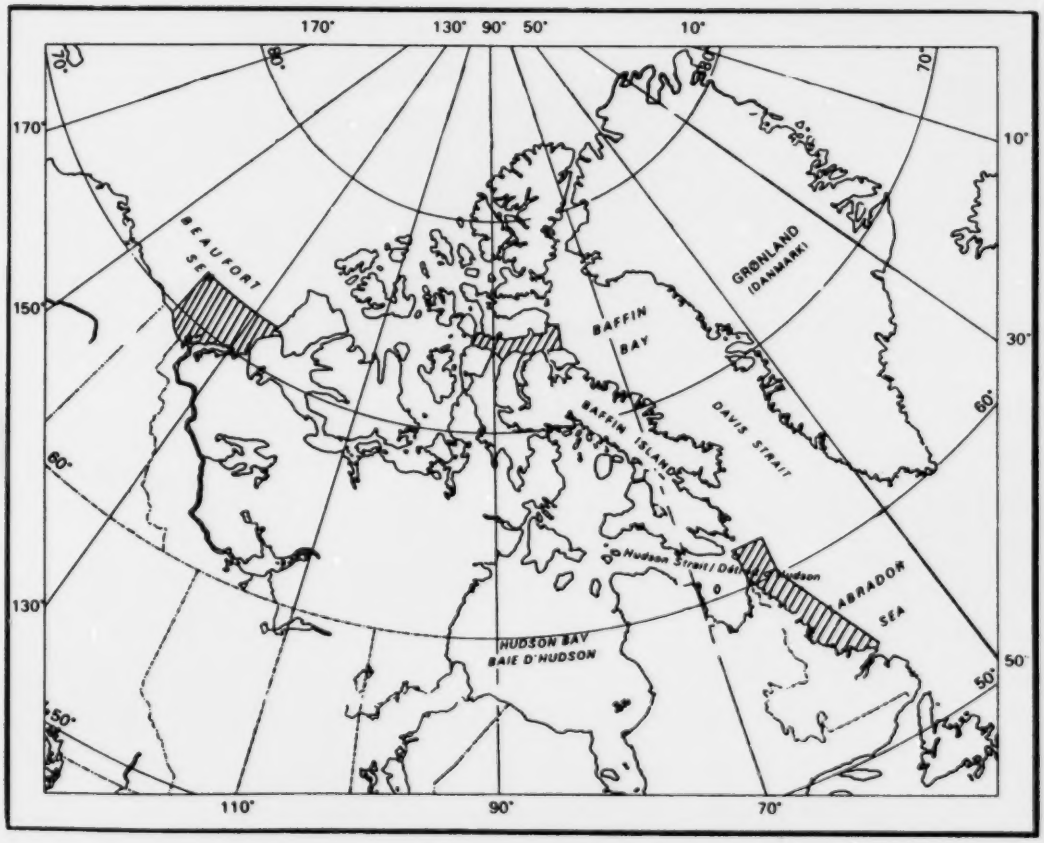

Figure 1.1 Location Map Showing Study Areas

The main objective of this study was to quantify the dynamics of different pack ice areas in terms of specific parameters of ice movement and geometry. Principal subject areas covered in this report include discussions of ice concentration, leads, and floes. Sub-categories treat specific characteristics such as lead opening and closing rates, lead refreezing and floe movements.

Three distinct regions, Beaufort Sea, Lancaster Sound, and Labrador Sea were selected as being of interest for hydrocarbon exploration and transportation and as having clearly defined differences in ice regimes. Hibernia was not included because pack ice is too infrequent to allow sufficient data acquisition.

The Beaufort Sea is characterized by an extensive seasonal pack ice cover bordered by the polar pack to the north and landfast ice to the south. Variations of hundreds of kilometres in the polar pack boundary lead to significant annual differences in ice dynamics within the predominantly first year pack covering offshore drilling locations between November and July.

The Lancaster Sound ice regime is largely controlled by the east/west location of the stable ice boundary which forms across Parry Channel between Resolute and Bylot Island. New ice is constantly being generated at this ice boundary and carried east into the vast expanse of the North Baffin pack by prevailing winds and currents. Ice influx from the Sound into Baffin Bay averaged 481 km^3/year from 1974 to 1978 (Dey, 1981).

The third geographic region evaluated in this study was the Labrador Sea. Here, the pack is comprised of individual floes driven into the coast or dispersed several hundred kilometres offshore, according to the movements of low pressure storm systems. Ice thicknesses are extremely variable, as dynamic floe interactions lead to roughness features many times thicker than the maximum theoretical level ice thickness of about 1.4 m. The Labrador Sea pack was the most difficult to categorize in this study, due to the large variations in surface features, floe distributions, and areal extent. Pack ice near the edge is strongly affected

by the propagation of ocean swells, leading to a characteristic gradation of floes proceeding into the pack from the ocean edge.

In summary, the study collects new ice statistics from publicly available remote sensing imagery, and reports on ice dynamics in three distinct regions with a diverse range of pack ice environments. The primary study objective was to generate quantitative data on pack ice dynamics. It was not the study intent to qualitatively describe the ice environment in detail. Many references provide overviews of the seasonal variation in ice conditions within the different regions (eg. Beaufort Sea - Markham, 1975, 1981; Lancaster Sound - Marko, 1982, Milne, 1978; Labrador Sea - Winsor and LeDrew, 1979).

2.0 METHODOLOGY

2.1 Literature Review

A literature search was conducted to obtain reference sources pertaining to the main subjects of ice movements, lead distributions and ice thickness (refreezing). A majority of the references dealt with ice motion.

Ice drift information was first collected and reported by beset whaling vessels in the 1890's. One of the earliest programs to study ice dynamics in detail, with the benefit of modern electronics, was AIDJEX conducted between 1970 and 1978. Five methods used by AIDJEX to measure ice drift included air photo analysis (Hartwell, 1972), satellite imagery (Hibler et al, 1976), ground surveys (Hibler et al, 1972) satellite navigation (Pritchard et al, 1977) and satellite located buoys (reported by Gulf Canada - McGonigal and Wright, 1975-1977). Over six years of satellite buoy data is now available for the Beaufort Sea, including two years of more accurate French Argos system measurements from 1981 to 1982 reported by Murphy et al, 1981 and 1983. At their best, these newer buoys can provide daily positions of an ice floe to within ± 500 m. Earlier buoys known as RAMS, using the older U.S. Nimbus satellite, provided position accuracies in the range ± 1 to 2 km. Limited buoy data is available for Lancaster Sound as part of the EAMES program.

One other method for measuring ice movement nearshore has successfully used an anchored cable through a hole in the ice. Changes in the cable length were used to record small winter motions of the landfast ice relative to the seabed. This device has provided continuous ice movements in the Beaufort Sea shallow water areas (less than 50 ft of water) for the years 1972-78 (see Spedding - Imperial Oil Limited). The cable technique was used inadvertently at several sites too close to the moving shear zone and cable limits were quickly exceeded.

Other than the landfast ice movement records, there is almost no publicly available data on semi-instantaneous or hourly ice floe velocities. Dome Petroleum Limited has conducted several years of floe measurements at their drillsites using a microwave offshore positioning system. Limited release of this data in graphical form is presented in Marcellus and Morrison (1982).

Satellite imagery has proved to be the most popular, economical means of measuring ice floe displacements over periods of days. References include Markham, 1975; Marko 1976, 1982b; and Schwab, 1978.

Landsat with a scale of 1:1,000,000, and a resolution capability of 100 m, provides the most useful imagery for ice motion studies. There is minimal distortion between images, and slight orbital fluctuations maintain scale to within 10%. Unfortunately, Landsat is limited to daylight cloud free hours, a scarce commodity over much of the arctic offshore. The result is a total lack of imagery from early November until late February, and the loss of up to 85% of available images at other times due to excessive cloud. In spite of these problems sufficient overlapping daily images can be found to track individual floes for several days.

A major weakness of previous studies of interest to this study is the lack of any consistent record of ice concentrations associated with reported ice motions. Schwab (1978) provides a notable exception.

2.2 Geographic Subdivisions

Three geographic areas of Canada's arctic coastline were selected for this study, the southeastern Beaufort Sea, Lancaster Sound and the Labrador Coast. These regions were selected because they may all be affected by future petroleum developments and they have different ice climatologies. Each of the regions was further divided into sub-regions to enhance potential regional differences in the

data. Every piece of data was grouped according to date and sub-region.

Figure 2.1 shows the Beaufort Sea study area and its sub-regions. The area is bounded by Cape Bathurst to the east, Herschel Island to the west; 71°N latitude to the north and coastline to the south. Sub-regions were selected to separate shear zone ice and landfast ice. No attempt was made to collect images showing areas north of 71°N because petroleum development in those areas are unlikely. Some data was collected north of 71°N, and was used for comparison with data collected by others (i.e. AIDJEX was roughly 73°N).

Lancaster Sound was divided into three sub-regions (see Figure 2.2). The western sub-region (Zone A) is the smallest because it is usually covered by landfast ice in the spring. Zone B between Prince Leopold Island and Admiralty Inlet had the best data coverage. This was opportune as ice in Zone B was in motion during most years. The eastern mouth of Lancaster Sound is covered by Zone C. A number of authors have studied iceberg, floe, or buoy velocities in Zone C, but their data could only be included for comparison, as it lacked specific floe size and ice cover information.

The Labrador Coast area was divided into four sub-regions parallel to the coastline (see Figure 2.3). A small landfast ice zone exists within each sub-zone, but all the data was collected from the larger offshore moving pack ice area. Ice velocities within the northern part of Zone A may have been affected by Hudson Strait. Measurements due east of Hudson Strait were identified to allow recognition of any interference affects. All the sub-regions along the Labrador Coast are even in width.

In general, the large quantity of data available for the Beaufort Sea allowed the selection of specific sub-regions which separated the shear zone, landfast ice, and Mackenzie delta regions. The choice of sub-regions in Lancaster Sound was governed by the location of inlets. Some authors have further subdivided the region into north and south halves of the channel according to known current loops.

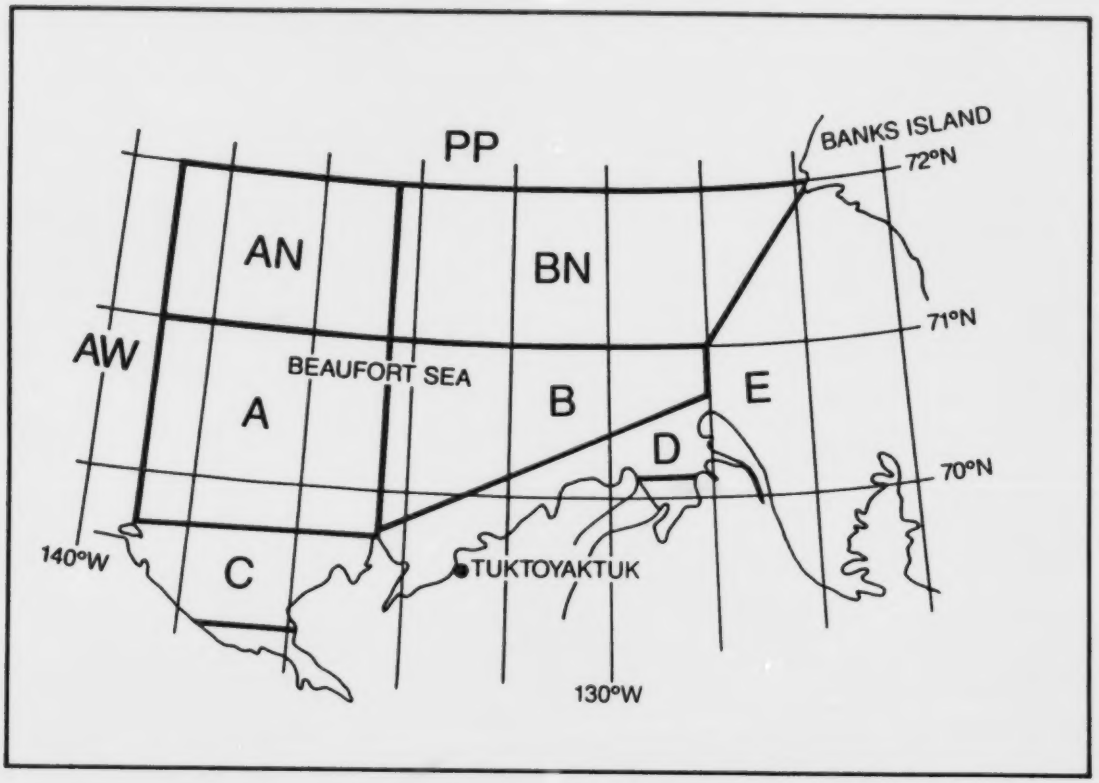

Figure 2.1 Beaufort Sea Location Map

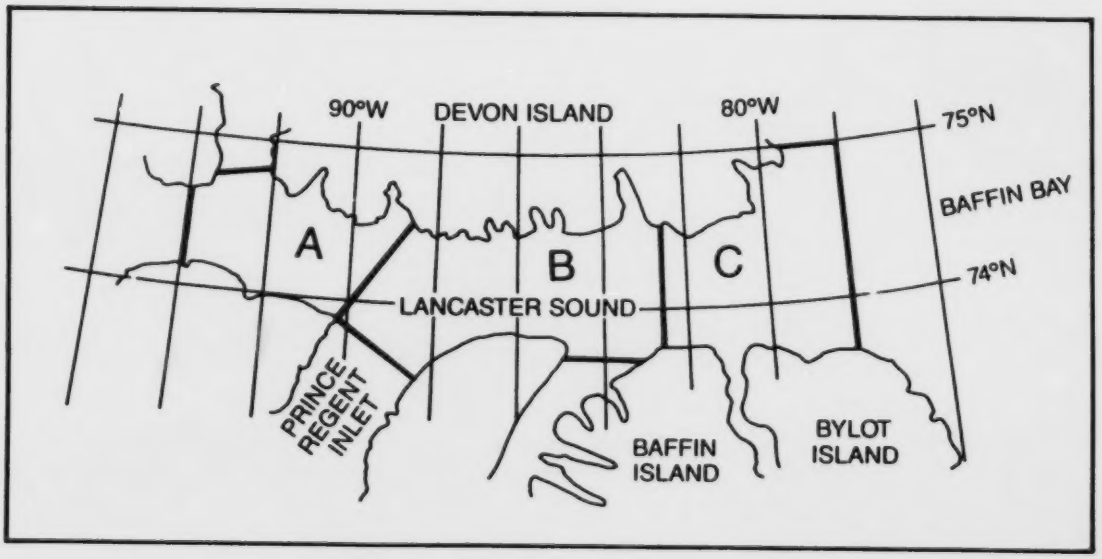

Figure 2.2 Lancaster Sound Location Map

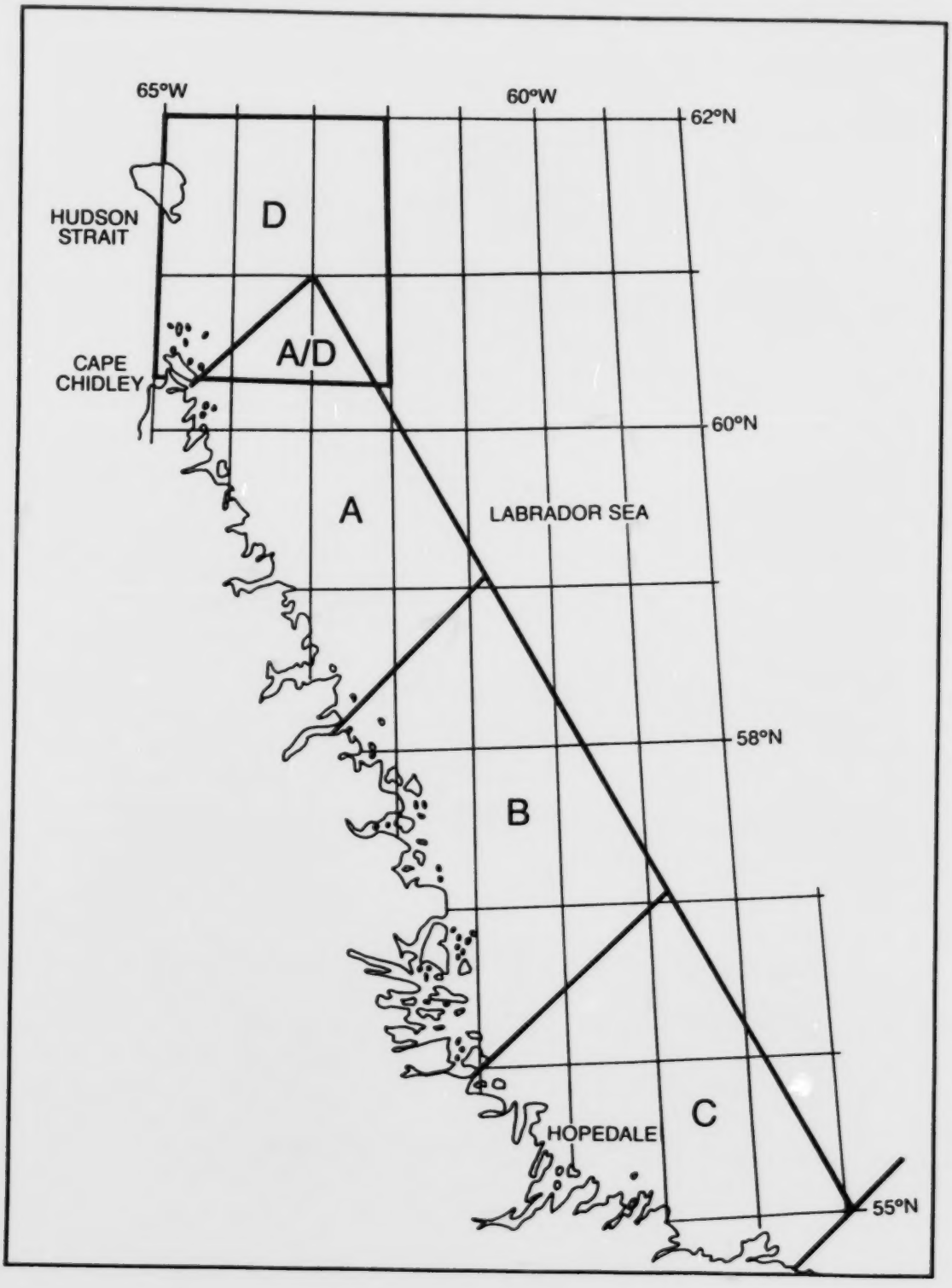

Figure 2.3 Labrador Coast Location Map

Selection of sub-regions along the Labrador Coast was more arbitrary, and was confined to the separation of north-south trends.

2.3 Ice Statistics: Definitions and Sources

Ice dynamics in the three geographic areas of this study were defined with the following statistics:

Floe Size
Ice Cover - Concentration in Tenths
Ice Displacement
Direction of Motion
Floe Rotation (only for Lancaster Sound Landsat Imagery)
Date
Lead Frequency (where possible)

Other data such as floe size distribution, and median ice cover were included to aid comparison with other studies, and to give a better understanding of the occurrence of extreme ice features. Where possible, data collected for this study was compared to information in the literature.

This study relied on acquisition of remote sensing imagery, satellite and airborne, to study ice conditions from February to July in the three regions of interest (Figures 2.1 to 2.3). It was not possible to obtain sufficient mid-winter imagery due to limitations of darkness and poor contrast. Fall conditions were not covered because the new ice cover is extremely mobile. Floes and leads are either too dynamic or not clearly defined, as the thin ice cover is constantly being broken up and ridged. In addition, satellite coverage ceases within three weeks of freeze-up offshore, severely restricting the number of available images.

Floe displacements were measured using the following definition: "A floe was defined as any planar area of ice surrounded by visible cracks or open water." The only exception to this definition

occurred in the floe distribution determination for the Labrador Coast. Aerial photography was available at a scale of 1:6,000 which allowed a distinction to be made between the new ice and the thicker ice which had drifted south. The patches of thicker ice surrounded by thinner ice were counted as floes.

The definition of a lead was more difficult because during spring break-up the ice reaches a state where it either has a lot of leads or a lot of floes. For this study any distinct lineal, open water features bounded by ice on both sides and greater than 5 km in length were counted as leads. Many leads were counted which were at the limits of image resolution. Large patches of open water adjacent to land were not included as leads.

A summary of rules used for collection and data entry (on a computer) is shown in Table 2.1.

Table 2.1 Data Collection and Entry Rules

1. If an ice floe crossed from pack ice to open water between images, the ice concentration was taken as 5/10.

2. If a lead crossed through more than one sub-region the region containing most of the lead was used to label the lead location.

3. A range of lead widths was recorded to show the maximum and minimum lead width.

4. If a shore lead was measured (open water between coast and pack ice in Lancaster Sound) the ice concentration was taken as 8/10.

5. Concentration of ice was taken as 9/10 for lead measurements unless rule 4 applied.

2.3.1 Median Ice Cover

Pack ice concentrations were tabulated from the AES ice charts. Total ice concentrations were tabulated in the groups 4/10 to 6/10 (loose pack), 7/10 to 8/10 (close pack) and 9/10 to +9/10 (very close pack) ice cover. A single concentration value was extracted for each sub-region, year, and two week interval by area averaging the data (i.e. if 1/3 of the sub-region was covered by 3/10 ice cover and the other 2/3 by 9/10 ice cover the area average = 1/3 * 3/10 + 2/3 * 9/10 = 7/10). Overall average concentrations for each sub-region and two week interval were derived from the average of 11 years of data (1975-1985).

2.3.2 Ice Velocities

The primary objective of this study was to determine ice displacement rates at various times of the year. Many authors report ice velocities but very few consider floe size and ice cover. This study used an analysis of 225 Landsat and 37 SLAR images to provide a data base containing velocity, floe size, ice cover, and direction of motion information. Landsat and SLAR information was at a nominal scale of 1:1,000,000 (1 mm on image = 1 km full scale). Three pairs of SLAR imagery were obtained at a scale of 1:500,000, and one at 1:250,000 (Appendix A).

Estimates of daily ice motion were made by using images temporally separated by one, or in some cases, two days. A further screening of potential imagery selected images with 15% or less cloud cover. In some cases images were used with greater than 15% cloud cover if they were viewed prior to purchase. In the case of the SLAR imagery, each potential pair was viewed before selection. Most of the SLAR images covered Lancaster Sound, so that each swath band had a land reference. Figures 2.4 and 2.5 show respectively, examples of Landsat and SLAR imagery of Landcaster Sound. Appendix A

Figure 2.4 **March 21, 1981 Landsat Image Showing Pack Ice North of Cape Bathurst (Image Scale = 1:1,000,000)**

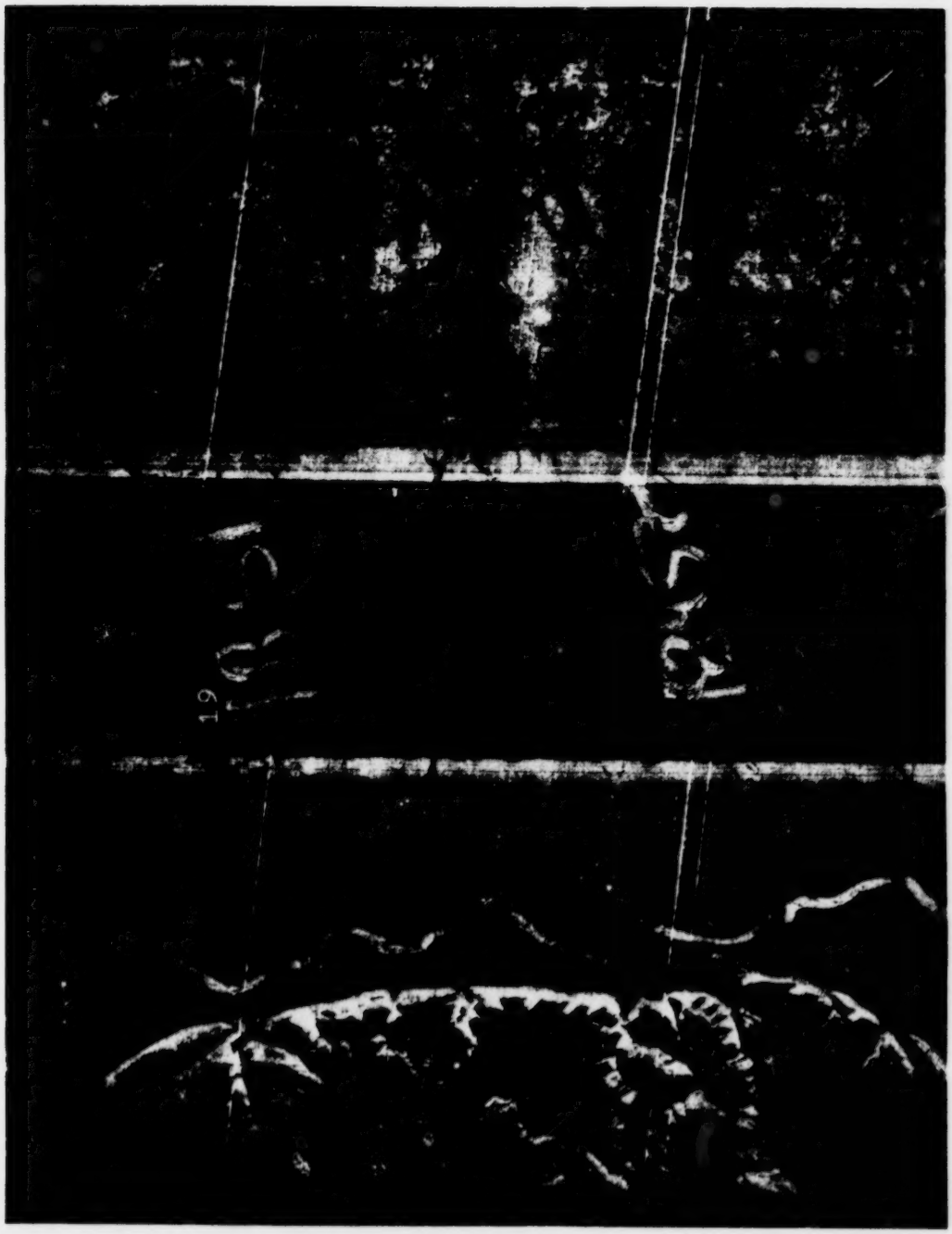

Figure 2.5 **July 17, 1983 SLAR Image Showing Pack Ice in Lancaster Sound (Image Scale = 1:500,000)**

contains a listing of Landsat and SLAR images used in this study.

Ice velocity was measured by determining the daily floe displacement relative to land, or the lead closure rate. An overlay technique was used to transfer information from one image to another. The reference coastline, each floe and each lead were traced onto a piece of vellum paper. The vellum was placed on top of the next day's image and the displacement of the floe or lead was measured. The geometric centre of a floe was used for displacement measurements. Lead measurements were relative, so the change of lead width was measured and not the movement of the lead relative to land. All displacements were measured relative to True North. The accuracy of the measurements depended on the scale of the image and the length of reference coastline in the image area. Ten floes and leads were sampled per image pair.

Most of the data has position accuracies of ± 1 km. Some of the Labrador coast measurements (sub-region D) may be in error by as much as ± 3 km due to the small lengths of available reference coastline. Figure 2.6 shows example data entries for a floe and for a lead.

REGION -- LABEL */M/YR	BEAUFORT Δt (hours)	SEA a (km)	E b (km)	ΔN (km)	ΔE (km)	ΔØ (deg)	CONC (Tenths)	BEARING (deg)
A/JUL/74	24.0	3.0	2.0	0.0	0.0	0.0	7	45
B	24.0	4.0	1.5	2.0	0.0	0.0	7	0
C	24.0	9.0	5.0	1.0	1.0	10.0	7	45
D	24.0	4.0	2.0	2.0	0.0	0.0	7	0
F	24.0	6.0	3.0	2.0	-1.0	0.0	7	333
C	24.0	9.0	5.0	0.0	3.0	10.0	7	90
D	24.0	4.0	2.0	4.0	4.0	5.0	7	45
F	24.0	6.0	3.0	3.0	3.0	5.0	7	45
P	24.0	6	5	1E-04	0	0	7	0
Q	24.0	14	11	1E-04	0	0	7	0
A/JUN/75	48.0	7.0	5.5	15.0	-40.0	-25.0	3	291
B	48.0	5.0	5.0	27.0	-30.0	55.0	1	312
Where:	*/M/YR =	Floe label,	Month,	Year		Δt =	time	interval
	a, b =	Major &	Minor	floe	axes			
	ΔN, ΔE, ΔØ =	Change of	floe	position	to North	to East	& floe	rotation
	Conc =	Ice cover						

Figure 2.6 Example Data Format for Floes and Leads

As shown in Figure 2.6, the date of the image and the pack ice category (4-6/10, 7-8/10, 9-9+/10) were recorded. Ice cover was visually estimated. The date and time of each Landsat image was encoded within the Landsat image number. Each SLAR image date was available in a catalogue of images, and the actual time of the imagery was available from flight logs.

Only one aerial photograph mosaic pair was found within the study areas. Most aerial photography either lacked a good coordinate fix, or was not taken on consecutive days. More images exist, but are not available for public use. When available, aerial photography can provide very detailed information, as shown in the 1:2,600 image in Figure 2.7.

Figure 2.7 **March 24, 1982 Aerial Photograph Showing Pack Ice in the Labrador Sea (Image Scale = 1:2,600)**

Once all the ice data were recorded, they were put into a spreadsheet type computer program (Microsoft Multiplan). Ice velocity, floe area and movement direction were calculated using a computer. Calculations of the maximum and average monthly velocities were made for each sub-region. The data was entered into a plotting program to allow a graphic representation of data.

Where possible, data from the literature review was extracted for comparison with the data base generated for this study. Buoy drift rates, iceberg drift rates, and floe drift rates were compared to the data base. In some cases data outside the study area was shown as there was no other information. In all cases, data from the literature were distinguished, and notes on their sources included.

2.4 Wind Statistics

2.4.1 Wind Speed Dependence on Cloud Cover

The Landsat images were selected for this study on the basis of 15% or less cloud cover. Consequently, the ice movements measured are those accompanying winds occurring at the lower cloud concentrations. This sample space may not contain the more extreme ice speeds concurrent with storm winds (and potentially overcast conditions). To test this hypothesis, wind speed and cloud cover statistics obtained from the Atmospheric Environment Service (AES) were analyzed in order to evaluate the concurrence of the two meteorological elements. For lack of offshore data, one onshore station with sufficient length of record was selected for each geographical area studied, as follows.

a) Beaufort Sea: Tuktoyaktuk, 1958-1983 (37,990 records);
b) Lancaster Sound: Resolute A, 1953-1983 (222,975 records);
c) Labrador Coast: Hopedale, 1953-1983 (206,939 records).

For each station, data were separated into two groups:

a) observations of wind speeds at 0 to 20% cloud cover, and
b) wind speeds at more than 20% cloud.

The percent frequency of the above two cloud cover groups within each wind speed interval was determined for the three onshore stations.

2.4.2 Offshore Wind Statistics

Data on frequency of wind speed and direction were also acquired from AES. Table 2.2 shows the distribution of observations by month at offshore sites falling within the study regions (Figures 2.1 to 2.3). Original printouts are contained in Appendix B.

Table 2.2 Data Base on Offshore Wind Statistics

Area	Regions Lat	Regions Long	Period of Records	No. of Records Feb	Mar	Apr	May	Jun	Jul	Aug
Beaufort Sea	A,B,C,D (Figure 2.1)		1952-1979	*	*	*	*	*	850	2330
Lancaster Sound	as per Figure 2.2		1899-1979	*	*	*	58	43	481	3351
Labrador Coast	A/D,A,B,C (Figure 2.3)		1882-1979	35	206	218	31	223	2044	2862

*Number of records negligible or null.

It can be seen that the majority of the available offshore wind records fall in the summer months of July and August coincident with the frequency of vessel observations. Additional wind information was extracted for Hopedale on the Labrador coast, and Ocean Station Bravo to compare the differences between shore station and offshore data. In studying relationships between winds and ice dynamics, only those months and locations with reasonable data coverage were used. A

major difficulty with the offshore wind data is its non-uniformity between months, (Table 2.2) and between years. Table 2.3 shows how over 2/3 of the offshore wind data set is concentrated in only one to three years of record.

Table 2.3 Annual Non-Uniformity of Offshore Wind Statistics

Area	Month	% of Record	Period
Beaufort Sea	July	62	1979
Lancaster Sound	May	97	1970, 1977
	June	73	1977
	July/August	77	1975-79
Labrador Coast	March	91	1965
	April	89	1965-67

For the selected months, the relative frequencies of speed and of direction of winds were tabulated and graphed for comparison with corresponding probability distributions of ice speed and direction of movement.

Even with the above selection procedure, some subsets of data are of questionable quality. For wind data, the spatial distribution of observations in each study area is not known, and the distribution of observations between years is in most cases highly non-uniform.

For ice movements, the distribution between subareas is also non-uniform. Owing to these limitations, the selected subsets of data were used with caution in making inferences on the wind-ice movement relationships. No attempt was made to provide a quantitative assessment of ice speed and wind speed distributions. Average values are compared and discussed in Section 3.5.2.

2.5 Refreezing of Pack Ice Leads

When a lead in the pack ice is open, the water surface is a heat source for colder air above the water. If the water is at or near

its freezing point, about -1.8°C for most sea water, the heat loss will result in formation of ice. If sufficient ice is produced, the lead will be covered in a new ice layer. The timing of this new ice formation will compete with the closure of the lead to determine which physical process will control the distribution of oil.

A number of processes are involved in the transfer of heat to and from the air-water interface, and the subsequent formation and behaviour of ice on the surface of the lead. Figure 2.8 depicts the many processes occurring while a lead is open. If there is no wind, heat will be lost from the water to the air, producing a skim of new ice. This ice will grow as fast as heat can be transferred from the water below to the air above, and depends on the air temperature and the thickness of the insulating ice layer. If there is a wind or a current the ice, as it is produced, will be transported away, leaving open water for more ice production. Eventually, this ice will pile up against the boundary of the lead and will ultimately cover the lead. As ice is produced at the water surface, the salt is generally excluded from the ice. This increase of salinity in the underlying water may cause a density instability to develop, and may result in a turnover of the water column, bringing warmer deep water to the surface. This would act to slow the production of ice.

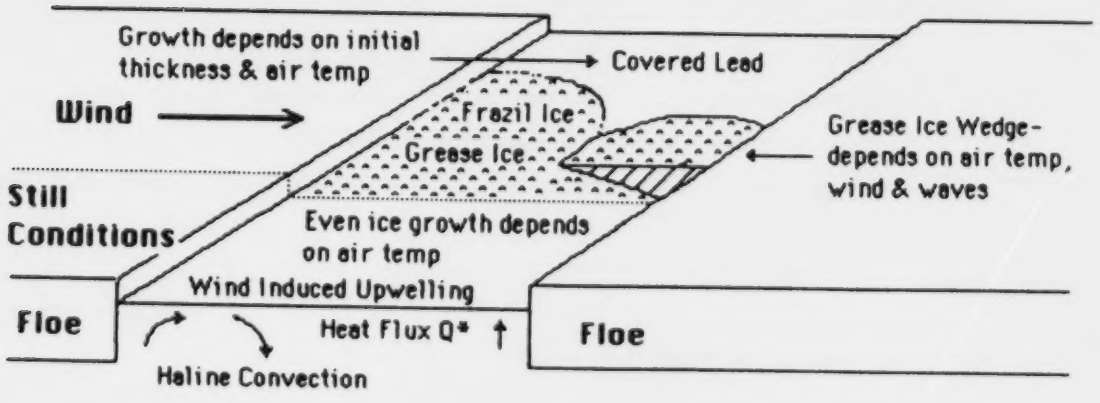

Figure 2.8 Lead Refreezing Processes

Each of the processes depicted have been studied and some have been modelled. No experimental study has been found in the literature which examines the problem of lead refreezing specifically, but an estimate of lead refreezing rates may be made using data from related studies.

The growth of ice has been generalized for Canadian waters by Burns (1974). Using the classical equation for ice growth, he relates the theoretical growth rates to measured growth rates, and provides a rough method for determining the thickness of ice given the temperature regime over time. The equation takes the following form:

$$D\ L_f\ dH = a\ K_i\ (T_w - T_a)/H_m/\ dt \qquad (1)$$

where

D = ice density (taken as 920 kg m^{-3})

a = constant correcting for included air (Burns suggests 0.94)

L_f = latent heat of fusion of water (taken as 320 kj kg^{-1}, at -1.6°)

dH = change in ice thickness (metres)

K_i = thermal conductivity of ice (taken as 2.5 W $m^{-1}deg^{-1}$)

T_a, T_w = temperature of the air and water

H = ice thickness (metres)

dt = time interval (hours)

This equation is integrated to give the form:

$$H_{t2}^2 - H_{t1}^2 = 2.87 \times 10^{-5} \times \text{Freezing Degree Hours} \qquad (2)$$

This equation may be used to determine the growth of ice from an open lead under conditions with no wind or current. It is similar to the equation used by Bauer and Martin (1983) in their model treatment of ice growth.

If there is any wind, the ice will be transported away from the site of formation, leaving open water to produce more ice. This effect is well documented for polynyas and leads (Dunbar, 1981; Topham et al, 1983; Smith et al, 1983; den Hartog et al, 1983; Martin and

Kaufmann, 1981). Dunbar (1981) quotes Kupetski (1962) who determined that the open water of the North Water annually produced 4.5 times as much ice as the equivalent covered area.

Photographs of leads under windy conditions show grease ice formation, movement, and pile-up (Martin and Kaufmann, 1981). The formation of grease ice in leads has been modelled by Bauer and Martin (1983).

Estimates of ice growth under wind conditions are all based on the determination of the heat flux to the air from the water, and are usually calculated assuming all the heat removed from the water is provided from the latent heat of vapourization, as the water will likely be at the freezing point. This assumption is acceptable as the latent heat of vapourization is much higher than the heat capacity of water and will be the major heat source. The heat flux consists of four components:

$$Q^* = Q_S + Q_L + Q_{lw} + Q_{sw} \qquad (3)$$

where

Q_S is the sensible heat flux
Q_L is the latent heat flux
Q_{lw} is the long wave radiation flux

and

Q_{sw} is the short wave radiation flux

Andreas et al (1979) measured the heat flux over small leads (6-10 m), and Bauer and Martin (1983) developed a model of heat flux over large leads (0.5 km). The environmental conditions of Andreas et al (1979) are mild, whereas those of Bauer and Martin (1983) are severe. The results of both workers may be simplified by plotting heat flux against a "wind chill" factor, $U\ (T_w - T_a)$, where U is wind speed in m s^{-1}. The flux equations may then be included in the equation for the production of ice, assuming all the heat is from the heat of fusion, to give two equations for ice production, one for small leads and mild wind chill, and the other

for large leads and severe wind chill. Lo (1980) has pointed out that the heat flux may decrease in larger leads due to fog formation above the leads, but no experimental data could be included in this analysis. The equations are:

$$P = 1.2 + 0.0312\ U\ (T_w - T_a) \qquad (4)$$

and

$$P = 3.0 + 0.0204\ U\ (T_w - T_a) \qquad (5)$$

P = Production Rate (kg $m^{-2}h^{-1}$)

U = Wind Speed (m sec^{-1})

Equation (4) will be used for mild conditions (wind chill less than 200 m sec^{-1} °C), equation (5) for severe conditions (wind chill greater than 200 m sec^{-1} °C).

The time required to cover a lead may be estimated by integrating the ice production rate over the dimensions of the lead as the lead is covered. This integration is logarithmic, with the final stages of covering becoming infinitely slow, as the area for ice production approaches 0. By using 95% coverage and factoring it up to 100%, coverage times may be estimated according to equation (6) below:

$$t_c = 827\ P/H \qquad (6)$$

where

H is the final covered ice thickness (m).

It should be noted that for leads wider than 50 m, coverage times are independent of lead width.

The results using this equation correspond closely to Bauer and Martin's (1983) results when their choice of ice thickness and environmental conditions are used. The weak point in this analysis is the estimation of the final ice thickness. Bauer and Martin (1983) developed a model based on wave action and wind induced current to determine the thickness of the grease ice wedge built up

at the end of the lead, and subsequently covering the lead. Their tank results have shown that the modelled thickness is typically only one-half of the observed thickness. By doubling their model results, and plotting against wind speed, an estimate of grease ice thickness of $H = 0.06\ U$ is used for the present analysis.

The other factors depicted in Figure 2.8 have been examined. The effect of haline convection in small (less than 1 m) leads was examined by Foster (1972). The circulation of water in a lead caused by the exclusion of salt during freezing was modelled by Kozo (1983). His model broke down in a current of 5 cm s^{-1}, but showed significant circulation in quiet conditions. No attempt has been made to include the introduction of warm, deep water in the present analysis, as the general oceanographic conditions for these areas are not well defined. Some factors may be considered. Schaas and Galt (1973) modelled heat flux as determined by water structure, and pointed out that any overturning of the water column will slow icing by introducing warmer deep water, and that any factors which reduce this turnover will encourage icing. A density or salinity discontinuity, such as occurs in the Beaufort Sea, insulates the upper layer from the deeper heat source. Horizontal currents had a similar but smaller effect.

Buckley et al (1979) showed the presence of wind induced upwelling at pack ice edges. This effect may influence lead refreezing in the case of large leads.

The analysis for refreezing times for leads in the three regions studied will be determined using the equation for calm conditions, equation (2), rearranged to give the time for production of 0.2 m of ice, selected as being a thickness which allows most forms of light transport. The times for coverage under mild and severe wind conditions will be determined using either equation (4) or (5), depending on the mean climatic conditions. The climatic conditions used in each case are those provided by the "Canadian Climate Normals 1951-1982" for weather stations in each area. The Beaufort Sea area is represented by data from Nicholson Peninsula and Tuktoyaktuk. The Lancaster Sound area is represented by data

from Resolute Bay, and the Labrador area by data from Hopedale. The marine data collected for each area did not have sufficient data for the time periods of interest. The data used from each station are minimum, mean, and maximum monthly temperatures, and mean and maximum winds. The lead refreezing rates are presented in Section 3.6.

3.0 RESULTS AND DISCUSSION

3.1 Pack Ice Concentrations

Figures 3.1 to 3.3 show median bi-weekly ice concentrations for the different regions. This information is an important indicator of the relative importance of a particular pack ice environment within the different offshore areas of interest for hydrocarbon exploration.

Ice concentration is considered the single most important pack ice descriptor. At low ice concentrations (less than 4/10) it seems unlikely that ice dynamics will play a major role in modifying or controlling oilspill behaviour. As concentrations reach 7/10, individual ice floes are contacting one another, and the potential exists for substantial ice/oil interaction. Eventually, as the pack closes up and becomes a continuous sheet of bonded ice, leads appear and become an important natural means for oil containment or spreading depending on dynamics of the situation. Table 3.1 shows a simplified comparison of the most important characteristics of the ice regime in the three main areas.

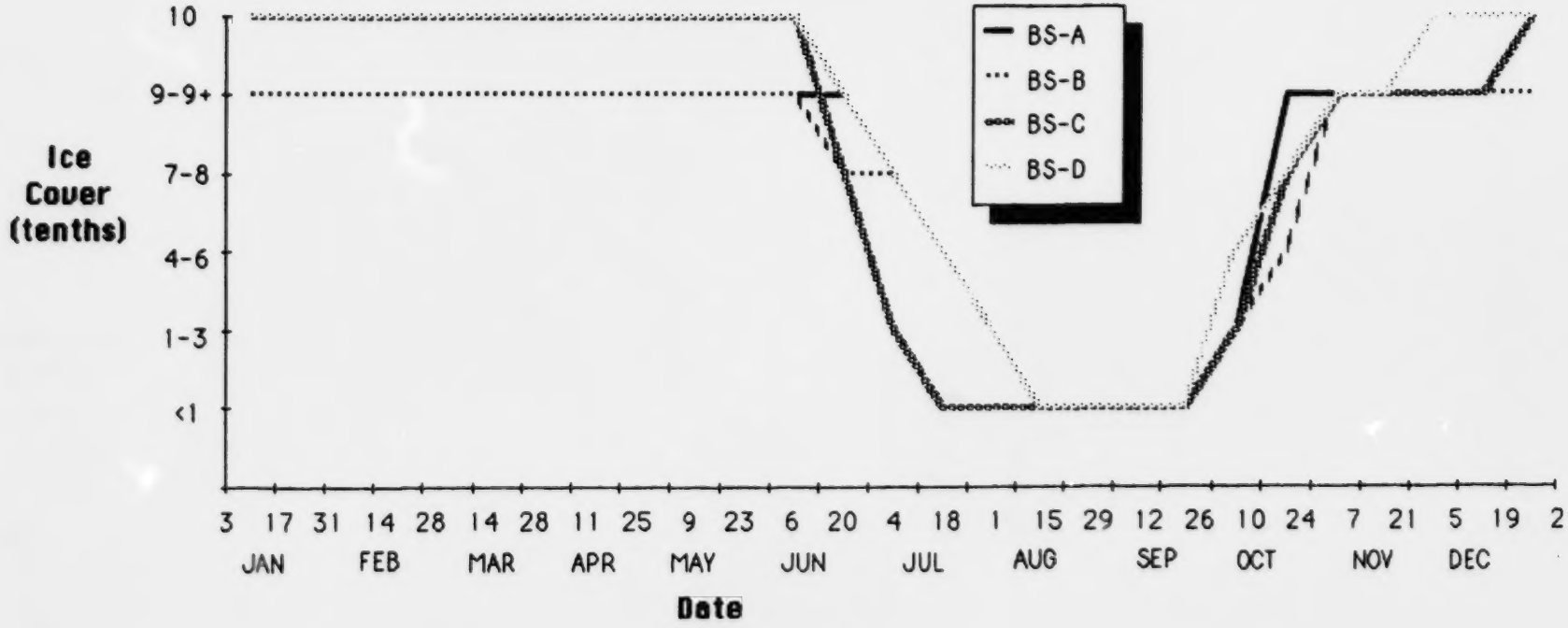

Figure 3.1 Median Bi-Weekly Ice Concentration - Beaufort Sea

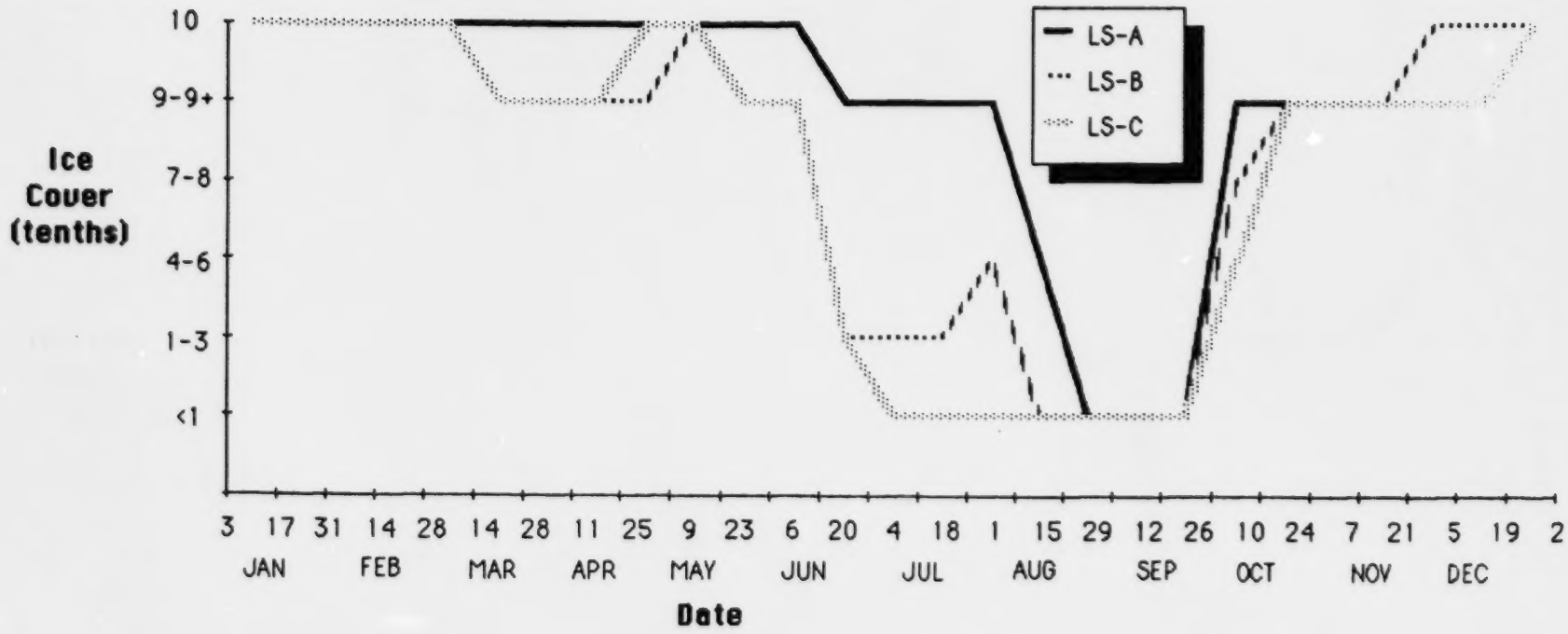
10
9-9+
7-8
4-6
1-3
<1
Ice Cover (tenths)
LS-A
LS-B
LS-C
3 17 31 14 28 14 28 11 25 9 23 6 20 4 18 1 15 29 12 26 10 24 7 21 5 19 2
JAN FEB MAR APR MAY JUN JUL AUG SEP OCT NOV DEC
Date

Figure 3.2 Median Bi-Weekly Ice Concentration - Lancaster Sound

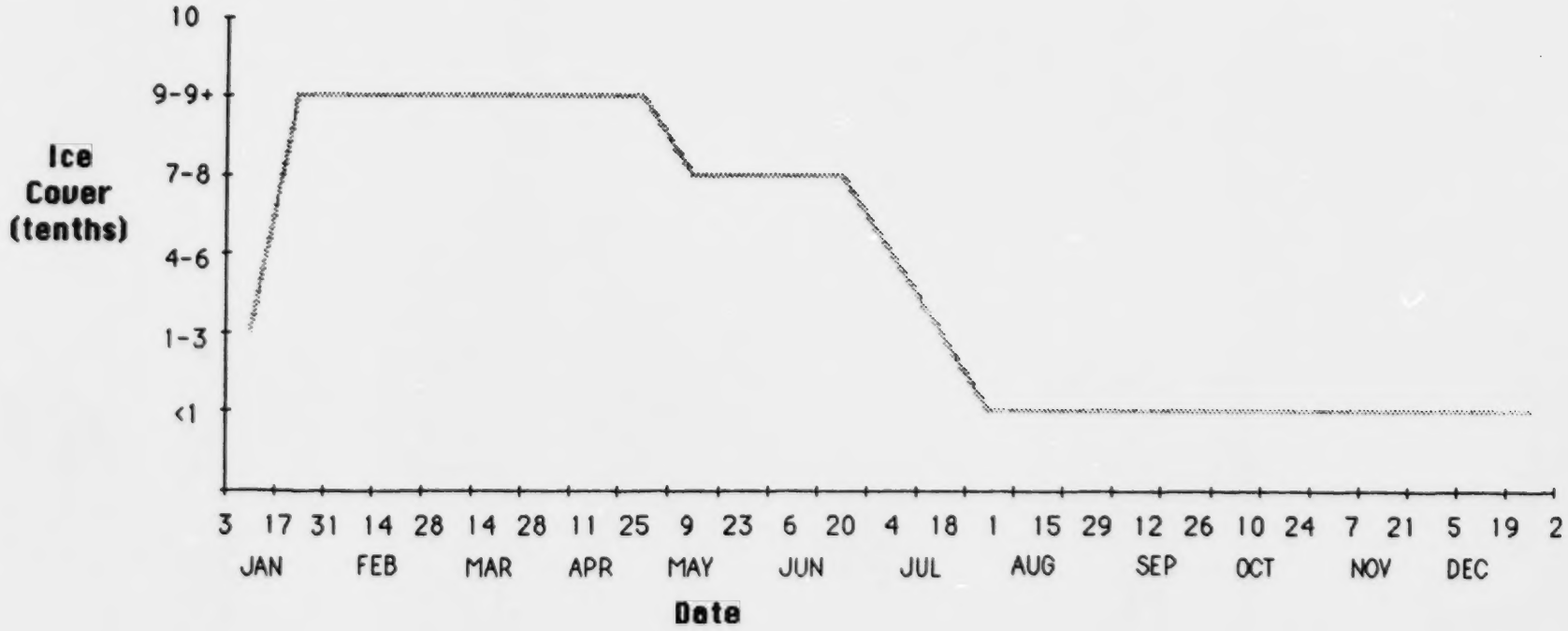

Figure 3.3 Median Bi-Weekly Ice Concentration - Labrador Sea

Table 3.1 Regional Comparison of Ice Regimes

	Beaufort Sea	Lancaster Sound	North Labrador Sea
Freeze-Up	Oct 5 ± 15 days	Oct 10 ± 10 days	Jan 10
Break-Up	July 16 ± 20 days	June 3 ± 40 days	June 20
Single Most Important Physical Control on the Ice Environment	Position of Polar Pack Relative to Shore	- East/West Location of Stable Ice Edge - Prevailing Winds	- Storm Tracks - Ocean Currents
Maximum Level Ice Thickness	1.8 m	1.9 m	1.4 m
Weeks of:			
7-8/10 Ice Floes	2 weeks	2 weeks	8 weeks
4-6/10 Floes	4	3	2
9-9+ Leads	34	30	16*
<4/10 Ice	12 weeks	17 weeks	26 weeks

*For Labrador Sea 9-9+/10 ice is still predominantly composed of individual floes. Lead patterns are transient and not well formed.

The Beaufort Sea region has the greatest number of weeks of 9/10 and greater ice cover (over twice as many weeks as the Labrador Sea).

Four to eight/tenths can be considered the maximum range of pack ice concentrations where the movement and interaction of individual floes will play a major role in affecting oil behaviour and fate. In lesser ice concentrations an oil spill can essentially be treated as an open water situation. In higher concentrations, individual floes gradually loose their identity, and linear openings in the cover known as leads become the major pack ice characteristic impacting oil distribution.

From Table 3.1, the three regions can be summarized as follows according to the proportion of the year when average pack ice conditions will impact an oil spill through a) individual floe dynamics and b) leads.

Table 3.2 Regional Summary of Average Pack Ice Duration

	% of Year by Region		
Pack Type	Beaufort Sea	Lancaster Sound	Labrador Sea
a) 4-9/10, Floes	11	10	50
b) 9/10+, Leads	65	58	Not Estimated

This simplified comparison indicates that in Lancaster Sound and the Beaufort Sea, open to close pack ice conditions persist on average for about 10% of the year, concentrated in a 5 to 6 week period preceding break-up. Both Arctic regions have almost complete ice cover for over half the year. During this period, leads and openings (polynyas) exist as evidence of continuing pack ice motion.

The Labrador Sea is not as readily characterized in terms of a simple division between leads and floes. Instead of a rapid, predictable build-up and drop in ice concentrations characteristic of the arctic ice cycle, the marginal ice zone in the Labrador Sea tends to be much more variable both between years and within a single winter season. From previous descriptions and evaluation of remote sensing imagery in this study, floe interactions are considered to be much more important than leads in potentially controlling oil behaviour and fate in the Labrador Sea.

3.2 Leads

3.2.1 Distribution of Data

Figures 3.4 and 3.5 show the distribution of lead statistics collected in this study for the Beaufort Sea and Lancaster Sound.

In the Beaufort Sea, 85% of the remote sensing imagery suitable for the analysis of leads falls in the month of March, with the remainder in April. Sixty-two percent of the data was collected for Regions A and B of most interest for deep water offshore exploration (see Location Map, Figure 2.1).

In Lancaster Sound, the data is spread over the period March to August, with half of the measurements in April and July. The break-up of Lancaster Sound proceeds from east to west. Logically, most leads in April were in the central Region B (Figure 2.2), while July leads were concentrated in far western Region A, where the ice cover is last to clear.

Figures 3.6 to 3.8 show examples of lead dynamics in the Beaufort Sea and Lancaster Sound. Figures 3.3 and 3.4 show the closure of lead systems over a 24 hour period off the Tuktoyaktuk Peninsula. Figure 3.8 presents a pair of Landsat images showing the opening of lead systems in Lancaster Sound between March 30 and March 31, 1981.

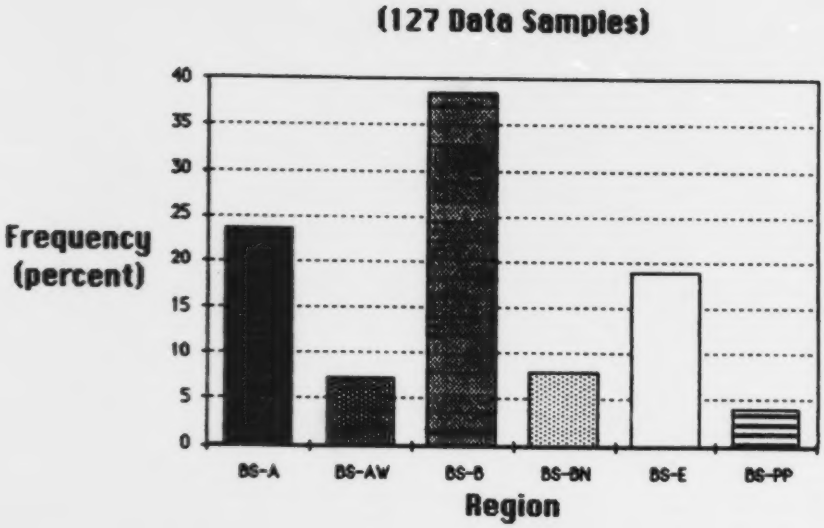

Figure 3.4 Distribution of Beaufort Sea Lead Statistics by Region

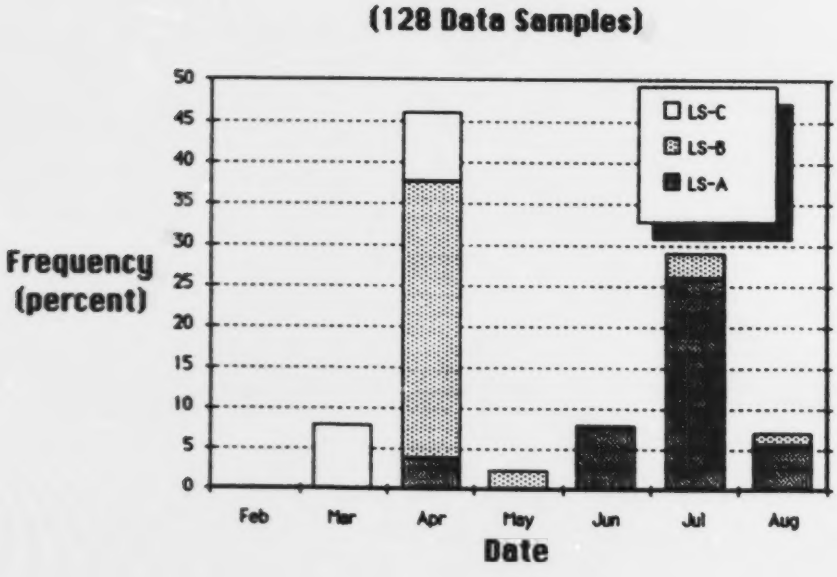

Figure 3.5 Distribution of Lancaster Sound Lead Statistics by Month

Scale 1:1,000,000

Figure 3.6 Overlay of Landsat Image, March 10, 1975 Showing Well Defined Lead Systems in the Beaufort Sea

Figure 3.7 Landsat Image of Same Area as Figure 3.6 Showing Compressed Pack Ice and Lead System Closure, on March 11, 1975

March 30, 1981, 1707 h

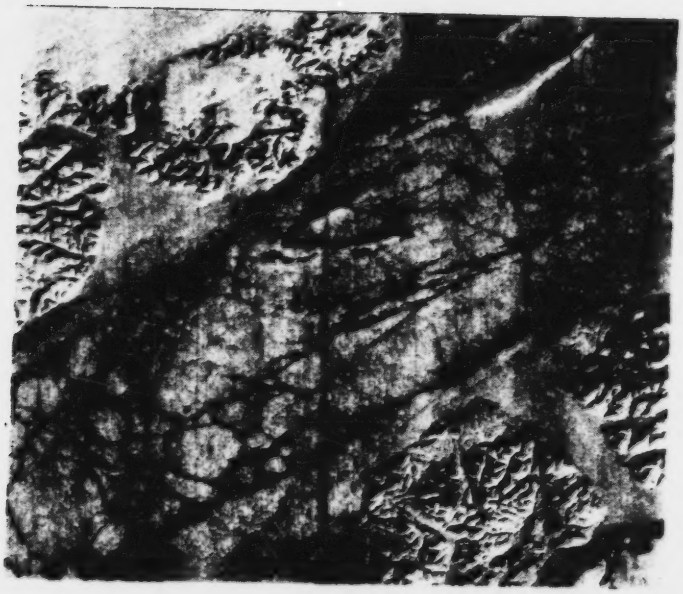

March 31, 1981, 1712 h

Figure 3.8 Comparison of Lead Appearance in Lancaster Sound Over 24 Hour Period

3.2.2 Lead Dimensions

Figures 3.9 and 3.10 show the frequency distribution of lead widths for the Beaufort Sea and Lancaster Sound. With similar sized data sets (127 and 128 measurements respectively) these graphs show almost identical distributions with over half the leads less than 500 m wide.

Regional variations are shown in a stacked bar graph format. In each case, the number of leads in a particular width category and region, is presented as a percent frequency of the total number of leads measured in all regions. In this way the sum of all bars in the graph = 100%. The regional distributions of lead widths are shown by the height of a particular shaded block. For example, Figure 3.10 shows that of all leads measured in Lancaster Sound (128), 25% were in Region A and had a width of 0 to 0.5 km, 18% (43-25) were in Region B and had a width of 0 to 0.5 km and so on. Fifty-two percent of all leads fell into the 0 to 0.5 km category. There are no significant regional differences in lead dimensions within Lancaster Sound.

Figure 3.9 presents lead width data in six Beaufort Sea regions (Figure 2.1). Only three of these areas have enough data to justify regional comparisons, BN, B, and A. Of these, Region BN, the area north of 71° stands out as having almost no leads greater than 500 m width. Amundsen Gulf (Region E) with only ten measurements shows an equal frequency of large and small leads.

In summary the lead width distributions appear to follow a negative exponential relationship within the range of values measureable off Landsat. It must be emphasized that for every lead large enough to appear on a satellite image (several hundred metres wide) there will be tens or hundreds of smaller leads and cracks which could also play a role in oil spill distribution in a dynamic ice cover.

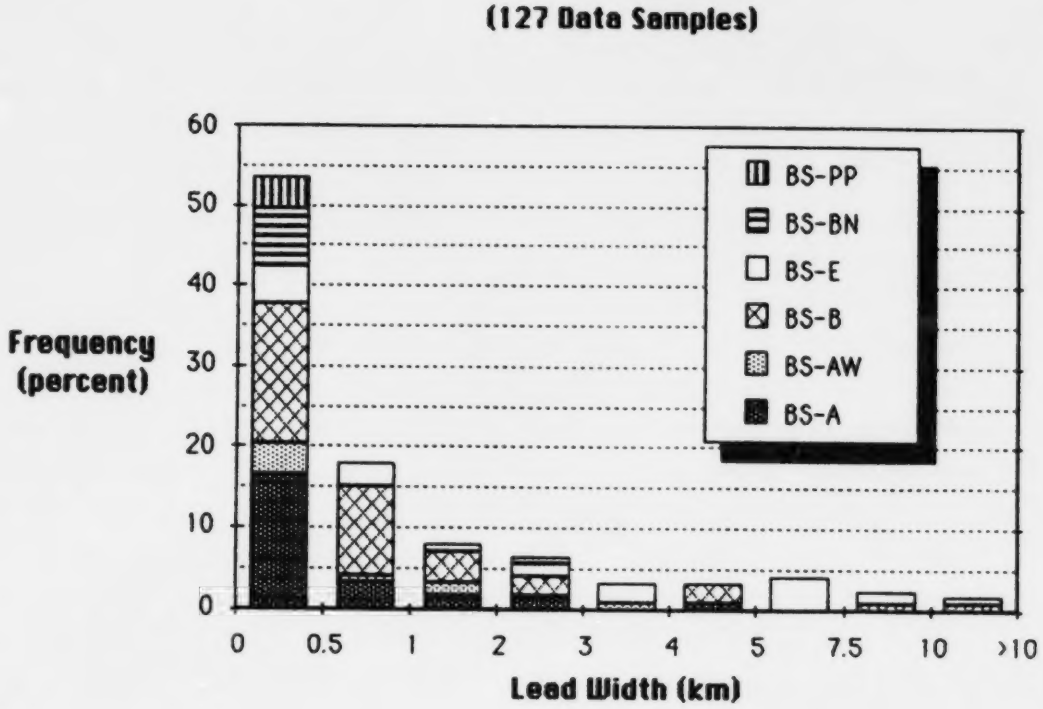

Figure 3.9 Distribution of Lead Widths - Beaufort Sea

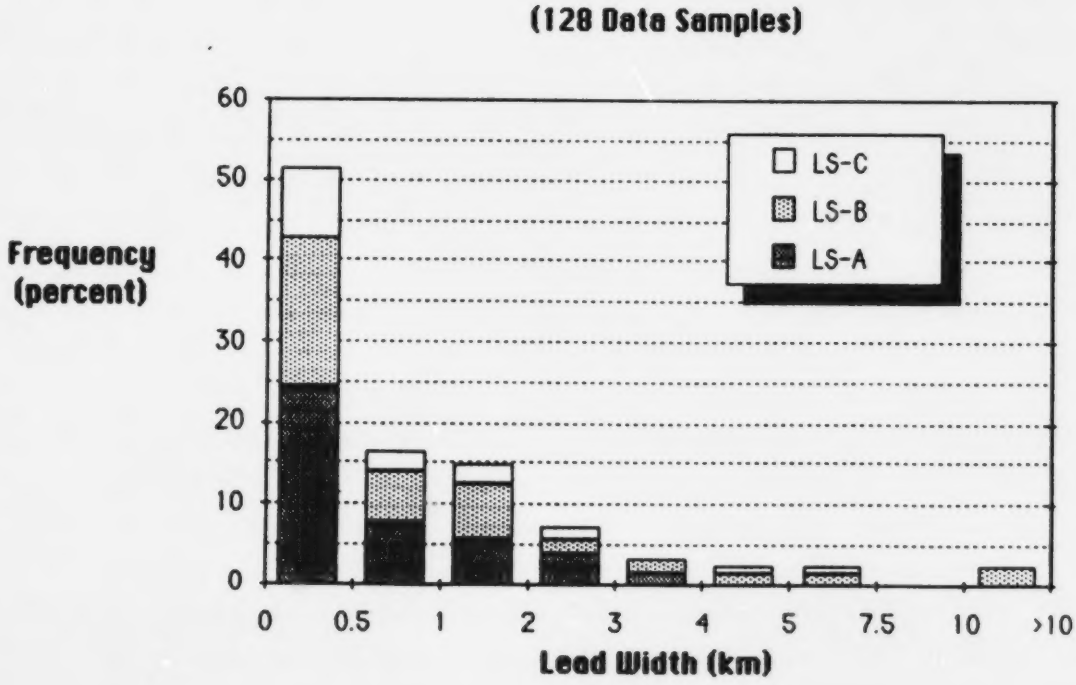

Figure 3.10 Distribution of Lead Widths - Lancaster Sound

Some indication of the potential numbers of small leads can be gained from analysis by Hall (1977) using April 1972 aerial photography over the polar pack in the vicinity of the AIDJEX camp in the Alaskan Beaufort Sea (Figure 3.11).

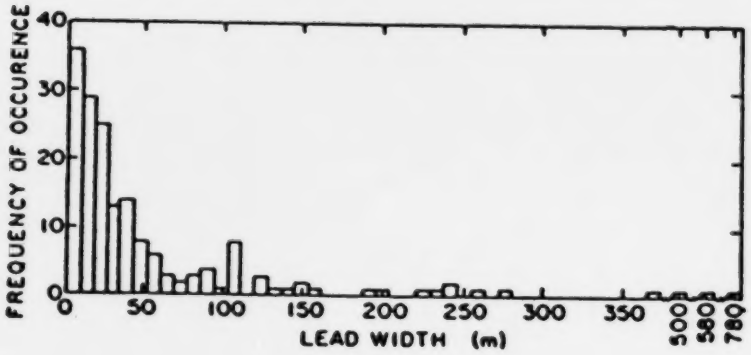

Figure 3.11 Lead Width Distributions in the Polar Pack, April 1972 (Hall, 1977)

The AIDJEX research showed that for leads less than 50 m wide, 70% were less than 50 m width and 40% less than 20 m in width. The 1972 aerial photography data looked at leads from zero to 800 m, while the Landsat analysis conducted in this study looked at leads from about 100 m to 10 km.

In the Beaufort Sea, 46% of all leads were between 100 m and 1 km. Hall's analysis showed 26 leads between 100 and 800 m, vs 137 between 0 and 100 m. On this basis, there could be 137/26, or about 5 times more leads in the ice than can be documented from Landsat imagery. Hall's data was collected over the polar pack.

Wadham's (1975) showed that in flying south from the polar pack into the seasonal pack ice south of 72°N, the total number of leads per kilometre increased from a mean of 0.18/ km to 0.72/km. Interestingly, the 50 percentile lead width of about 30 m identified in Hall's analysis agrees with the

Birdseye flights carried out by the U.S. Navy from the early 1950's to 1966. In the winter shear zone they reported about 0.4 leads/km < and >30 m (Wadhams, 1975).

From the available March Landsat imagery showing leads in the Beaufort Sea, a limited set of 25 observations was made of lead aerial density in #/hectare (Figure 3.12).

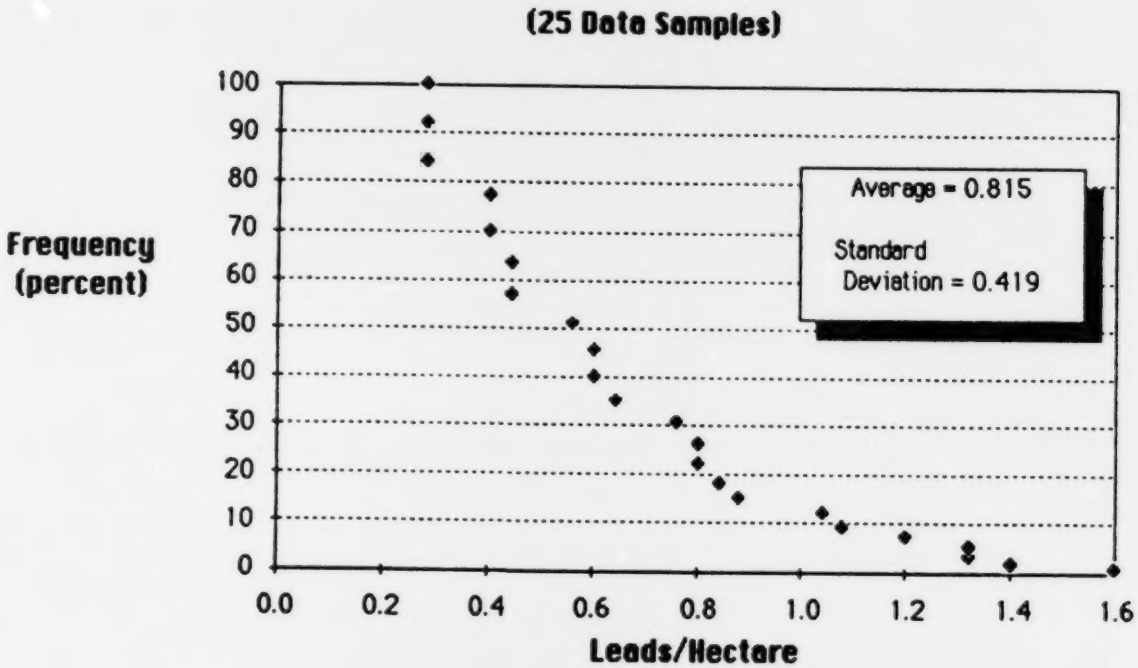

Figure 3.12 Cumulative Probability of Lead Density

3.2.3 Lead Orientation

The bearings of leads measured in the Beaufort Sea and Lancaster Sound are plotted in Figures 3.13 and 3.14. There are no strongly preferred lead orientations but trends agree with the overall directional motions of the pack ice relative to the local shorelines and fast ice boundaries. In the Beaufort Sea, leads tend to parallel the shore. Region B off the Tuktoyaktuk Peninsula shows a bias towards NE/SW leads while Region A off Mackenzie Bay favours an E/W orientation.

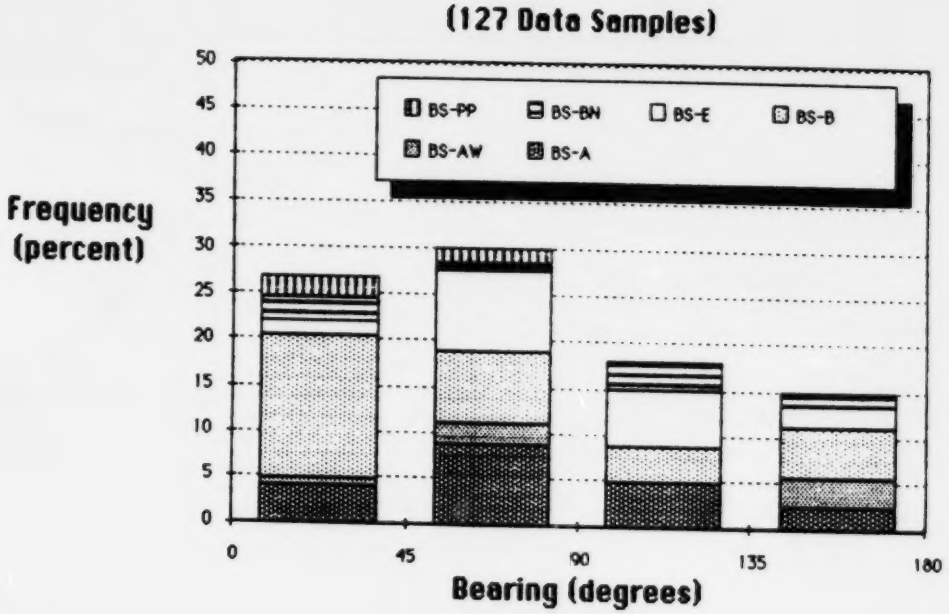

Figure 3.13 Beaufort Sea Lead Orientation

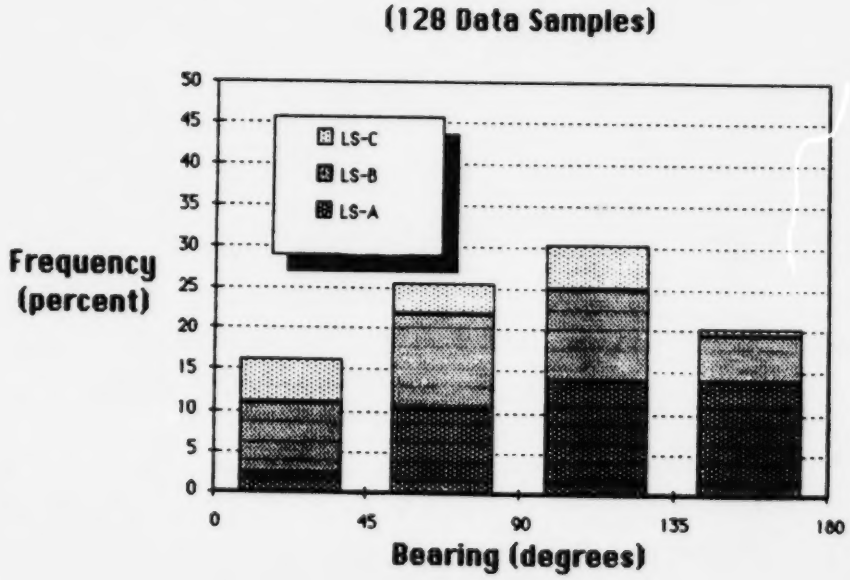

Figure 3.14 Lancaster Sound Lead Orientation

In Lancaster Sound, there is a slight trend to NW/SE oriented leads in the most westerly Region A. The other two regions lack any preferred lead orientations, but tend more to an E/W alignment paralleling the coastlines. Intuitively, as the ice is funnelled away from the stable ice edge, leads would be expected for change from a cross channel to a long channel orientation (see example Landsat image shown in Figure 3.8).

3.2.4 Lead Opening and Closing Rates

The distribution of lead opening and closing rates is probably of most interest in terms of modelling lead pumping mechanisms. Figures 3.15 and 3.16 show percent frequency of occurrence of measured rates of change in lead width. Positive rates signify opening and negative rates indicate closing. Both Lancaster Sound and the Beaufort Sea appear as expanding ice environments, that is, openings are favoured over closing by a ratio of 5:1. Peak movement rates encountered during opening events tend to be two to five times higher than rates measured during closings. Lancaster Sound experiences lead opening rates as high as 17 km/day, compared to a peak value of less than 10 km/day measured in the Beaufort Sea. The percent occurrence of closure events is similar for the two regions, but closure rates tend to be higher and more evenly distributed in the Beaufort Sea.

Regional differences in lead dynamics within the study areas are not clear. Few lead closures were observed in Lancaster Sound Region C, which is to be expected in an area where the sound is opening out into Baffin Bay.

The Beaufort Sea seems to be divided into expanding and contracting regions. Amundsen Gulf (E), and the offshore Mackenzie Bay (A) regions showed only opening leads. Limited data for the polar pack (PP) showed only closing leads. Amundsen Gulf is a known area of ice arching between

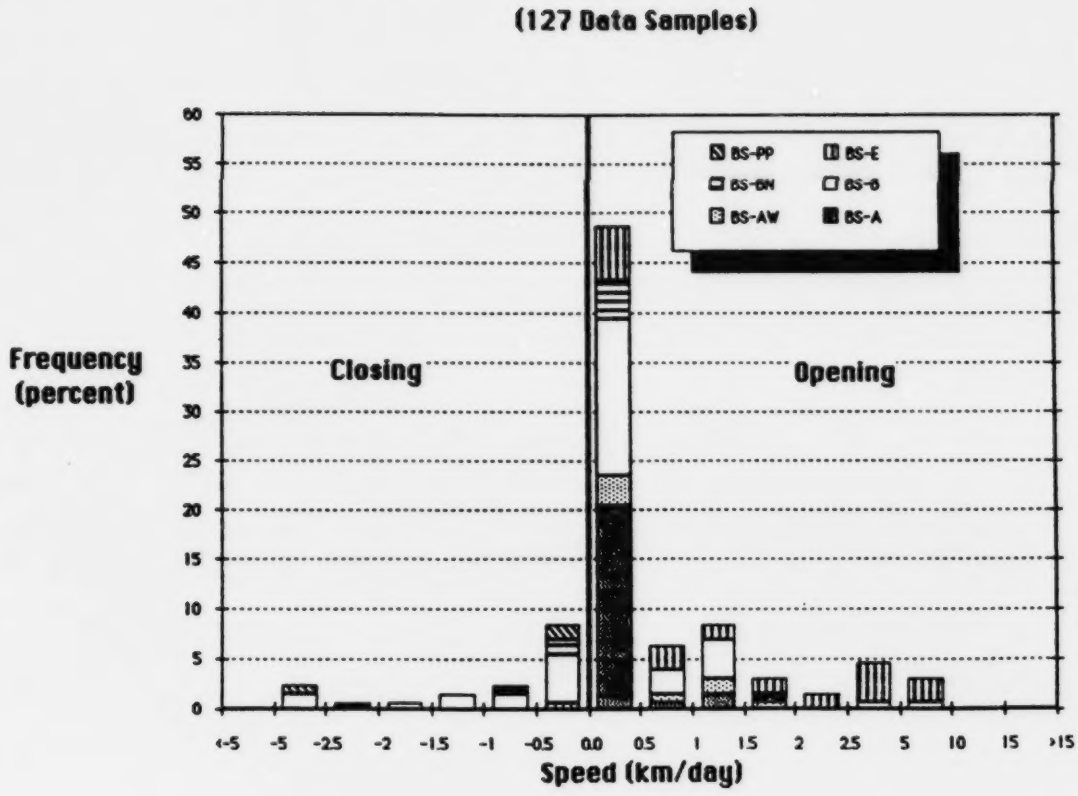

Figure 3.15 Lead Opening and Closing Rates - Beaufort Sea

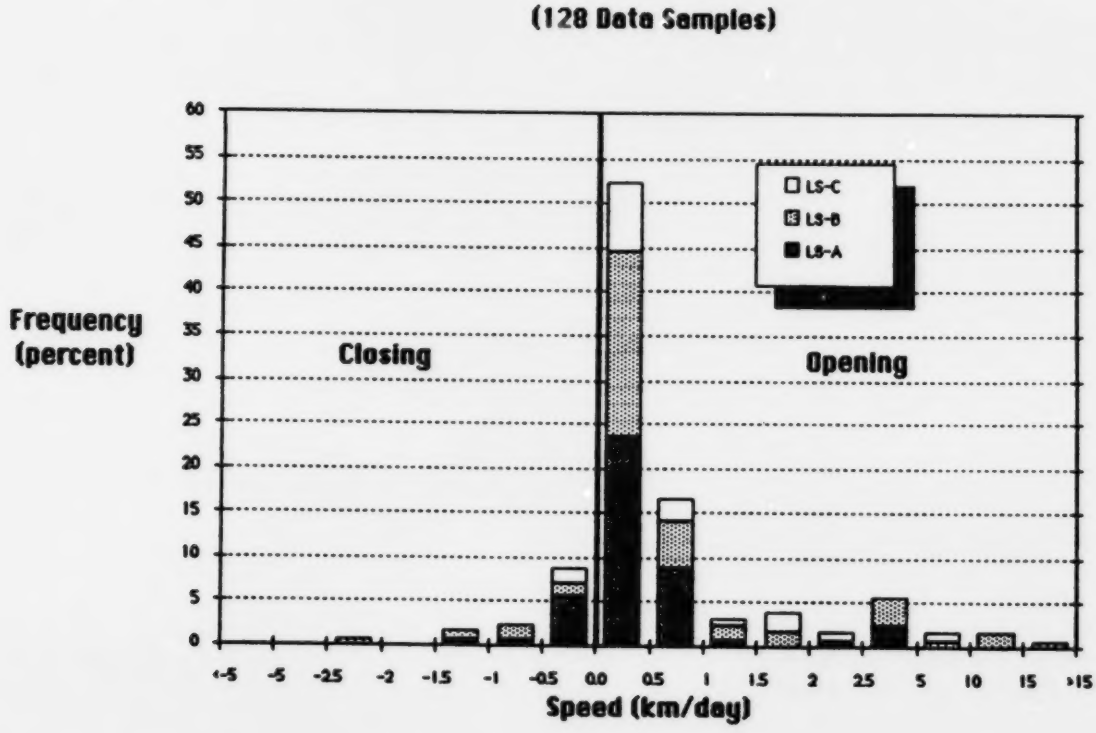

Figure 3.16 Lead Opening and Closing Rates - Lancaster Sound

Banks Island and the Parry Peninsula. Ice drifts to the west away from this arch for much of the winter.

Region A offshore of Mackenzie Bay showed a strong trend to very slow movement rates, opening at between 0 and 0.5 km/day. This region tends to mark the point where the seasonal pack ice begins to be squeezed between the northerly trending Yukon/Alaskan coast, and the polar pack in its winter journey westward into Soviet waters.

Figures 3.15 and 3.16 clearly show that over 50% of lead motions occur at rates less than 0.5 km/day. Caution should be exercised in drawing conclusions about instantaneous lead motions, from 24 hour displacements shown here. There are known to be significant differences between short and long term ice floe drift rates in low ice concentrations. Leads would tend to contract and expand in a more uniform manner, as the surrounding pack ice acts to damp rapid transient motions. As a first approximation, the average rates of lead openings and closings are less than 20 m/hour.

A unique data set on potential short term lead closure rates is contained in personal observations of ice track closure behind icebreakers. Table 3.3 summarizes findings provided by J.D. Bradford, Chief Intergovernmental Ocean Science Affairs Division, Fisheries and Oceans.

Table 3.3 Icebreaker Track Closure Observations
(Source: Bradford, Personal Communication)

Location	Date	Ice Thickness	Closure Rate
		cm	m min^{-1}
Barrow Strait	Oct/73	28	30
Baffin Bay	Apr/70	121	0.8
N.W. Baffin	May/70	38	4.6
Lancaster Sound	May/70	46	15.2
Lancaster Sound	May/70	152	6.1
Grand Banks	Mar/71	23	2.1
Lancaster Sound - Maximum for this study			1.73

3.3 Floes

Leads are the dominant pack ice characteristic affecting oil distribution in the Beaufort Sea and Lancaster Sound. Thick first year floes in these areas are only present for 4 to 6 weeks during break-up offshore. Ice concentrations quickly reduce to the point where there are only scattered floes, which will have limited impact on oil spill behaviour.

The Labrador Sea is a very different ice environment in that the pack is a mixture of older first year floes from Baffin Bay and Davis Strait, and younger ice forming in-situ between the floes. The Beaufort Sea and Lancaster Sound are areas of ice efflux, while the Labrador Sea is an area of significant ice influx. Floes are the dominant feature in the Labrador Sea. Leads only occur temporarily when large floes divide.

Figure 3.8 showed a mixture of thicker ice floes and leads in young ice in Lancaster Sound on March 30/31, 1981. Figure 3.17 shows an example of floes moving away from the stable ice edge in Lancaster Sound on April 25, 1977. The larger floe "C" is actually a conglomerate of thicker first year floes within a grey-white ice matrix. New ice is forming at the ice edge and gradually thickening as it moves east.

Figure 3.18 shows a pair of images north of Kugmalit Bay in the Beaufort Sea, separated by 24 hours (June 28 to June 29, 1980). Break-up is well advanced, and large floes tens of kilometres across are breaking off the remaining landfast ice in the lower right. Offshore the pack ice is being compressed from a concentration of about 7/10 on June 28 to over 8/10 on June 29. The dynamics of pack ice in conditions such as shown here would play a major part in controlling the physical process of oil spreading, weathering and dispersion into the water column.

Labrador Sea pack ice can take on an infinite number of extremely complex formations, from large areas of grey to grey-white ice less than 1 foot thick, to conglomerates of thicker first year floes. This mixture of young ice sheets and older floes is in a constant state of flux. Figures 3.19 and 3.20 show examples of the appearance of changing Labrador Sea pack ice conditions between February and April 1979.

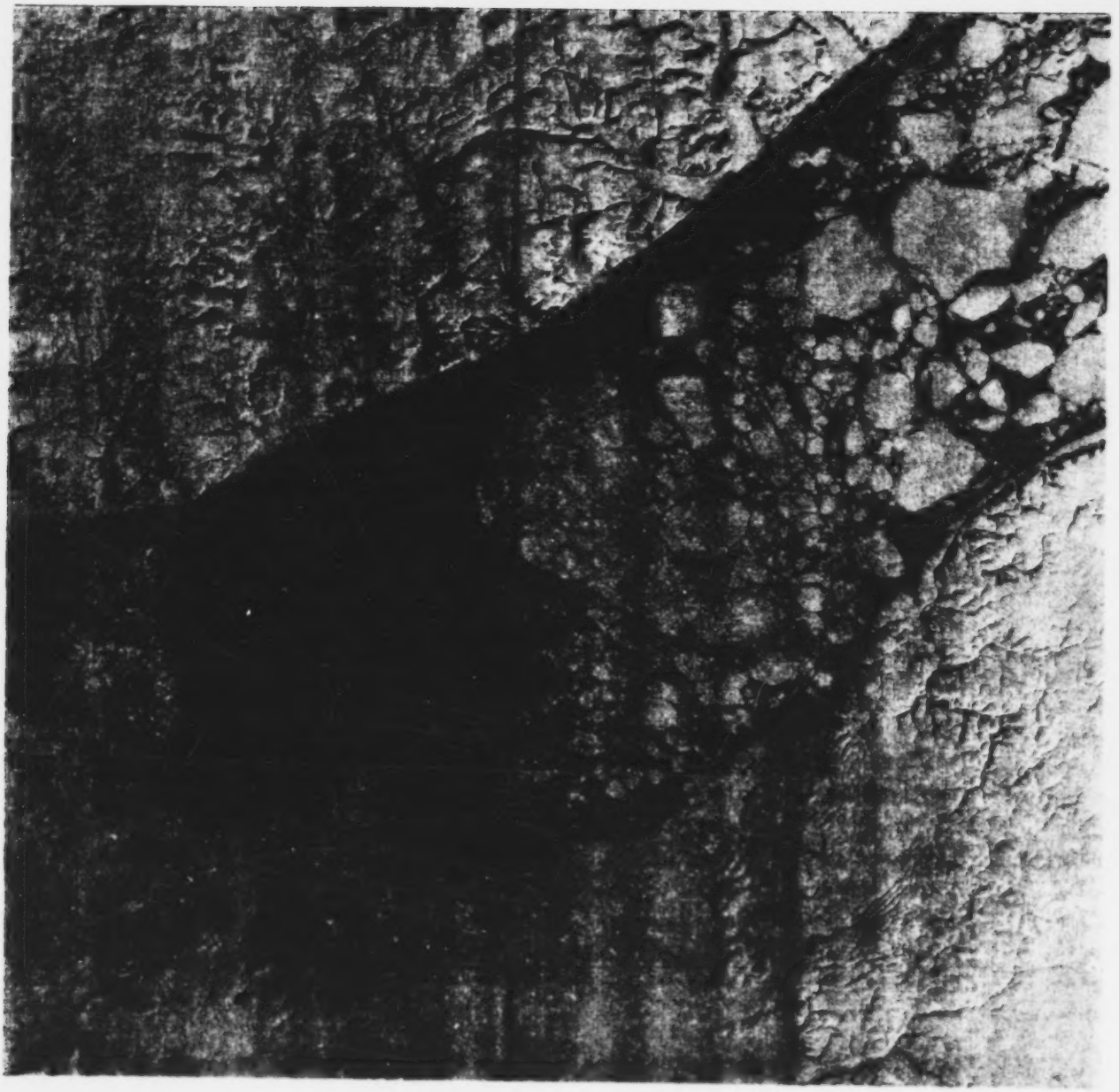

Figure 3.17 Lancaster Sound Landsat Image, April 25, 1977 Scale 1:1,000,000

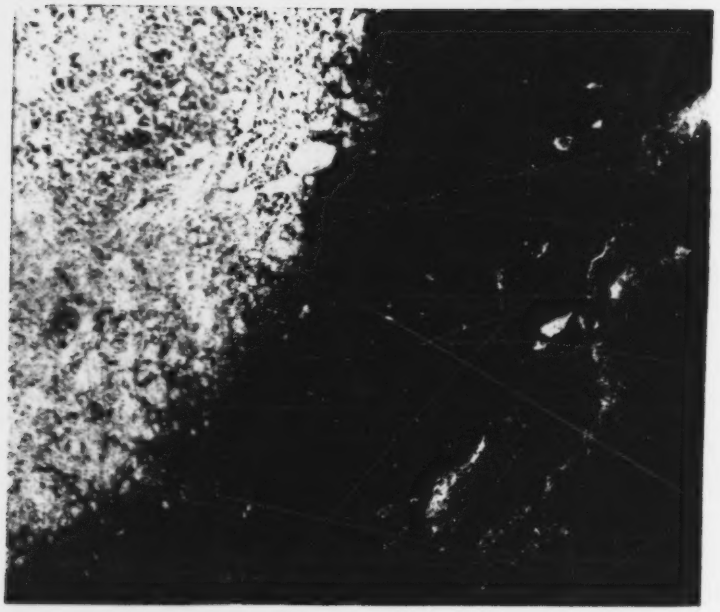

June 28, 1980

June 29, 1980

Figure 3.18 Landsat Images Showing 24 Hour Changes in Pack Ice Concentration in the Beaufort Sea North of Kugmallit Bay

Scale 1:1,000,000

Figure 3.18 Landsat Image Showing Labrador Sea Pack Ice, February 22, 1979

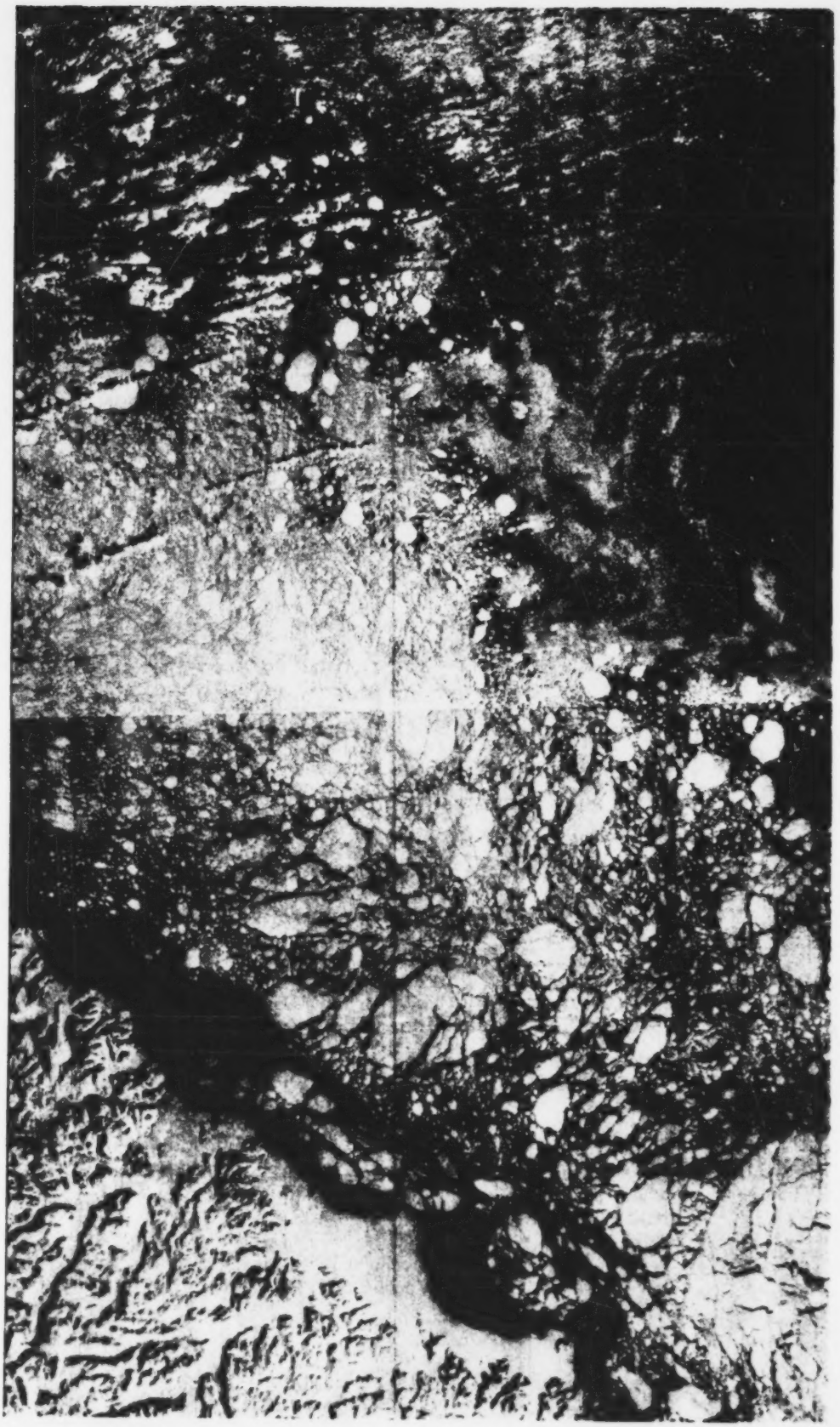

Scale 1:1,000,000

Figure 3.20 Labrador Sea Pack Ice Conditions, April 1, 1979

3.3.1 Distribution of Data

Figures 3.21 to 3.23 show the distribution of floe data collected in the three geographic areas according to month, ice concentration, and floe area. Floes were clearly identifiable for a longer period in Lancaster Sound than the Beaufort Sea (April to August vs June to July). Floes examined in Lancaster Sound after June probably resulted from break-up in surrounding waterways leading into Parry Channel. A small number of floes (10% of the total number) were tracked in the Amundsen Gulf region of the Beaufort Sea in March and May. The data set of floes off the Labrador Coast concentrated on the month of April with smaller subsets in February, March, May and June (all less than 20% of the total).

In terms of grouping the floe data by ice concentration, most information was collected in the 7/10 to 8/10 range, where floes are largely in contact. This is the concentration range considered most important in terms of oil/ice interaction. The Lancaster Sound data set contains the most uniform distribution of measurements over a wide range of ice concentrations. In all, 702 floes were tracked during the study, 215 in the Beaufort Sea, 382 in Lancaster Sound, and 105 in the Labrador Sea.

The smallest observable floe which could be followed between consecutive statellite images was about 1 km^2. Figure 3.23 shows that the Labrador Sea and Beaufort Sea data sets represent much smaller floes than in Lancaster Sound, where floe areas of 150 to 200 km^2 were frequently encountered.

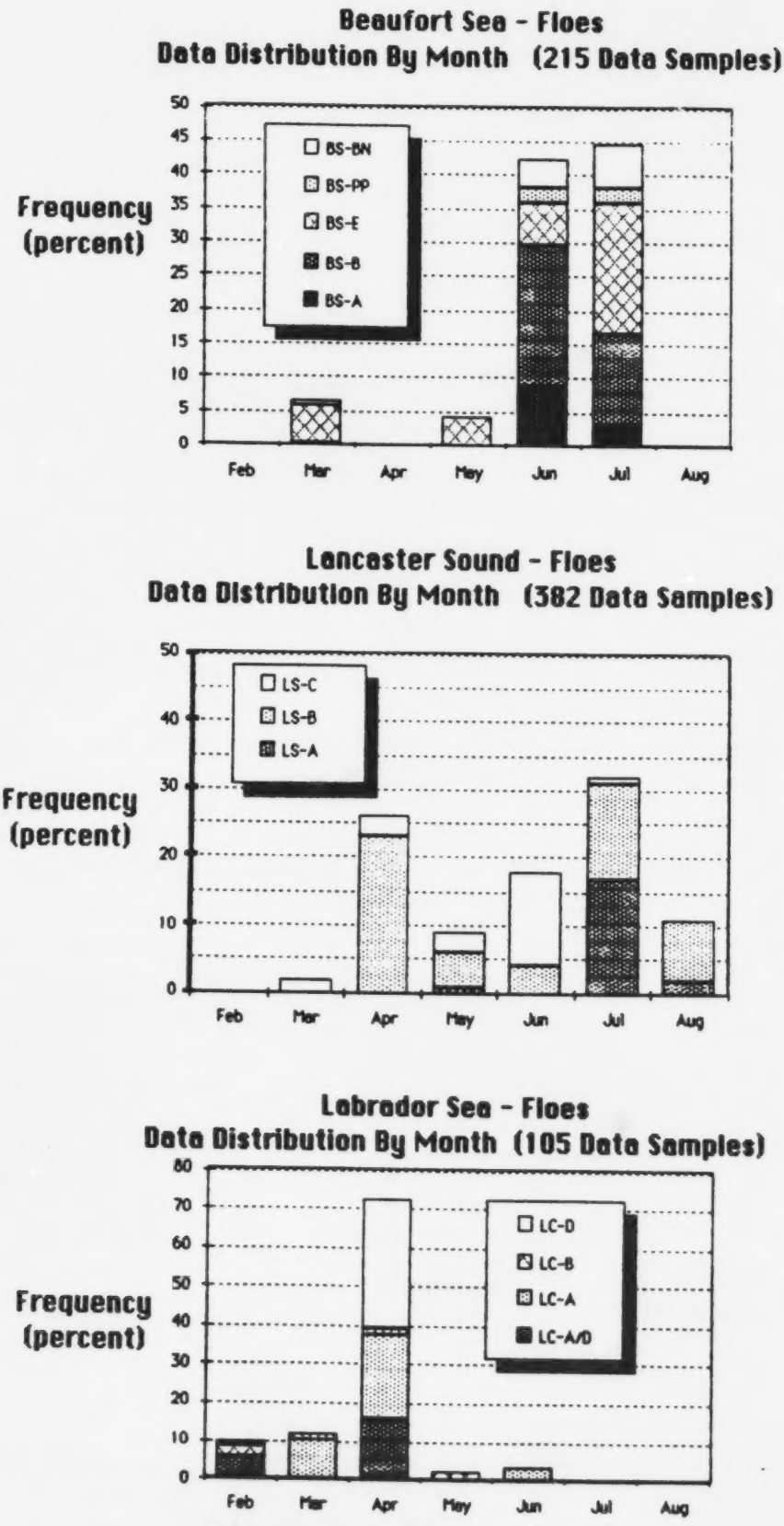

Figure 3.21 Floe Data Distribution According to Month

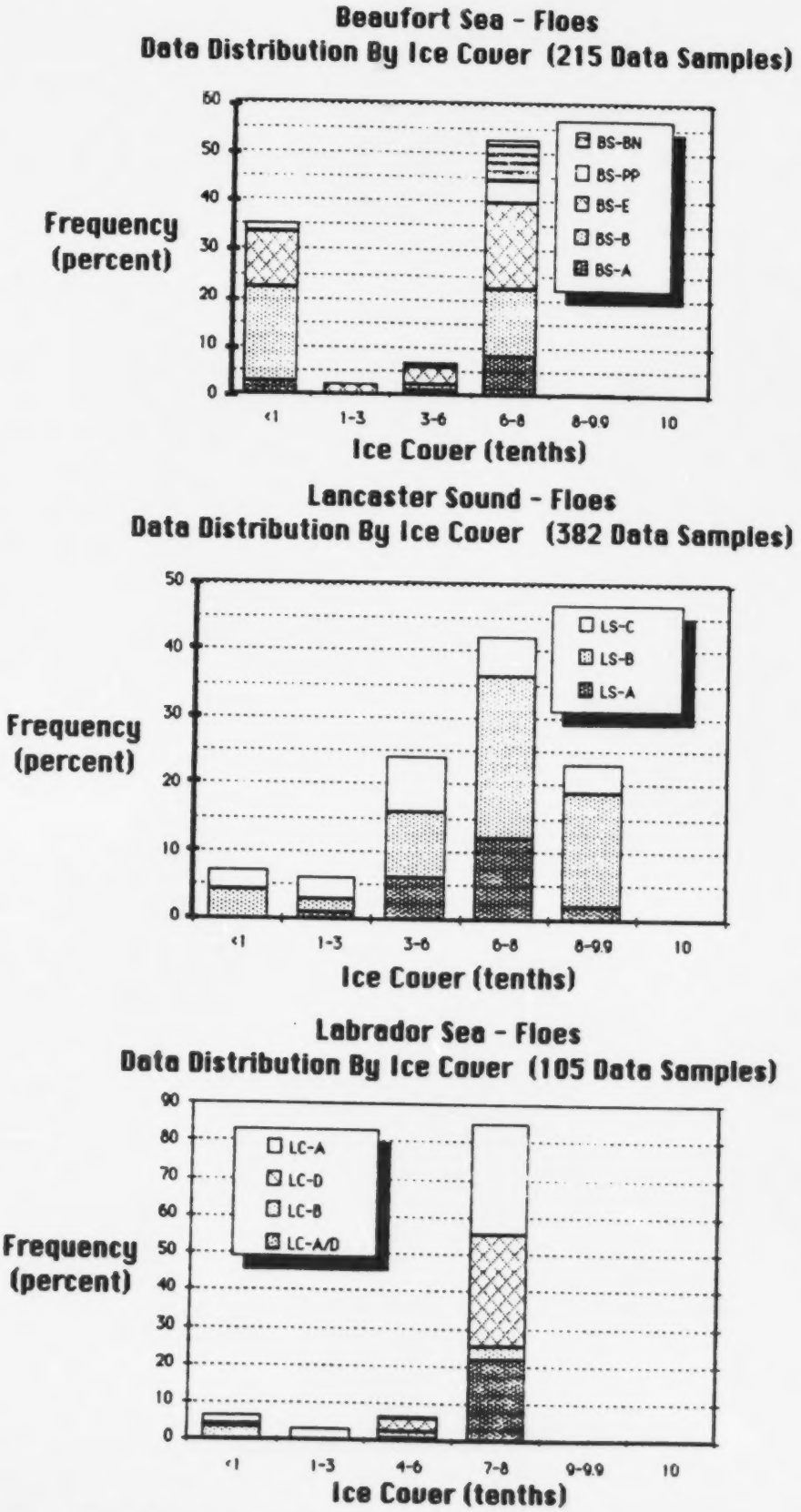

Figure 3.22 Floe Data Distribution According to Ice Concentration

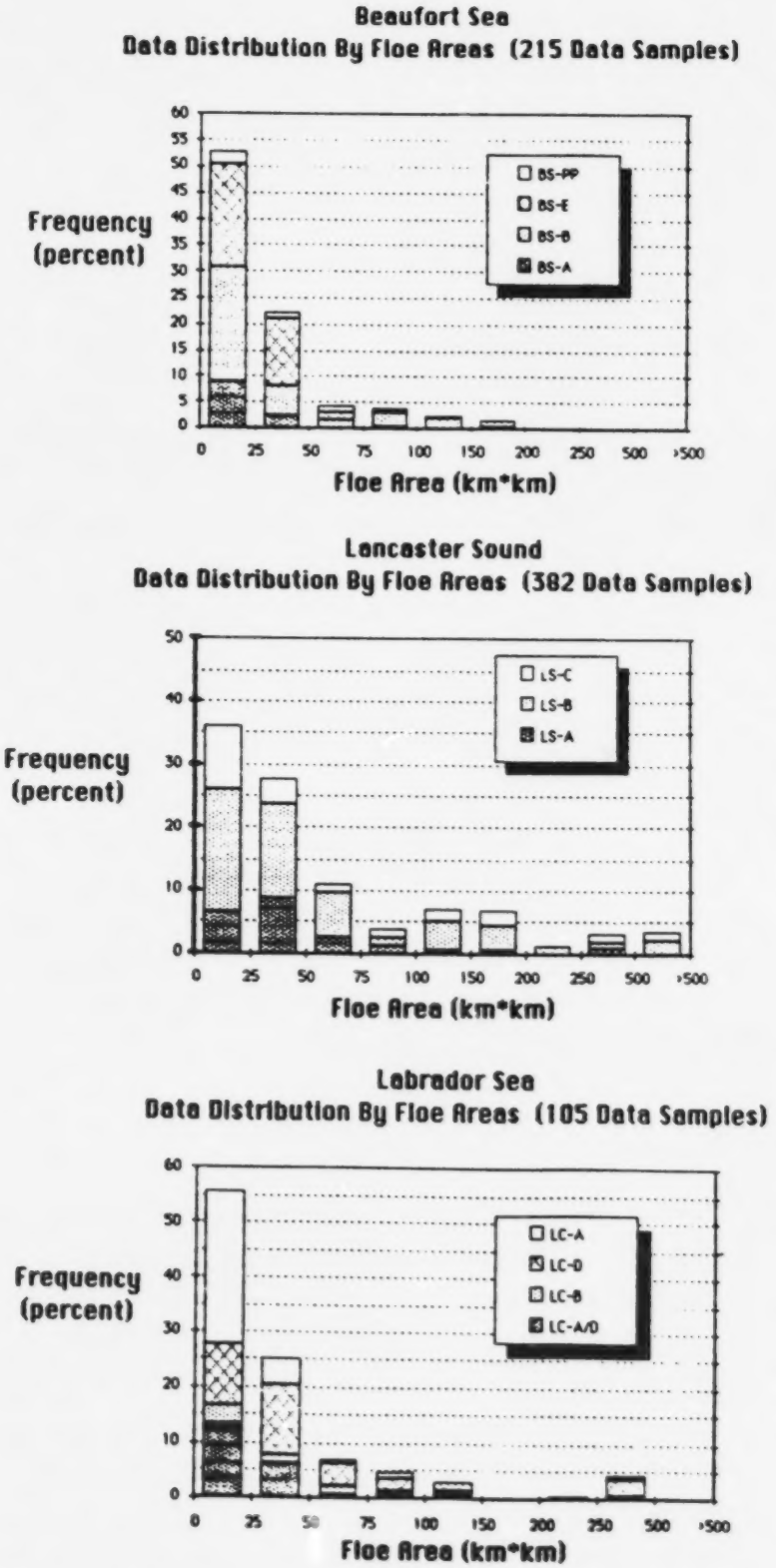

Figure 3.23 Floe Data Distribution According to Floe Area

3.3.2 Floe Velocities

Floe velocity analysis is presented in five groups of graphs listed as follows:

1. Frequency Distribution of Floe Speed
   - All Months
   - Monthly (Appendix C)

2. Frequency Distribution of Direction of Floe Movements

3. Relationship Between Average Ice Floe Speed and Ice Concentration
   - All Months, Beaufort Sea and Lancaster Sound

4. Relationship Between Average Ice Floe Speed and Floe Area
   - All Months, Lancaster Sound only

5. Comparisons with Other Data Sources
   - Beaufort Sea and Lancaster Sound

The graphs are intended to be self-explanatory. The text will serve to highlight significant trends and/or limitations of the data.

1. Floe Speed (Figures 3.24 to 3.26)

   These graphs show a distinct trend to higher floe speeds proceeding from the Beaufort Sea, to Lancaster Sound, to the Labrador Sea.

   In the Beaufort area fewer than 30% of the floes measured moved at speeds greater than 10 km/d, compared to about 45% in Lancaster Sound and 75% off Labrador. The upper decile velocities ranged from about 20 km/day in the two arctic areas to 30 km/day in the Labrador Sea.

The most rapid floe movements were observed in Amundsen Gulf (Region E) in the Beaufort Sea, at the entrance to Lancaster Sound (Region C) and off Hudson Strait (Region D). Monthly distributions of ice speed are contained in Appendix C.

2. Direction of Floe Movements (Figures 3.27 to 3.29)

Floe motions show a stronger trend to preferred directions in the two arctic areas than did lead orientations (Figures 3.13 and 3.14).

In the Beaufort Sea floe movements tend to be towards the west in agreement with previous buoy drift data. In Lancaster Sound, floes move predominantly from west to east into Baffin Bay. Labrador Sea floe movements are highly variable in direction but tend in a southerly direction, or perpendicular to the coastline. Almost no northerly movements were recorded.

3. Ice Floe Speed vs Concentration

It appears to be a reasonable hypothesis that floe motions should decrease as pack ice concentration increases. Almost certainly this would be the case with instantaneous motions. Surrounding floes would tend to oppose very rapid short term movements. Unfortunately, hourly or finer time scale measurements are not publicly available. The Landsat analysis in this study uses floe displacements over a 24 hour period. Figures 3.30 and 3.31 indicate that this period is too long to detect a statistically significant variation in floe speed with ice concentration. In spite of the limitations of the available data both graphs show a trend to larger fluctuations in speed at lower ice concentrations as well as a reduction of approximately 30% in average speed between 1/10 and 8/10 ice cover.

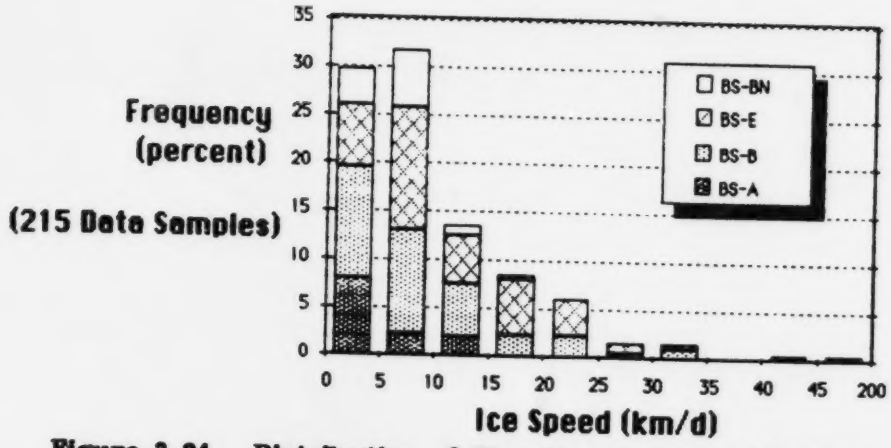

Figure 3.24 Distribution of Floe Speeds - Beaufort Sea

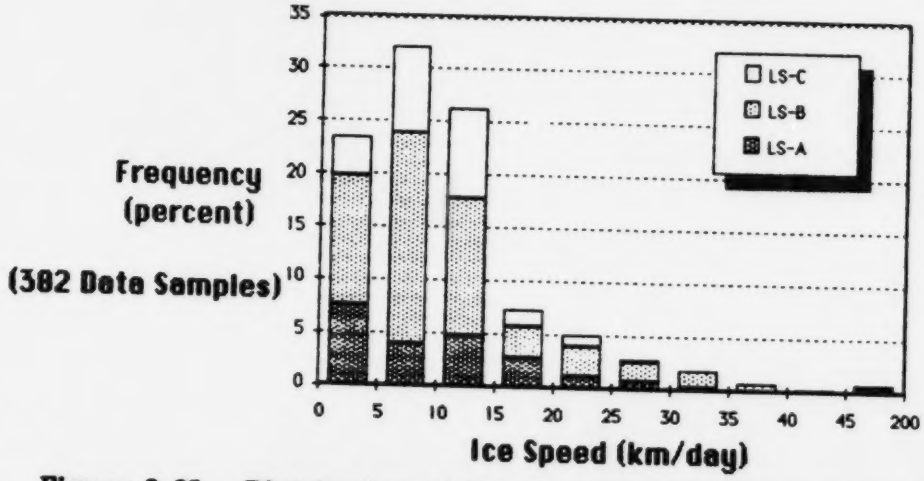

Figure 3.25 Distribution of Floe Speeds - Lancaster Sound

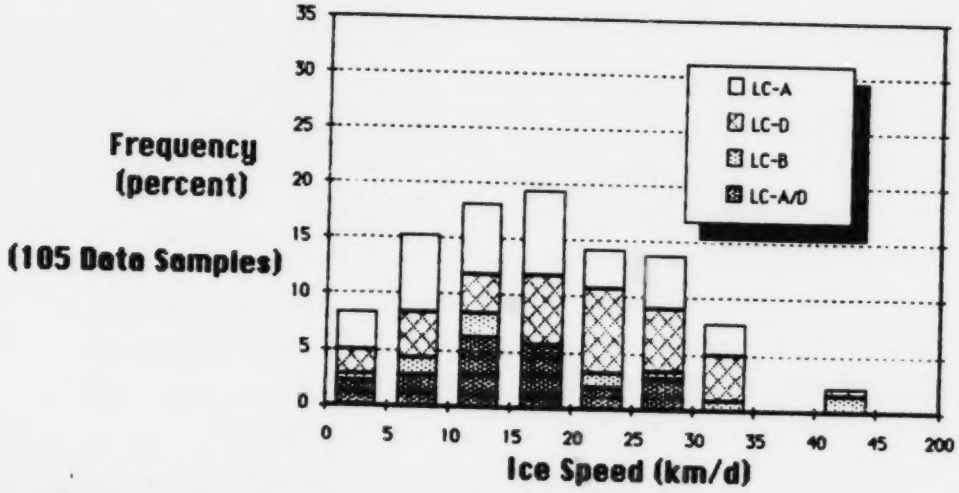

Figure 3.26 Distribution of Floe Speeds - Labrador Sea

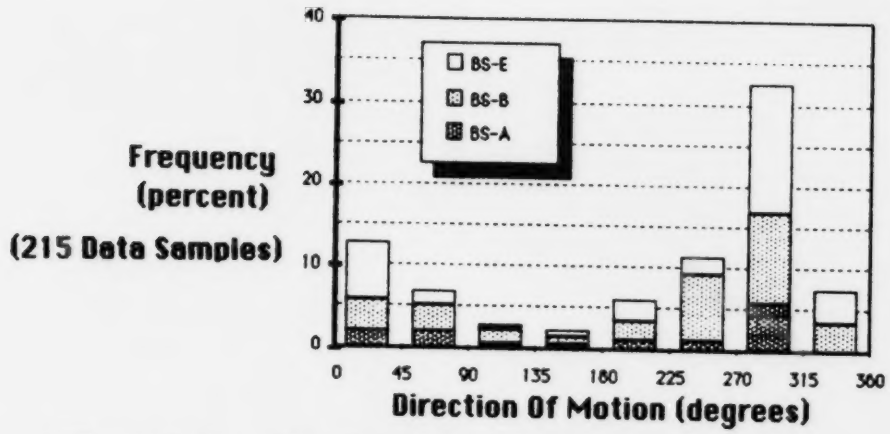

Figure 3.27 Direction of Floe Motion - Beaufort Sea

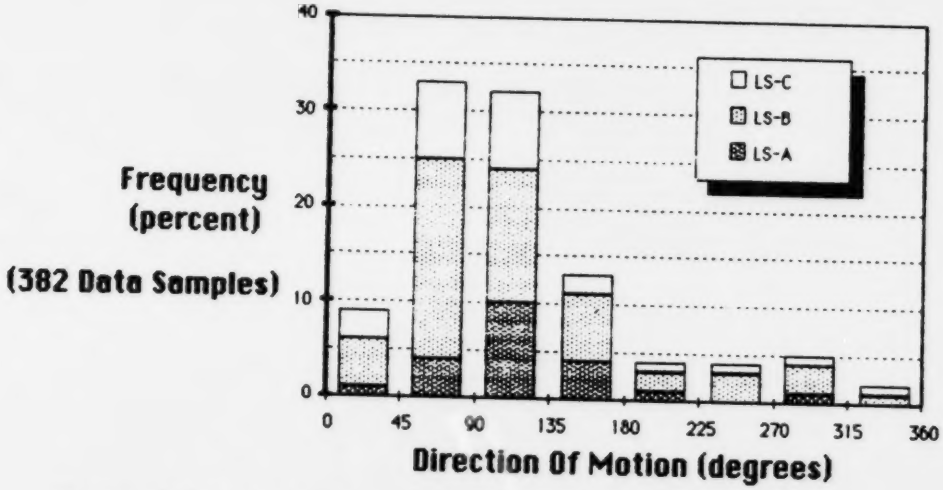

Figure 3.28 Direction of Floe Motion - Lancaster Sound

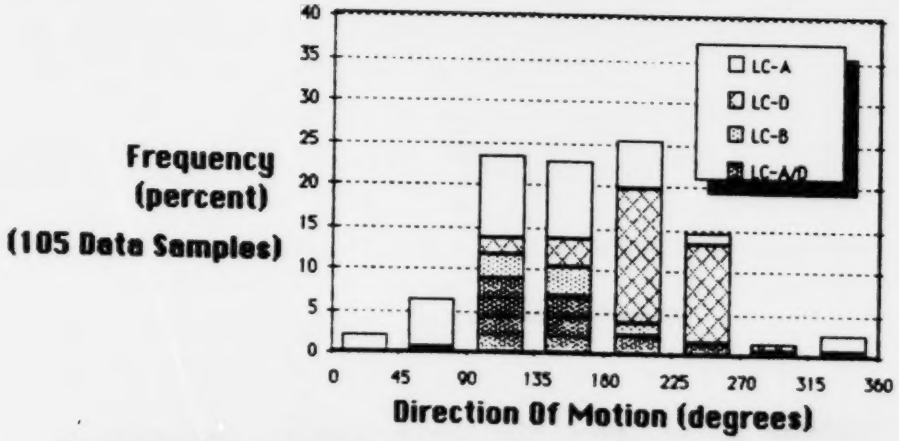

Figure 3.29 Direction of Floe Motion - Labrador Sea

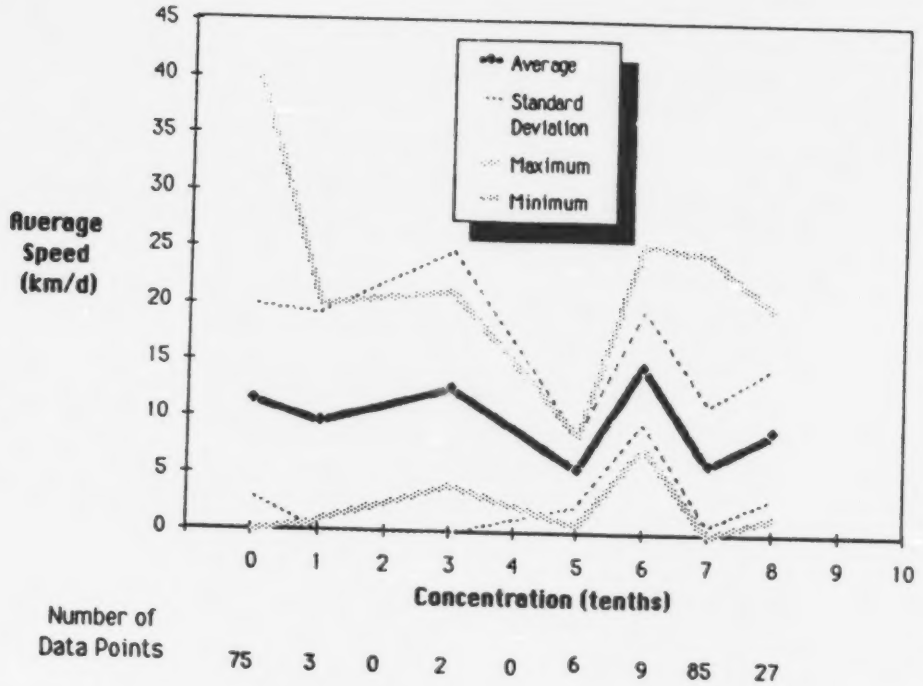

Figure 3.30 **Variation in Ice Speed with Concentration - Beaufort Sea**

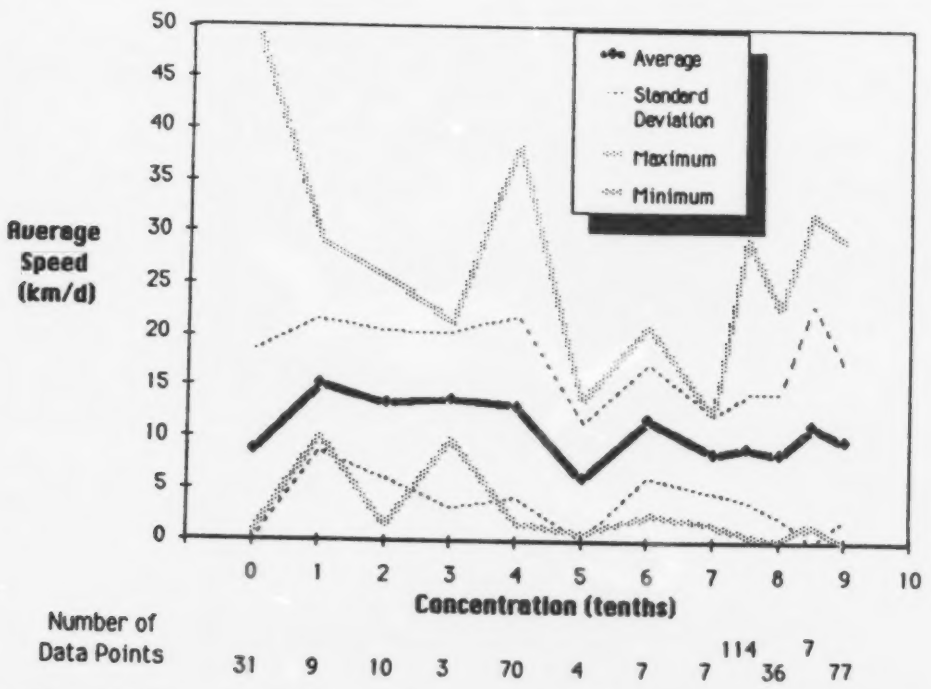

Figure 3.31 **Variation in Ice Speed with Concentration - Lancaster Sound**

4. Variation in Floe Speed with Floe Size

Floe movements are principally controlled by wind and current stress acting across a floe area. The balance between hydrodynamic resistance and environmental driving forces will not necessarily be achieved at the same speed for all floe sizes. To explore this possibility, Figure 3.32 was prepared showing the relationship between ice speed and floe area for the Lancaster Sound which had the most evenly distributed data set with regard to floe size (Figure 3.23).

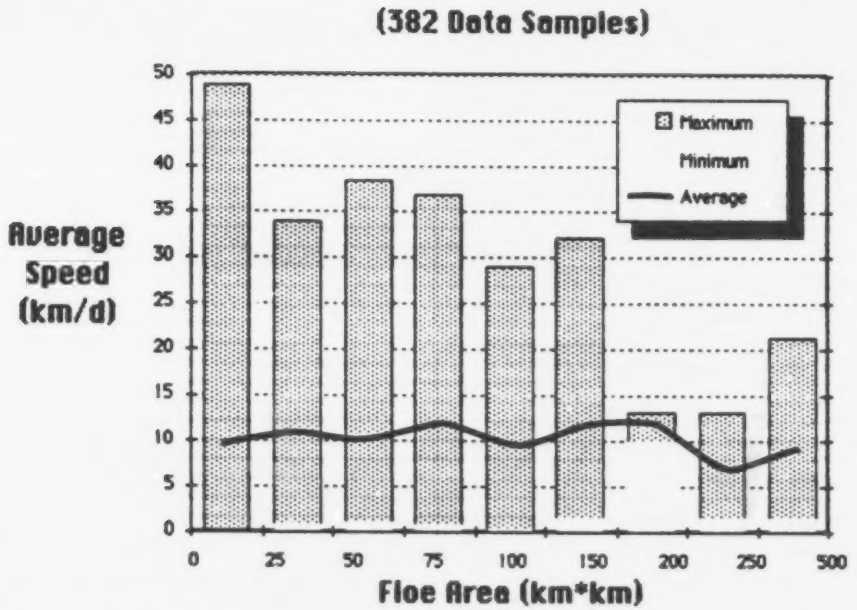

Figure 3.32 Variation in Ice Speed with Floe Area - Lancaster Sound

There is a large range in average values for the different regions, but there appears to be no apparent relationship between a floe's size and its speed of motion.

5. Comparison with Other Data Sources

Figure 3.33 compares the cumulative probability distribution of floe speeds derived for the Beaufort Sea in this study, with previous work by Schwab using a similar analysis technique. Results compare favourably within five percent over most of the speed range. It should be noted that Schwab's data is available from Gulf Canada Resources Inc. on a restricted release basis.

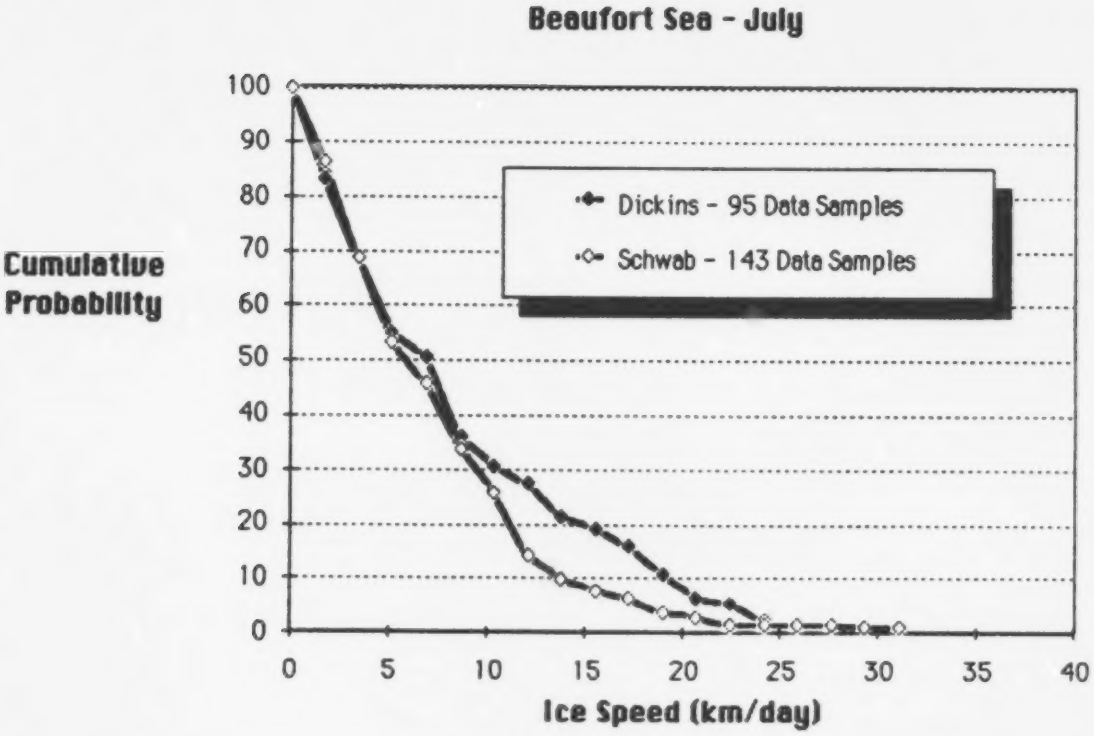

Figure 3.33 Cumulative Probability of Ice Speed Comparison with Schwab (1978)

Figures 3.34 and 3.35 compare monthly average floe speeds reported by different authors for the Beaufort Sea and Lancaster Sound. In Figure 3.34 it should be noted that the curve plotted for McGonigal and Wright was derived from satellite buoy data, which tended to give lower ice

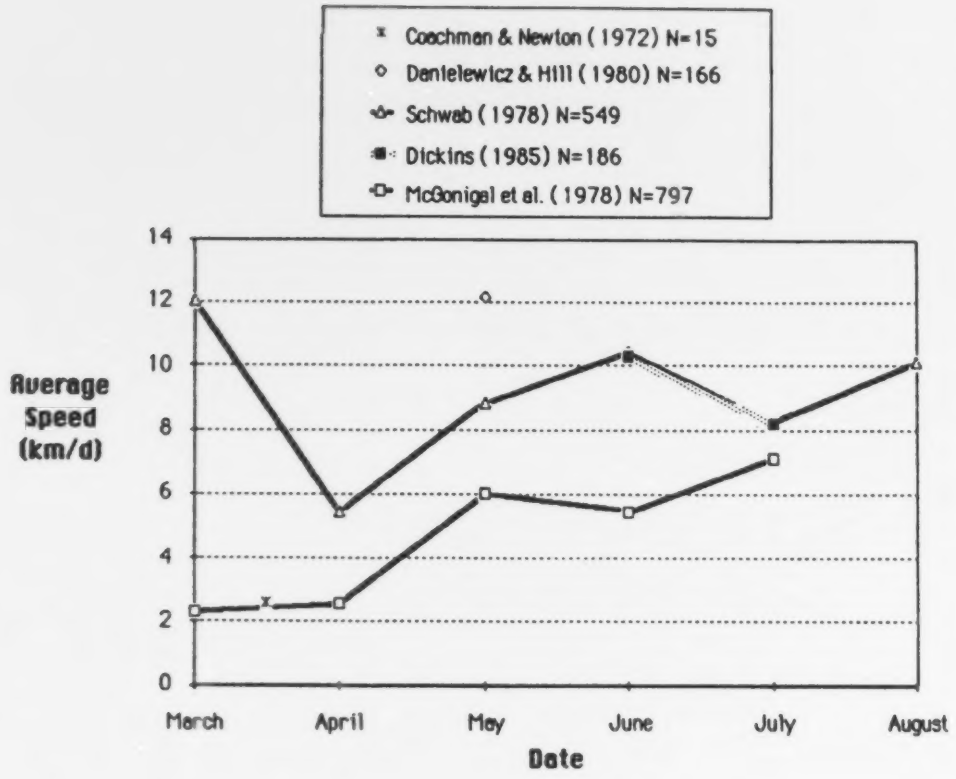

Figure 3.34 Comparison of Reported Floe Speeds for the Beaufort Sea

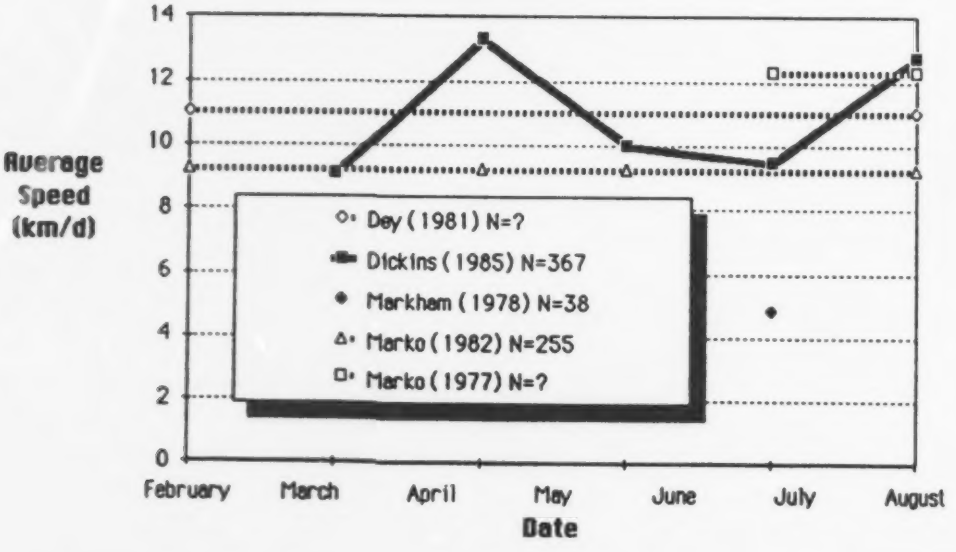

Figure 3.35 Comparison of Reported Floe Speeds for Lancaster Sound

speeds than free floes observed by Schwab using Landsat. Data derived in this study for the months of June and July agree almost exactly with Schwab's analysis.

The data from this study effectively doubles the previous Lancaster Sound ice speed data base. Results agree favourably with previously estimated values (Figure 3.35).

3.3.3 Ice Floe Size

Three floe size distributions were developed through the course of this study, one using 1:500,000 SLAR imagery in the Beaufort Sea for May (Figure 3.36), one using 1:20,000 aerial photography in the Labrador Sea in March, and one using a very small scale 1:2,600 aerial photo mosaic in the Labrador Sea on the same date. Figure 3.36 shows that half of the visible floes were less than about 2 km^2.

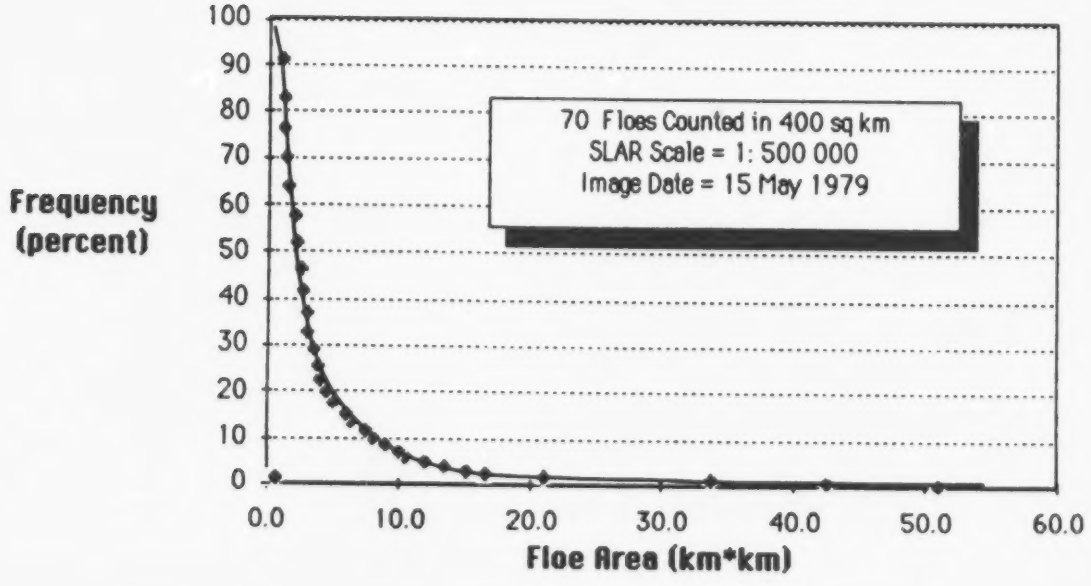

Figure 3.36 Beaufort Sea Floe Size Distribution from SLAR

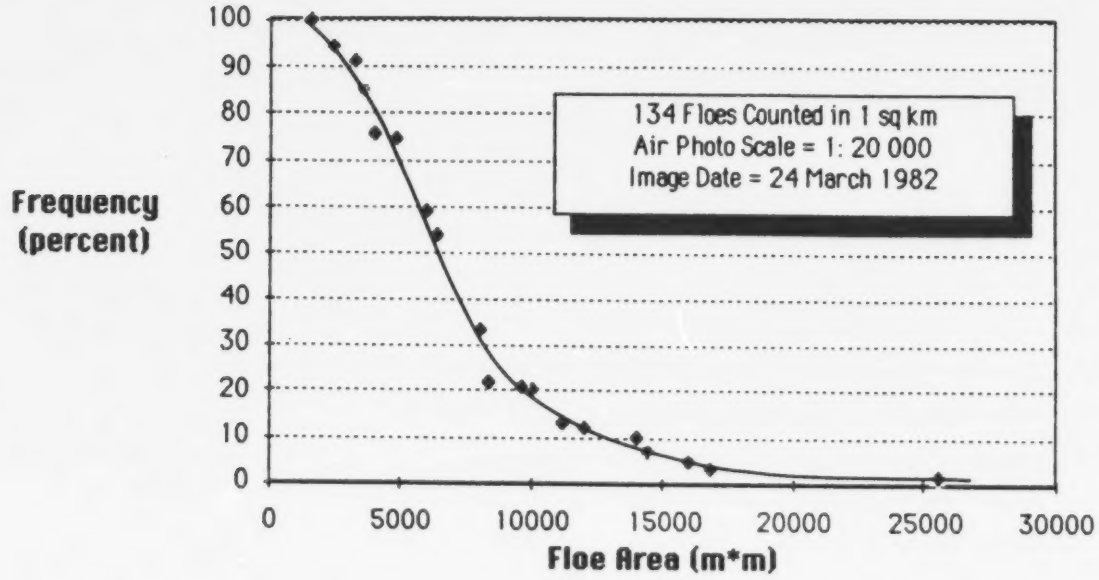

Figure 3.37 **Labrador Sea Floe Size Distribution from 1:20,000 Scale Photography**

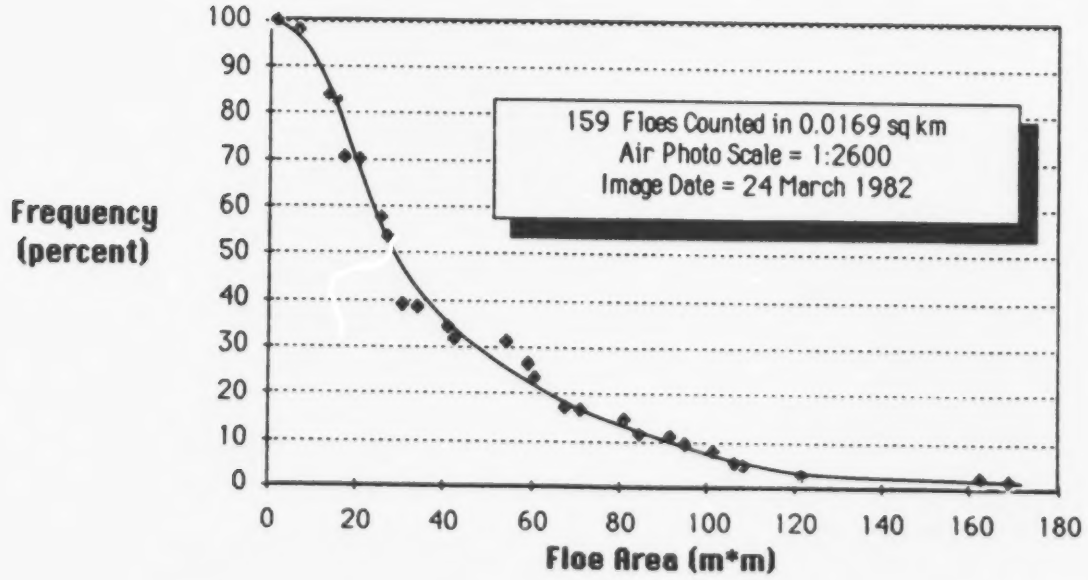

Figure 3.38 **Labrador Sea Floe Size Distribution from 1:2,600 Scale Photography**

Floe size distributions are highly dependent on the scale and resolution of the remote sensing imagery. This fact is clearly demonstrated by Figures 3.37 and 3.38. At a scale of 1:20,000 the median floe area is approximately 7,000 m^2. With a scale of 1:2,600 the median area becomes 30 m^2, which is of the same order as floe sizes recorded in surface surveys of the Labrador Sea ice pack (FENCO, 1977).

3.4 Ice Freeboard

The freeboard of ice is defined here as the height of the ice surface above sea level at the ice edge. For landfast ice, the freeboard can be accurately calculated from the total ice thickness, by assuming densities of seawater and ice. The main problem in using this approach offshore is that there is a wide range of ice ages and ice roughness, which leads to significant variations in ice freeboard.

Leads tend to be sharply delineated features with level ice of approximately the same thickness on each side of the lead. The distribution of freeboards at lead edges is assumed to follow the distributions of ice ages. These distributions will shift to progressively thicker ice forms as the winter progresses. Actual measured distributions of level ice thickness offshore are almost non-existent. One data set is available for the Canadian Beaufort Sea using a bottom mounted sonar device recording ice drafts moving over a fixed point (Hoare et al, 1980). This data showed that average first year ice thickness offshore was about 40 cm less than the adjacent landfast ice along the Beaufort coast.

The only offshore measurements of ice thickness in Lancaster Sound were taken during the Manhattan tests in May 1970 (reported in Milnes and Smiley, 1978).

Descriptions of the Labrador Sea pack indicate that freeboard will not be related to level ice thickness. Floes are extremely irregular in cross section and commonly have a raised lip at the edge, as a

result of the grinding action within the pack (Appendix D contains sample Labrador Sea floe cross-sections).

Monthly average freeboards, representative of lead edges, are tabulated for the Beaufort Sea based on offshore ice thickness reported by Hoare et al, and for Lancaster Sound based on theoretical maximum level ice growth as a function of residence time within the Sound.

Average level ice thicknesses for the offshore regions of Lancaster Sound, will be substantially less than for landfast nearshore ice. For example, first year ice at Resolute reaches an average thickness of 180 cm between October and June. Ice forming at the stable edge and drifting east into Baffin Bay will typically reside in the Sound for about one month. In the coldest part of the winter (December to February) this exposure would result in a maximum ice thickness of about 80 cm. Ridging and ice rubble will create areas of thicker ice and, at break-up, floes broken away from the fast ice can temporarily clog the Sound with much thicker level ice than normal for the winter period.

For the Labrador Sea, freeboards have been measured off individual ice floe profiles carried out by C-CORE and FENCO (Winsor and LeDrew, 1979; FENCO, 1977). Table 3.4 shows monthly freeboard estimates for the Beaufort Sea and Lancaster Sound, and values of Labrador Sea floe measurements made in December 1976 and February 1977.

Table 3.4 Representative Ice Freeboard

	Beaufort Sea		Lancaster Sound*1	Labrador Sea
	Avg	Max	Max	Measured Values
	cm		cm	
October	2	5	6	
November	3	5	9	
December	4	10	11	- Freeboard
January	8	13	12	Min 0.2 m Avg 0.9 m
February	11	17	11	Max 2.3 m
March	15	20	11	- 40 to 80 cm (19 floes)
April	18	21	9	
May	20	23	5	Freeboard Min 0.6 m
June	20	-	24*2	Avg 1.4 m Max 2.8 m
July	5-15	-	18*2	
August	-	-	-	
	from Hoare et al (1980)			from Winsor and LeDrew, 1979; FENCO, 1977

*1 Based on assumed 10 km/day ice drift for 26 days Prince Leopold to Navy Board Inlet. Ice Growth from Resolute Bay records related to freezing degree day accumulations (monthly) after Milne and Smiley (1978).

*2 Reflects thicker first year floes breaking away from the fast ice edge (from Resolute June/July records - Richardson and Burns (1975)).

Note: Ice freeboard has been calculated as 0.126 x Ice Thickness based on Ice s.g. 0.9, Water s.g. 1.03

3.5 Wind Effects on Ice Dynamics

3.5.1 Modification of Measured Ice Speeds to Reflect Cloud Cover Wind Speed Bias

Ice movement statistics collected in this study depended almost entirely on Landsat imagery obtained in the visible spectrum on nearly cloudless days (maximum 15%). As described in 2.4.1 a correlation was requested from AES to ensure that our fair weather data accurately represented the complete distribution of wind speeds in all cloud covers.

Results shown in Figures 3.39, 3.40 and 3.41 demonstrate that for the onshore stations analyzed, higher wind speeds are associated predominantly with increased cloud cover. Skies with cloud cover in excess of 20% (i.e. no Landsat imagery used) occur about 90% of occasions when winds exceed 60 km h^{-1} at all three stations.

This correlation indicates that random sampling of ice motions from Landsat imagery will be biased toward slower movement rates and will likely miss extreme motions associated with storm events. Table 3.5 compares the frequency of a given wind speed occurring in <20% cloud cover to the equivalent frequency for all cloud covers. Above 30 km h^{-1} there are significant differences in frequency, the fair weather case typically seeing less than half the strong wind events that actually occurred.

The average wind speed for all cloud covers is between 13% and 24% higher than the average wind speed associated with clear sky (<20% cover) conditions. Assuming that a similar correlation holds true for offshore areas, it is concluded that average ice speeds sampled from Landsat imagery in this and other studies are underestimated by about 20%.

Correcting for extreme ice movements associated with severe storm events is not possible given the uncertainties in the tails of the wind speed distributions and lack of direct cloud cover/speed correlations offshore.

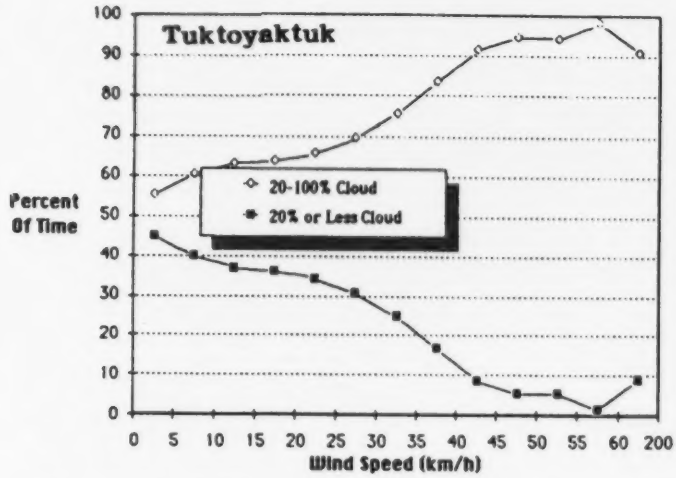

Figure 3.39 Percent of Time Cloud Cover Found for Given Wind Speed

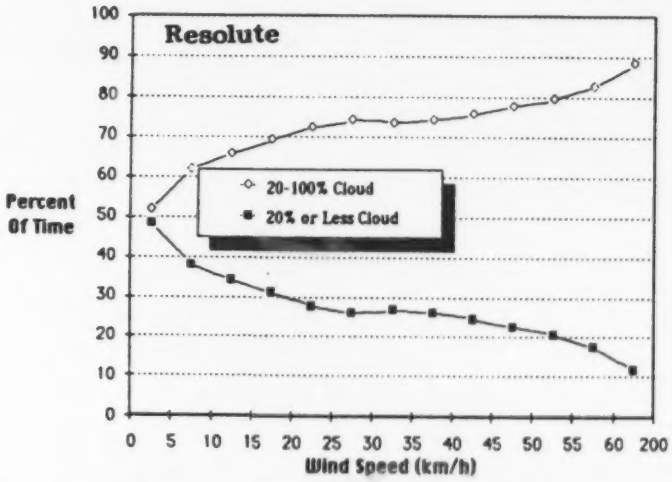

Figure 3.40 Percent of Time Cloud Cover Found for Given Wind Speed

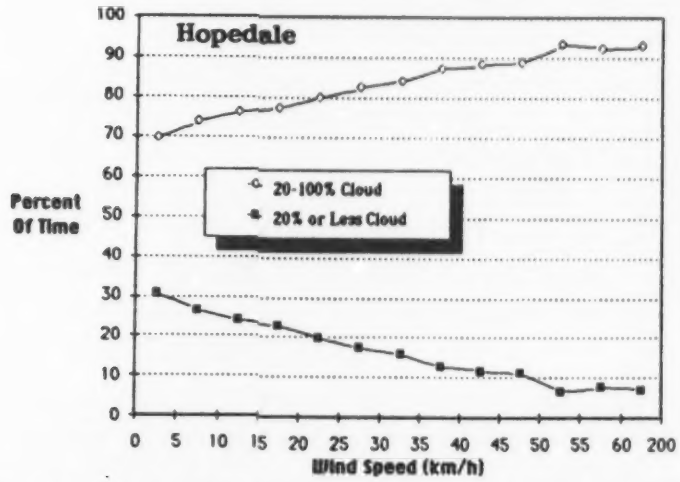

Figure 3.41 Percent of Time Cloud Cover Found for Given Wind Speed

Table 3.5 Comparison of Relative Frequency of Wind Speeds in Cloud Cover <20% to all Cloud Covers

Wind Speed (km/h)	Cloud Cover and Location					
	Resolute A		Hopedale		Tuktoyaktuk	
	0-20%	0-100%	0-20%	0-100%	0-20%	0-100%
0- 5	21.71	14.39	15.23	10.58	11.52	8.94
5- 10	14.64	12.31	16.50	13.24	15.38	13.52
10- 15	14.66	13.71	14.29	12.58	24.08	22.76
15- 20	12.95	13.45	17.95	16.58	21.42	20.68
20- 25	9.29	10.79	10.13	10.76	12.93	13.23
25- 30	7.90	9.71	12.79	15.32	8.88	10.16
30- 35	7.08	8.51	7.44	9.86	3.82	5.39
35- 40	4.23	5.24	2.40	3.99	1.59	3.35
40- 45	3.15	4.14	1.42	2.57	0.21	0.86
45- 50	1.96	2.82	1.01	1.89	0.10	0.64
50- 55	1.14	1.78	0.24	0.74	0.04	0.24
55- 60	0.76	1.40	0.29	0.80	0.01	0.17
60-200	0.51	1.74	0.36	1.09	0.02	0.08
	100	100	100	100	100	100
x =	17.3	21.4	17.1	20.8	15.6	17.7
s =	13.2	15.4	11.0	13.4	8.6	10.0
$(x_{100} - x_{20})/x_{20}$	24%		23%		13%	

3.5.2 Comparison of Average Winds and Ice Velocity

A rigorous correlation of floe velocity and wind velocity is not possible owing to the lack of coordination between ice and wind observations in time and space. Nevertheless, a trend is observed between the average regional speeds of the two elements. No trend was found for directions.

Table 3.6 summarizes the average speeds. It can be seen that the average daily floe speeds amount to about 2 to 3% of the wind speeds. The ice to wind speed ratio in the last column of Table 3.6 has been adjusted by a 20% reduction of the wind

speed to reflect the bias of our Landsat sample towards slower winds (see previous Section 3.5.1).

The adjusted ratio obtained in this study compares well with estimates by others, ranging from 2 to 5% for ice to wind speed ratios. Markham (1976) reported a median ratio of about 2.5% for floe drifts in June-July 1973, in Amundsen Gulf and off Western Banks Island. His floe direction/wind direction correlation was not conclusive, but the data trend indicated between 20 and 30 degrees deflection to the right of the wind vector.

Table 3.6 Wind Speed/Ice Floe Speed Comparison

Region	Average Speed		V_i/V_w	Modified* V_i/V_w V_w reduced 20%
	Ice Floe km/day	Wind km/h		
Beaufort Sea	9.44 (A+B+BN)	25.7 (July only)	0.015	0.019
Lancaster Sound	9.48 (A+B+C)	28.3 (July only)	0.014	0.017
Labrador Coast	17.51 (A/D+A+B)	28.5 (April only)	0.026	0.032

*According to Section 3.5.1

3.6 Refreezing of Pack Ice Leads

The analysis of lead refreezing rates described in Section 2.5 has been applied to climatic data for four weather stations in the three areas. The results are presented in the following tables. Tables 3.7 to 3.9 include the data used to calculate the refreezing parameters. The data are from the "Canadian Climate Normals 1951-1981." Gaps in the tables are caused by data which results in ice melt rather than refreezing. During certain months, no lead refreezing would be expected.

Table 3.7 Beaufort Sea Climate

Tw = Water Temp (°C)

Ta = Air Temp (°C)

Wind Chill Units (m sec^{-1} °C)

Nicholson Peninsula

	Tw-Ta		Wind Chill		
Month	Mild	Mean	Max	Mean	Max
January	23.9	27.5	30.9	137	455
February	25.2	29.2	31.4	144	410
March	21.4	24.9	29.0	123	443
April	12.4	16.2	20.0	81	306
May	0.5	4.1	7.5	29	121
June					
July					
August					
September					
October	4.0	6.3	8.7	39	164
November	14.8	18.1	21.3	100	391
December	20.7	24.1	27.7	109	485

Tuktoyaktuk

	Tw-Ta		Wind Chill		
Month	Mild	Mean	Max	Mean	Max
January	23.4	26.8	30.0	122	292
February	24.1	27.5	30.7	125	290
March	21.1	24.9	28.6	103	294
April	11.2	15.6	19.9	66	177
May	-0.7	3.1	6.8	16	66
June					
July					
August					
September					
October	3.4	6.1	8.6	31	93
November	14.6	18.1	21.6	87	210
December	20.5	23.6	26.9	113	239

Table 3.8 Lancaster Area Climate

Resolute Airport

	Tw-Ta			Wind Chill	
Month	Mild	Mean	Max	Mean	Max
January	26.8	30.5	34.1	182	824
February	28.0	31.6	35.2	174	909
March	26.2	29.8	33.4	152	779
April	17.6	21.5	25.4	118	706
May	6.1	9.3	12.5	49	274
June					
July					
August					
September	1.3	3.5	5.6	21	135
October	10.4	13.5	16.7	79	390
November	19.3	22.9	26.4	120	711
December	24.1	27.7	31.3	151	661

Table 3.9 Labrador Area Climate

Hopedale

	Tw-Ta			Wind Chill	
Month	Mild	Mean	Max	Mean	Max
January	10.5	14.3	18.1	91	427
February	9.4	13.8	18.1	86	422
March	5.1	9.4	13.6	59	366
April		3.3	7.0	19	200
May			0.3		7
June					
July					
August					
September					
October					
November		1.8	4.4	12	104
December	6.3	9.7	13.1	67	444

Tables 3.10 to 3.12 include the calculated grease ice thicknesses, grease ice coverage times, and times to achieve 20 cm of new ice growth under still conditions. Again, gaps in the tables are caused by melting conditions.

Table 3.10 Beaufort Sea Lead Refreezing

Nicholson Peninsula

	With Wind Chill				Still Conditions			
	Grease Ice Thickness			Coverage Time		0.2 m Growth		
Month	Mean	Max	Wind	Mean	Max Wind	Min	Mean	Max Tw-Ta
	m	m		hr	hr	hr	hr	hr
January	0.3	0.9		48	63	58	51	45
February	0.3	0.8		45	60	55	48	44
March	0.3	0.9		51	66	65	56	48
April	0.3	0.9		70	86	112	86	70
May	0.4	1.0		175	154	2780	339	185
June								
July								
August								
September								
October	0.4	1.1		134	155	348	221	160
November	0.3	1.1		67	87	94	77	65
December	0.3	1.1		51	71	67	58	50

Tuktoyaktuk

	With Wind Chill				Still Conditions			
	Grease Ice Thickness			Coverage Time		0.2 m Growth		
Month	Mean	Max	Wind	Mean	Max Wind	Min	Mean	Max Tw-Ta
	m	m		hr	hr	hr	hr	hr
January	0.3	0.6		48	57	59	52	46
February	0.3	0.6		47	55	58	51	45
March	0.2	0.6		49	60	66	56	49
April	0.3	0.5		68	70	124	89	70
May	0.3	0.6		161	117		448	204
June								
July								
August								
September								
October	0.3	0.7		123	115	409	227	162
November	0.3	0.6		64	70	95	77	64
December	0.3	0.5		53	59	68	59	52

Table 3.11 Lancaster Sound Lead Refreezing

Resolute Airport

Month	With Wind Chill: Grease Ice Thickness Mean (m)	Max (m)	Wind	Coverage Time Mean (hr)	Max (hr)	Wind	Still Conditions: 0.2 m Growth Min (hr)	Mean (hr)	Max (hr)	Tw-Ta
January	0.4	1.5		45	64		52	46	41	
February	0.3	1.6		43	63		50	44	40	
March	0.3	1.4		45	64		53	47	42	
April	0.3	1.7		59	83		79	65	55	
May	0.3	1.3		100	133		228	150	111	
June										
July										
August										
September	0.4	1.5		170	219		1070	397	248	
October	0.4	1.4		83	111		134	103	83	
November	0.3	1.6		55	80		72	61	53	
December	0.3	1.3		48	67		58	50	44	

Table 3.12 Labrador Sea Refreezing Rates (Interstices Between Floes)

Hopedale

Month	With Wind Chill: Grease Ice Thickness Mean (m)	Max (m)	Wind	Coverage Time Mean (hr)	Max (hr)	Wind	Still Conditions: 0.2 m Growth Min (hr)	Mean (hr)	Max (hr)	Tw-Ta
January	0.4	1.4		82	105		132	97	77	
February	0.4	1.4		84	105		148	101	77	
March	0.4	1.6		107	134		272	148	102	
April	0.3	1.7		210	211			421	199	
May		1.5			401				4630	
June										
July										
August										
September										
October										
November	0.4	1.4		222	241			772	316	
December	0.4	2.0		197	147		220	143	106	

It is clear from the tables, that predicted coverage times for leads in winter months are relatively constant, and that the differences which would be observed are predicted to be primarily differences in thickness. For the grease ice coverage times, the common result

is that the severe environmental conditions extend the coverage time. This is due to the increase in expected ice thickness. As the climate warms, as seen by comparing spring months to winter months, or by comparing the Lancaster area to the Labrador area, refreezing times become larger.

When the results of calculations using the equations used in this analysis are compared to the results of other workers, they are consistent. The calculated heat fluxes and ice production rates correspond to Bauer and Martin (1983), to Andreas et al (1979), to Schaas and Galt (1972), and to den Hartog et al (1983).

Three problems are associated with the grease ice coverage determinations. First, the thickness of the ice cover is only crudely estimated. No experimental or field data were found to give a better estimate than the equation used. Field data is critical in determining coverage times, as an underestimate will also underestimate coverage times. Second, the coverage time is independent of lead size, because in the integration, all lead dimensions cancel except for ice thickness. This mathematical result is limited to fairly large leads. A comparison of the results of the present analysis to the analysis of Bauer and Martin (1983), shows good correlation down to leads with 50 m fetch. However, leads smaller than this will probably not have the mature wind and wave conditions of the larger lead, and may be expected to behave more like leads subject to still conditions. Third, the transition from grease ice to consolidated ice is not well defined. After piling up at the lee edge of the lead, the grease ice has been shown to form a dense dead zone, where it behaves as a solid. It is likely that in the time taken for the lead to cover, most of this ice will consolidate to solid ice. This assumption is not documented.

The still condition ice growth calculations are standard, and compare well with other research (e.g. Burns, 1975).

4.0 CONCLUSIONS AND RECOMMENDATIONS

Leads are a much more common pack ice characteristic than individual floes in the Beaufort Sea and Lancaster Sound. When ice concentrations are between 4 and 8/10, as in spring break-up, floe motions will control the behaviour of oil spills. In these regions break-up lasts less than six weeks in a typical ice year. However, the Labrador Sea is an environment where individual floe interactions will be the major factor controlling oil spill behaviour and fate, rather than lead dynamics.

Where leads are common, they appear to be enlarging rather than contracting. Based on 24 hour ice displacement records, this trend to a diverging ice cover would indicate that lead pumping may not be an important factor affecting oil spill distribution within a pack ice environment. This preliminary conclusion requires verification using near instantaneous ice movement records.

Satellite remote sensing imagery is not satisfactory to derive actual distributions of lead width. Although relative displacements of large leads can be measured accurately, the numerous small leads less than 100 m wide are not detected.

Based on this study's results the following recommendations are made:

1. That future Beaufort Sea floe analysis concentrate on the spring break-up period where high quality industry SAR imagery is available on a daily basis along the entire coast. The break-up period is critical for oil spill behaviour. Oil still incorporated in landfast ice can be rapidly carried offshore in vast floes, and then dispersed over a wide area as these floes break down.

2. That the continued assessment of lead pumping utilize available aerial photography and near instantaneous ice velocity measurements to better understand the significance of irregular relative ice motions on a scale of meters.

3. That consideration be given to conducting a study of pack ice dynamics in a major offshore area not covered by this study: Baffin Bay/Davis Strait.

4. Than consideration be given to designing a field project to measure small scale lead and floe dynamics.

ACKNOWLEDGEMENTS

The success of this study depended to a large part on gaining access to a variety of remote sensing data sources. The authors wish to express their appreciation for the time and effort expended by a number of individuals who provided assistance with data acquisition, particularly:

- John Miller of Petro Canada
- Chris Hill of Dome Petroleum
- Bob Frederking of NRC
- Fred Geddes of the Atmospheric Environment Service
- Doug Bradford of Fisheries and Oceans
- Lynn Arsenault of Cold Region Remote Sensing

Many painstaking measurements of pack ice characteristics were carried out by Ingrid Bjerkelund, Peter Bein, and Michael Cassidy. Sections on correlation of ice movements and wind statistics was prepared by Peter Bein. Material on refreezing the pack ice leads was developed by Blair Humphrey.

The authors appreciate the cooperation of Gulf Canada Resources in releasing data on floe movements by Don Schwab.

REFERENCES

Agerton, D.J. and J.R. Kreider. Correlation of Storms and Major Ice Movements in the Nearshore Alaskan Beaufort Sea. POAC 1979. 97.

Andreas, E.E., C.A. Paulson, R.M. Williams, R.W. Lindsay and J.A. Businger. 1979. Boundary Layer Meteorology 17:57-91.

Atmospheric Environment Service. 1982. Canadian Climate Normals 1951-1980. Volume 1: Radiation. Volume 2: Temperature. Volume 4: Degree Days. Volume 5: Winds. Environment Canada, Ottawa.

Bauer, J. and S. Martin. 1983. J. Geophys. Res. 88:2917-2925.

Buckley, J.R., T. Gammelsrod, J.A. Johannessen, O.M. Johannessen and L.P. Roed. 1979. Science 203:165-167.

Burns, B.M. 1974. The Climate of the Mackenzie Valley-Beaufort Sea. Volume II. Environment Canada, Ottawa.

Coachman, L.K. and J.L. Newton. February 1972. Water and Ice Motion in the Beaufort Sea, Spring 1970. AIDJEX Bulletin No. 12, pp. 61-77.

Convey, A.D. 1972. Engineering Memorandum 1972 Grand Banks Aerial Reconnaissance. Amoco Canada Petroleum Co., Calgary, Alberta. Project #59-EC-40-72-9.

Croasdale, K.R. and L.G. Spedding. 1972. Landfast Ice Movement - Mackenzie Delta 1972. Imperial Oil Ltd., Production Research and Technology Service Laboratory Report. APOA-33-1, IPRT-5ME-72.

Culshaw, S.T. and B.R. LeDrew. 1977. Labrador Sea Ship in the Ice - A Pilot Study. In the Proceedings of the Port and Ocean Engineering for the Arctic Conference. St. John's, Nfld. Vol. II, pp. 1122-1131.

Danielewicz, B.W. and G.R. Pilkington. 1981. Selected Environmental Characteristics of Beaufort Sea Ice. Dome/Canmar Technical Report. GG-28.

den Hartog, G., S.D. Smith, R.J. Anderson, D.R. Topham and R.G. Perkin. 1983. J. Geophys. Res. 88:2911-2916.

Denner, W.W. and T.E. Keliner. 1981. Numerical Modelling Labrador Pack Ice Dynamics. In Proceedings of the Port and Ocean Engineering in the Arctic Conference, Quebec, Canada, Vol. III, pp. 1330-1347.

Dey, B. April 20, 1981. Monitoring Winter Sea Ice Dynamics in the Canadian Arctic with NOAA-TIR Images. J. Geophysical Research, Vol. 86, No. C4, pp. 3223-3235.

Dunbar, M.J. 1981. Polynyas in the Canadian Arctic. Occasional Papers 45. Canadian Wildlife Service. Environment Canada. pp. 29-44.

FENCO. Decmeber 1976. Davis Strait Ice and Oceanographic Investigation Winter (76/77) for Imperial Oil Ltd. APOA 128-1. GG-8.

Foster, T.D. 1972. J. Phys. Ocean. 2:462-469.

Frederking, R., M. Sayed, E. Wessels, A.J. Child and D. Bradford. 1984. Ice Interaction with Adams Island, Winter 1982-1983. IAHR Ice Symposium.

Hall, R.T. 1977. AIDJEX Modelling Group Studies Involving the Use of Remote Sensing Data. In preprints, Symposium on Sea Ice Processes and Models, Seattle.

Hartwell, A.D. May, 1972. Airphoto Analysis of Ice Deformation in the Beaufort Sea. AIDJEX Bulletin No. 13, pp. 1-34.

Hibler, W.D., W.F. Weeks, S. Ackley, A. Kovacs and W.J. Campbell. May, 1972. Mesoscale Strain Measurements on the Beaufort Sea Pack Ice (AIDJEX 1971). AIDJEX Bulletin No. 13, pp. 35-76.

Hibler, W.D., III, W.B. Tucker and W.F. Weeks. March 1976. Techniques for Using Landsat Imagery without Land References to Study Sea Ice Drift and Deformation. AIDJEX Bulletin No. 31, pp. 115-136.

Kozo, T.L. 1983. J. Geophys. Res. 88:2926-2934.

Kupetski, V.N. 1962. Gos i Oceanogr. Inst. Moskva 70:47-60. Quoted in Dunbar, 1981.

Lachapelle, A. 1981. Wind and Waves - Lancaster Sound. In Proceedings of the Port and Ocean Engineering in the Arctic Conference. Quebec, Canada, Vol. II, pp. 830-842.

LeDrew, B.R. and K.A. Gustajtis. November 1979. Oil Spill Scenario for the Labrador Sea. C-CORE EPS 3-EC-79-4.

Lindsay, D.G. 1977. Polar Continental Shelf Project. Patterns of Break-Up, Freeze-Up and Surface Roughness of Sea Ice in Selected Channels in the Canadian Arctic. Energy, Mines and Resources Canada. 256.

Lindsay, D.G. 1975. Sea Ice Atlas of Arctic Canada 1961-1968. Dept. Energy Mines and Resources, Ottawa, Canada.

Lindsay, D.G. 1977. Sea Ice Atlas Canada 1969-1974. Dept. Energy Mines and Resources, Ottawa, Canada.

Lindsay, D.G. 1981. Sea Ice Atlas of Arctic Canada 1975-1978. Dept. Energy Mines and Resources, Ottawa, Canada.

Lo, A.K. 1980. Internal Rep. ARQB-80-012L. Atmospheric Environment Service, Environment Canada. Downsview. Quoted in Andreas et al, 1979.

Marcellus, R.W. and T.B. Morrison. 1982. Ice Design Statistics for the Canadian Beaufort Sea. Canada Marine Engineering Limited, Calgary.

Markham, W.E. 1980. Ice Atlas, Eastern Canadian Seaboard. Environment Canada. AES, Toronto. 422.

Markham, W.E. October 1978. Ice Climatology of the Beaufort Sea. Technical Report No. 26. Reprinted. BSP 26.

Marko, J.R. July 1977. A Satellite-Based Study of Sea Ice Dynamics in the Central Canadian Arctic Archipelago. Institute of Ocean Sciences, 205-C-77-4.

Marko, J.R. and R.E. Thomson. February 20, 1977. Rectilinear Leads and Internal Motions in the Ice Pack of the Western Arctic Ocean. J. Geophysical Research, Vol. 82, No. 6. 468.

Marko, J.R. September 1976. Satellite Observations of the Beaufort Sea Ice Cover. Technical Report No. 34. Reprinted. BSP 34.

Marko, J.R. 1982. The Ice Environment of Eastern Lancaster Sound and Northern Baffin Bay. Environmental Studies No. 26. Indian and Northern Affairs Canada, Ottawa. GG-15.

Marko, J.R. and S. Bannerman. July 1982. Comparison of Observed and Simulated Ice Floe Drift and Relevence to Oil Spill Modeling Accuracy. Arctic Sciences for Institute of Ocean Sciences, Sidney, B.C.

Martin, S. and P. Kauffman. 1981. J. of Glaciology 27:283-313.

McGonigal, D. and B.D. Wright. 1978. Beaufort Sea Ice Movement. RAMS Buoy Data Analysis, 1975-1977. Volume I, Gulf Canada Ltd., Frontier Research Division. GG-2.

Milne, A.R. and B.D. Smiley. February 1978. Offshore Drilling in Lancaster Sound. Possible Environmental Hazards. Institute of Ocean Sciences. JJ-1.

Murphy, D.L., I.M. Lissauer and J.C. Myers. 1983. Movement of Satellite Tracked Buoys in the Beaufort Sea. USCG Avery Point, Groton, Conn. 334.

Murphy, D.L., P.A. Tebeau and I.M. Lissauer. 1981. Long-Term Movement of Satellite-Tracked Buoys in the Beaufort Sea - An Interim Report. USCG Avery Point, Groton, Conn. 335.

NORCOR. August 1977. Probable Behaviour and Fate of a Winter Oil Spill in the Beaufort Sea. Environmental Impact Control Directorate. EPS-4-EC-77-5.

Pritchard, R.S., M.D. Coon, M.G. McPhee and E. Leavitt. September 1977. Winter Ice Dynamics in the Nearshore Beaufort Sea. AIDJEX Bulletin No. 37, pp. 37-94.

Richardson, F.A. and B.M. Burns. 1975. Ice Thickness Climatology for Canadian Stations. Atmospheric Environment Service, Toronto.

Robe, R.Q., I.M. Lissauer and J.C. Myers. 1983. Beaufort Sea Drifting Buoys, USCG, Groton, Conn.

Rothrock, D.A. 1979. Modeling Sea-Ice Features and Processes. J. Glaciology, Vol. 24, No. 90. 466.

Schaas, R.H. and J.A. Galt. 1973. Arctic 26:208-221.

Seasat SAR Data Over Canada. Coverage and Sources. May 1982. The Radarsat Project Office, Ottawa.

Smith, S.D., R.J. Anderson, G. den Hertog, D.R. Topham and R.G. Perkin. 1983. J. Geophys. Res. 88:2900-2910.

Sowden. 1980. Selected Physical Characteristics - Background Report 1 - Lancaster Sound Regional Study. Indian and Northern Affairs Canada. Ottawa.

Spedding, L.G., P. McLellan and C. Soares. 1978. Summer Ice Floe Size and Distribution in the Southern Beaufort Sea. IPRT-IME-78.

Spedding, L.G. 1973. Landfast Ice Movement - Mackenzie Delta 1972-73. Imperial Oil Ltd., Production Research and Technology Services Report APOA-51-1, IPRT-23ME-73.

Spedding, L.G. 1975. Landfast Ice Movement - Mackenzie Delta 1973-74. Imperial Oil Ltd. APOA-67-1, IPRT-2ME-75.

Spedding, L.G. 1975. Landfast Ice Movement, Mackenzie Delta 1974-75. Imperial Oil Ltd. APOA-83-1, IPRT-26ME-75, Calgary.

Spedding, L.G. 1977. Landfast Ice Movement, Mackenzie Delta 1975-76. Imperial Oil Ltd. APOA-105-4, IPRT-1ME-77, Calgary.

Spedding, L.G. 1975. Landfast Ice Movement - Mackenzie Delta 1972-73. Imperial Oil Ltd. APOA-51-1, IPRT-23ME-75, Calgary.

Spedding, L.G. et al. 1978. Summer Ice Floe Size and Distribution in the Southern Beaufort Sea. Report IPRT-1ME-78.

Spedding, L.G. 1983. A Large Landfast Ice Movement. Paper presented at POAC 83, Helsinki.

Topham, D.R., R.G. Perkin, S.D. Smith and R.J. Anderson. 1983. J. Geophys. Res. 88:2888-2899.

Wadhams, P. Field Experiments on Wave-Ice Interaction in the Labrador and East Greenland Currents, Polar Record, Vol. 19, No. 121.

Wadhams, P. 1975. Sea Ice Morphology in the Beaufort Sea. Beaufort Sea Project Technical Report No. 36, Institute of Ocean Sciences, Sidney, B.C.

Wadhams, P. 1984. Arctic Sea Ice Morphology and its Measurement. Arctic Technology and Policy Proceedings of the Second Annual MIT Sea Grant College Program and Lecture Seminar. Eds: I. Dyer and C. Chryssostomidis.

Wadhams, P. and R.J. Horne. 1980. An Analysis of Ice Profiles Obtained by Submarine Sonar in the Beaufort Sea. J. Glaciology Vol. 25, pp. 401-424. GG-14.

Welch, J.P., I.M. Lissauer, G.L. Hufford, T.S. Ellis, B.D. Thompson, L.D. Farmer and R.R. Hiltabrand. 1977. Some Dynamics of Spilled Oil in a Fractured Ice Field in Buzzards Bay, Massachusetts. J. Ocean Engineering, Vol. 4, pp. 197-203.

Winsor, D.W. and B.R. LeDrew. November 1979. Ice Features Characterization - Labrador Offshore. Oil Spill Scenario for the Labrador Sea. Environmental Protection Service EPS 3-EC-79-4.

APPENDIX A

LISTING OF REMOTE SENSING DATA

SLAR IMAGERY USED IN STUDY

Lancaster Sound				Beaufort Sea			
Day	Month	Year	I.D. Number	Day	Month	Year	I.D. Number
21	July	78	NDZ 079	14	May	79	252
22	July	78	080	15	May	79	253
24	Aug	78	107	16	June	81	Dome/Canmar
27	Aug	78	110	17	June	81	Dome/Canmar
28	Aug	78	111	30	June	81	Dome/Canmar
02	Sept	78	115	01	July	81	Dome/Canmar
02	Sept	78	116	14	June	83	Dome/Canmar
26	Aug	79	290	15	June	83	Dome/Canmar
28	Aug	79	291	10	May	84	Dome/Canmar
29	Aug	79	292	11	May	84	Dome/Canmar
31	Aug	79	296				
02	Sept	79	297				
02	July	80	456				
03	July	80	457				
21	July	81	677				
22	July	81	678				
02	July	82	867				
04	July	82	869				
12	July	82	875				
13	July	82	876				
27	July	82	885				
28	July	82	886				
17	July	83	1087				
19	July	83	1089				
23	July	83	1092				
24	July	83	1093				
06	Aug	83	1102				
08	Aug	83	1104				
17	Aug	83	1111				
19	Aug	83	1112				
20	Aug	83	1113				
21	Aug	83	1114				
22	Aug	83	1115				

Landsat Imagery Used In Study

BEAUFORT SEA				
YEAR	DATE	MONTH	TR	FR
1973	16	JUNE	66	10
	18	JUNE	68	10
1974	11	MARCH	64	10
	12	MARCH	65	10
	13	MARCH	66	10
	16	MARCH	69	10
	18	MARCH	71	10
	6	APRIL	72	10
	7	APRIL	73	10
	5	MAY	65	10
	6	MAY	66	10
	16	JULY	65	10
	17	JULY	66	10
	18	JULY	67	9
	18	JULY	67	10
	19	JULY	68	9
**	19	JULY	68	10
1975	10	MARCH	68	9
	10	MARCH	68	10
	11	MARCH	69	9
	11	MARCH	69	10
	14	MARCH	72	10
	16	MARCH	74	10
	25	MARCH	65	10
	27	MARCH	67	10
	28	MARCH	68	10
	30	MARCH	70	10
	22	JUNE	64	10
	24	JUNE	66	10
	26	JUNE	68	10
1976	16	JULY	67	10
**	17	JULY	68	10
**	18	JULY	69	10
	19	JULY	70	10
**	20	JULY	71	10
**	20	JULY	71	11
	21	JULY	72	10
	21	JULY	72	11
1977	5	JUNE	67	10
	6	JUNE	68	10
	8	JUNE	64	10
	9	JUNE	65	10
1978	3	JULY	64	10
	4	JULY	65	10
	5	JULY	66	10
	6	JULY	67	10
	7	JULY	68	10
	8	JULY	69	10
	10	JULY	71	10
1979	7	MARCH	68	10
	8	MARCH	69	10
**	8	MARCH	69	11
**	9	MARCH	70	10
**	9	MARCH	70	11

D F DICKINS ASSOCIATES LTD.

Landsat Imagery Used In Study

BEAUFORT SEA				
YEAR	DATE	MONTH	TR	FR
** 1979	12	MARCH	64	10
	13	MARCH	65	10
	4	APRIL	69	10
	6	APRIL	71	10
	7	APRIL	72	10
	1	JULY	67	10
	3	JULY	69	10
1980	24	JUNE	66	10
**	26	JUNE	68	10
	28	JUNE	70	10
	29	JUNE	71	10
	30	JUNE	72	10
1981	19	MARCH	64	10
	20	MARCH	65	10
	21	MARCH	66	10
	22	MARCH	67	10
	24	MARCH	69	10
	26	MARCH	73	10
	29	MARCH	74	10
**	13	MAY	65	10
**	14	MAY	66	10
	7	JUNE	72	10
	7	JUNE	72	11
	9	JUNE	74	10
	9	JUNE	74	11
	20	JUNE	67	10
	21	JUNE	68	10
	23	JUNE	70	9
	23	JUNE	70	10
	23	JUNE	70	11
	24	JUNE	71	9
	24	JUNE	71	10
	24	JUNE	71	11
	25	JUNE	72	10
	25	JUNE	72	11
1982	1	MAY	67	10
	2	MAY	68	10
	7	JUNE	68	10
	9	JUNE	70	10
	23	JUNE	66	10
	25	JUNE	68	10
	26	JUNE	69	10
	27	JUNE	70	10
	27	JUNE	70	11
	28	JUNE	71	10
	28	JUNE	71	11
	29	JUNE	72	10
	30	JUNE	73	10
	30	JUNE	73	11
	10	JULY	65	10
	11	JULY	66	10
	12	JULY	67	10
	13	JULY	68	10
	14	JULY	69	10
1983	1	JUNE	68	10

D F DICKINS ASSOCIATES LTD.

Landsat Imagery Used In Study

BEAUFORT SEA				
YEAR	DATE	MONTH	TR	FR
1983	1	JUNE	68	11
	3	JUNE	66	11
	3	JUNE	66	10
1984	15	MARCH	68	10
	15	MARCH	68	11
	17	MARCH	66	10
	17	MARCH	66	11

Landsat Imagery Used In Study

LANCASTER SOUND				
YEAR	DATE	MONTH	TR	FR
* 1973	26	MAY	45	7
	27	MAY	46	7
1975	23	JUNE	47	7
	24	JUNE	48	7
1976	1	APRIL	42	7
	2	APRIL	43	7
	3	APRIL	44	7
	4	APRIL	45	7
1977	23	APRIL	42	7
	24	APRIL	43	7
	25	APRIL	44	7
**	26	APRIL	45	7
	24	JUNE	44	7
	25	JUNE	45	7
1981	30	MARCH	39	7
	31	MARCH	40	7
	4	APRIL	44	7
	5	APRIL	45	7
	6	APRIL	46	7
	19	APRIL	41	7
	20	APRIL	42	7
	8	MAY	42	7
	9	MAY	43	7
	24	MAY	40	7
	25	MAY	41	7
	10	JUNE	39	7
	11	JUNE	40	7
	12	JUNE	41	7
	13	JUNE	42	7
	14	JUNE	43	7
	15	JUNE	44	7
	16	JUNE	45	7
	18	JUNE	47	7
	2	JULY	43	7
	3	JULY	44	7
	4	JULY	45	7
	5	JULY	46	7
	6	JULY	47	7
1982	13	JUNE	38	7
	14	JUNE	39	7
1983	19	JULY	36	8
	17	JULY	38	7
	17	JULY	38	8
	15	JULY	40	8
	13	JULY	42	7
	13	JULY	42	8

Landsat Imagery Used In Study

LABRADOR COAST				
YEAR	DATE	MONTH	TR	FR
1974	1	APRIL	13	16
	1	APRIL	13	17
	1	APRIL	13	18
	2	APRIL	14	16
	2	APRIL	14	17
	2	APRIL	14	18
1975	19	FEB	13	17
	19	FEB	13	18
	20	FEB	14	17
	20	FEB	14	18
	9	MARCH	13	18
	10	MARCH	14	17
	10	MARCH	14	18
	23	APRIL	13	17
	23	APRIL	13	18
	23	APRIL	13	19
	24	APRIL	14	17
	24	APRIL	14	18
	24	APRIL	14	19
	25	APRIL	15	17
	25	APRIL	15	18
	25	APRIL	15	19
1976	10	MARCH	11	19
	10	MARCH	11	20
	11	MARCH	12	19
	12	MARCH	13	17
	12	MARCH	13	18
	12	MARCH	13	19
	13	MARCH	14	17
	13	MARCH	14	18
	26	APRIL	13	16
	26	APRIL	13	17
	26	APRIL	13	18
	27	APRIL	14	16
	27	APRIL	14	17
	27	APRIL	14	18
1978	19	MAY	10	20
	19	MAY	10	21
	20	MAY	11	20
	20	MAY	11	21
	8	JUNE	12	18
	8	JUNE	12	19
	9	JUNE	13	18
	9	JUNE	13	19

Landsat Imagery Used In Study

LABRADOR	COAST			
YEAR	DATE	MONTH	TR	FR
1979	21	FEB	9	20
	21	FEB	9	21
	22	FEB	10	20
	22	FEB	10	21
	1	APRIL	12	18
	1	APRIL	12	19
	2	APRIL	13	18
	2	APRIL	13	19
1982	29	APRIL	11	19
	29	APRIL	11	20
	30	APRIL	12	19
1984	7	APRIL	13	15
	7	APRIL	13	16
	7	APRIL	13	17
	7	APRIL	13	18
	8	APRIL	12	15
	8	APRIL	12	16
	8	APRIL	12	17
	8	APRIL	12	18

APPENDIX B

WIND STATISTICS

APPENDIX C

MONTHLY FLOE SPEED DISTRIBUTIONS

Beaufort Sea - July
Ice Floe Speed
(96 Data Samples)

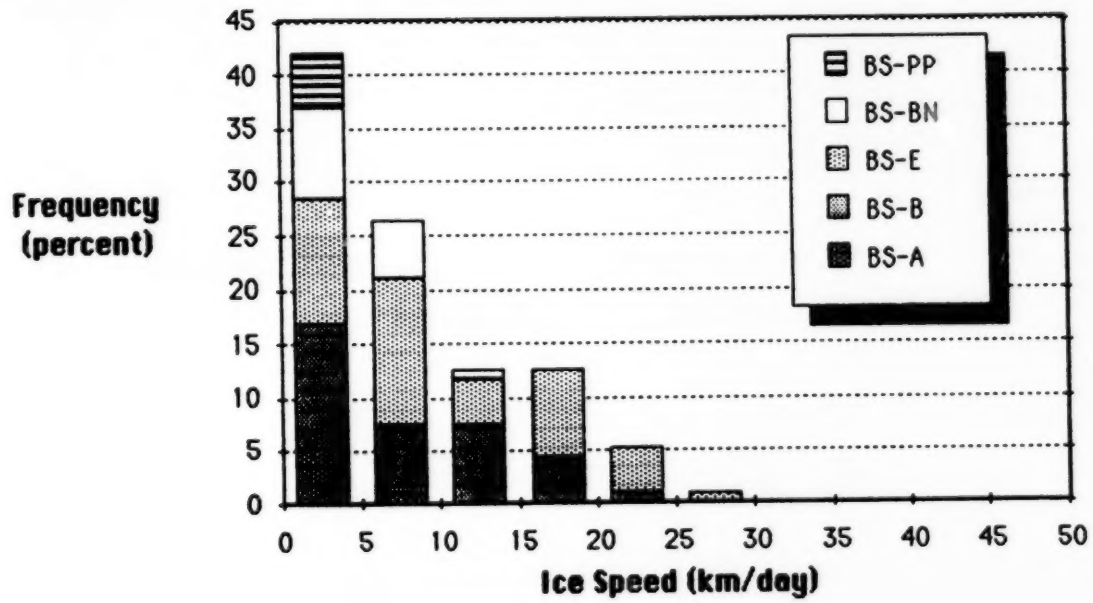

Lancaster Sound - May
Ice Speeds
(33 Data Samples)

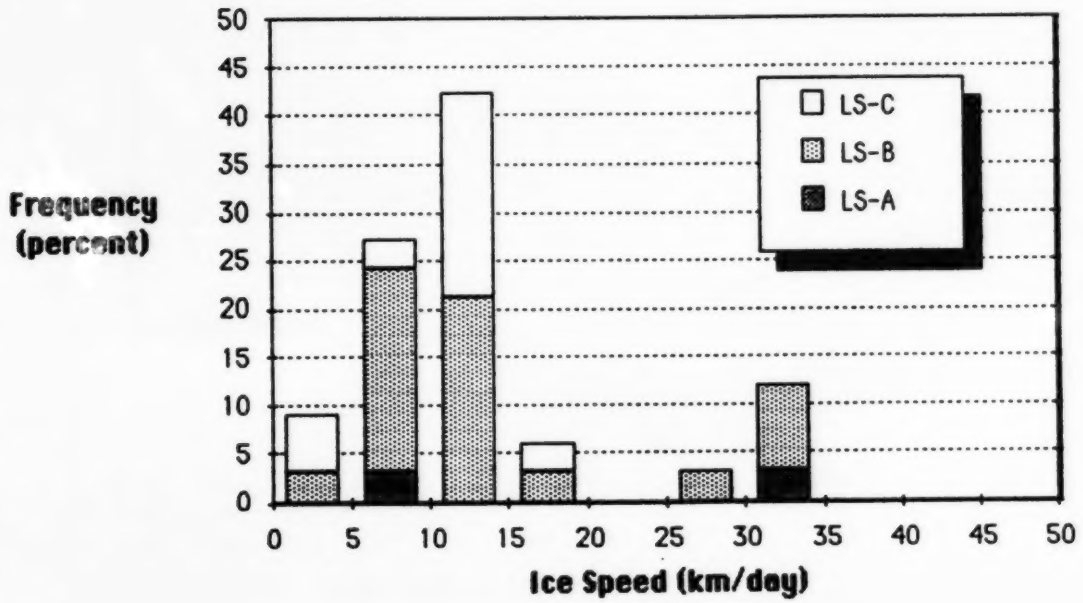

Lancaster Sound - June
Ice Speeds
(70 Data Samples)

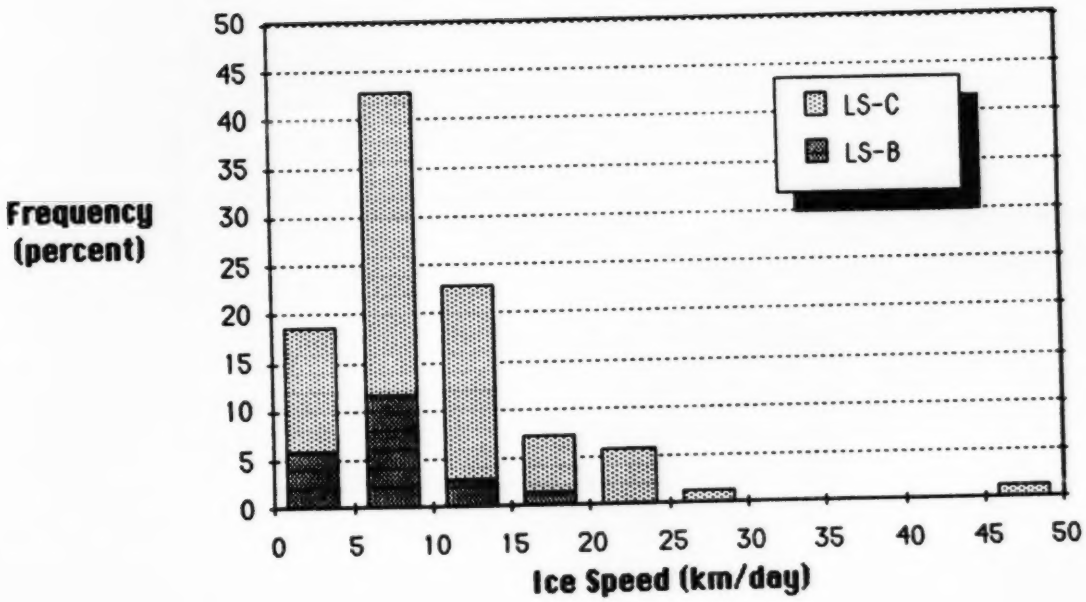

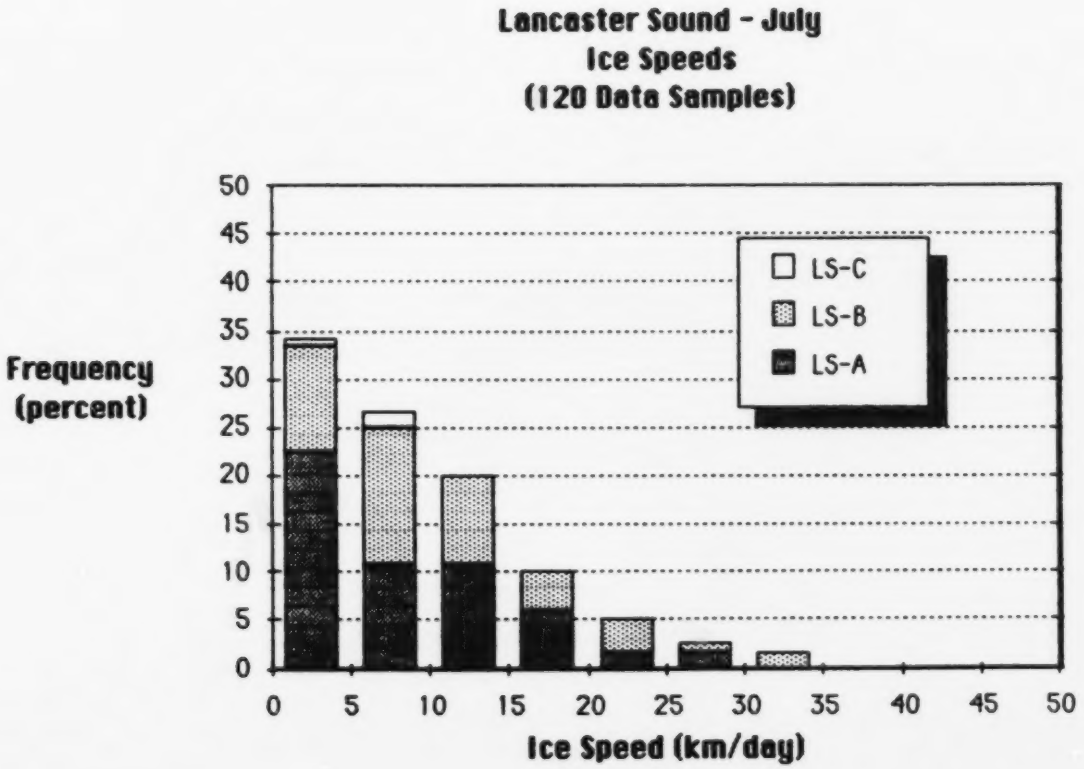
Lancaster Sound - July
Ice Speeds
(120 Data Samples)
Frequency
(percent)
50
45
40
35
30
25
20
15
10
5
0
0
5
10
15
20
25
30
35
40
45
50
Ice Speed (km/day)
LS-C
LS-B
LS-A

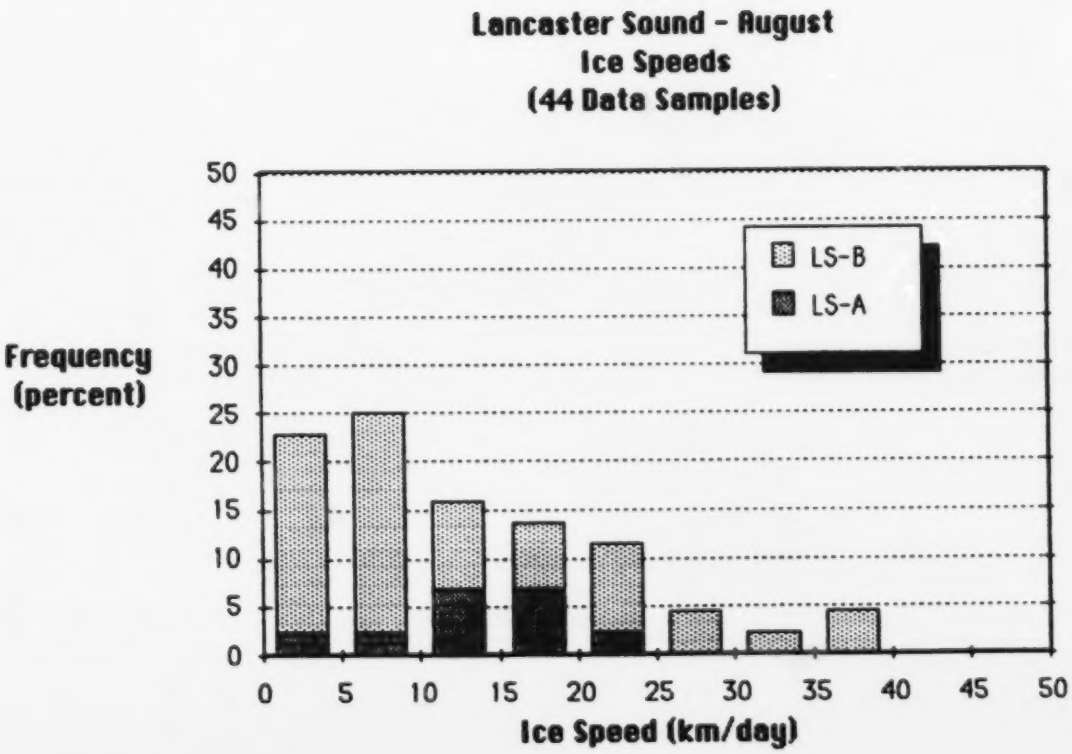
Lancaster Sound - August
Ice Speeds
(44 Data Samples)
Frequency
(percent)
50
45
40
35
30
25
20
15
10
5
0
LS-B
LS-A
0
5
10
15
20
25
30
35
40
45
50
Ice Speed (km/day)

Labrador Sea - March
Ice Speeds
(17 Data Samples)

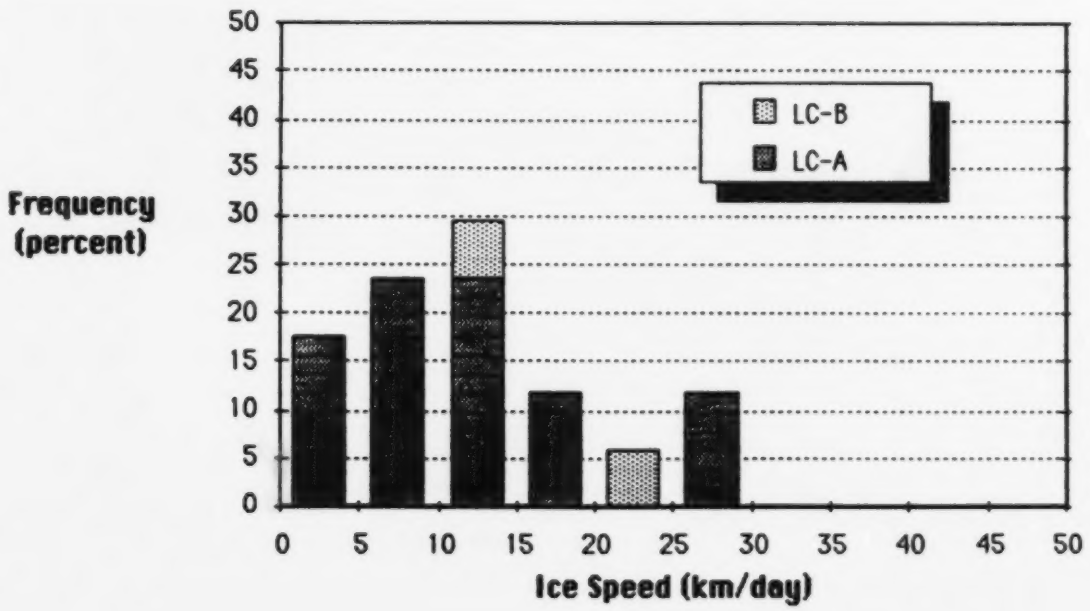

Labrador Sea - April
Ice Speed
(105 Data Samples)

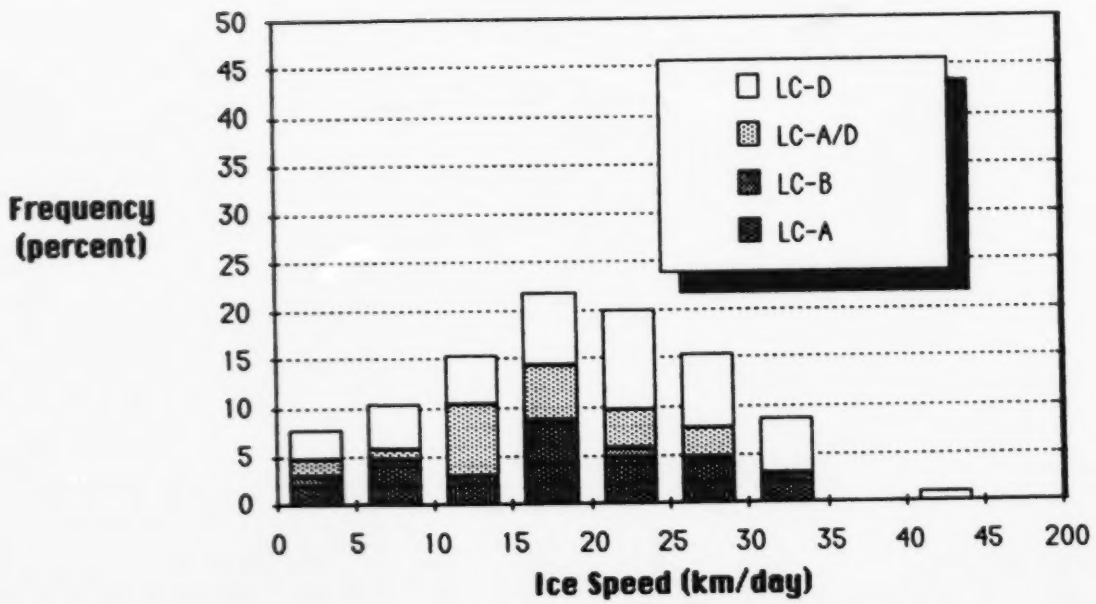

APPENDIX D

REPRESENTATIVE PROFILES OF LABRADOR SEA ICE CAKES

from LeDrew and Gustajtis, 1979

LINE 1-O
Saglek Area

date: 77 02 12
pos: lat; 58° 24' N
long; 61° 43' W

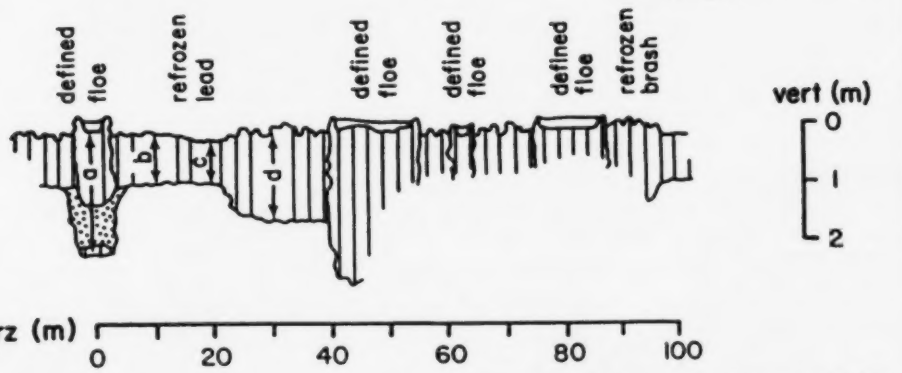

The letters represent thickness and core samples

a = 2·1m
b = 0·8m
c = 0·7m
d = 1·5m

Core series, 1-1 to 1-6

(a)

LINE 2-O
Saglek Area

date: 77 02 14
pos: lat; 58° 17' N
long; 61° 45' W

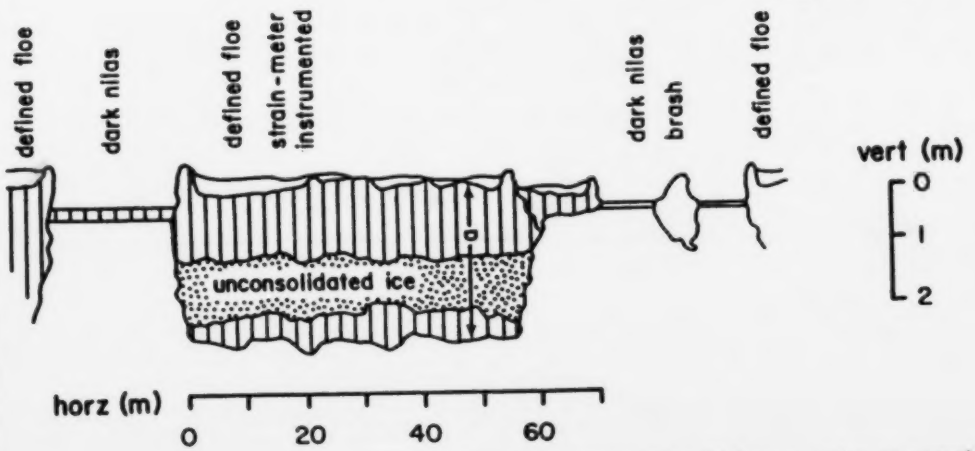

The letter represents thickness and core sample

a = 2·55m - 1·2m solid ice

Core series, A-1

(b)

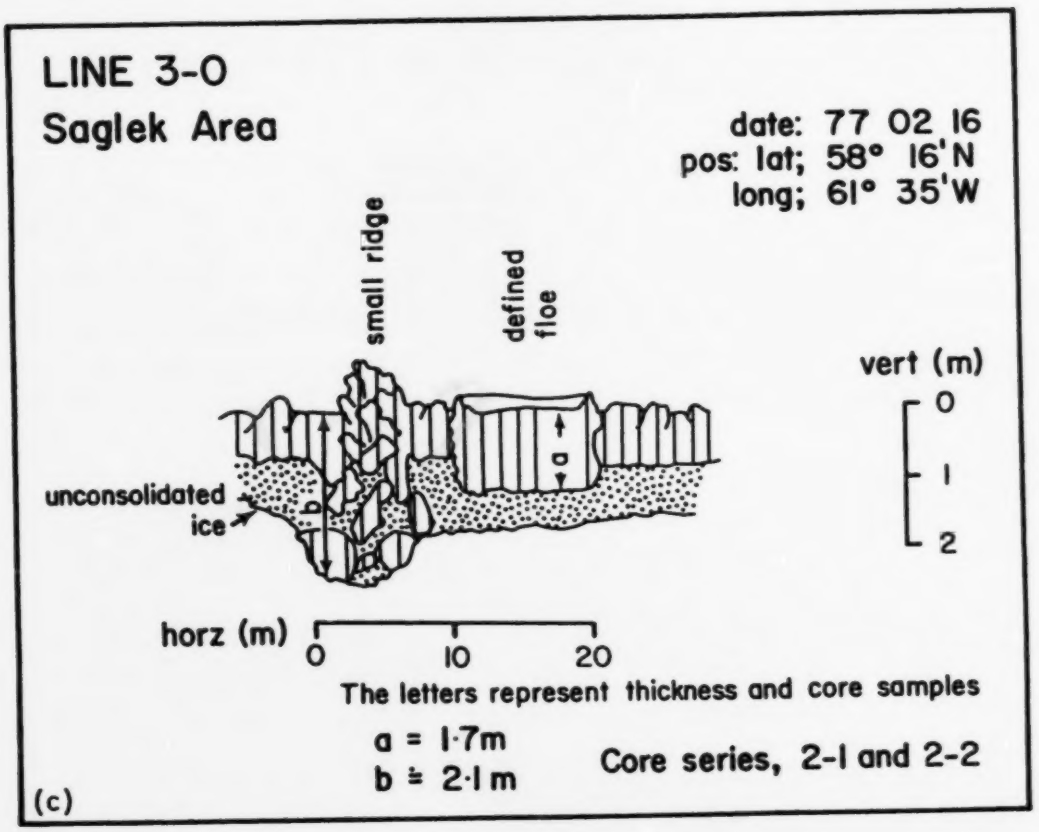
LINE 3-0
Saglek Area
date: 77 02 16
pos: lat; 58° 16'N
long; 61° 35'W
small ridge
defined floe
vert (m)
0
1
2
a
b
unconsolidated ice
horz (m)
0
10
20
The letters represent thickness and core samples
a = 1·7m
b ≅ 2·1 m
Core series, 2-1 and 2-2
(c)

LINE 4-0
Hopedale Area

date: 77 02 19
pos: lat; 56° 03'N
long; 57° 50'W

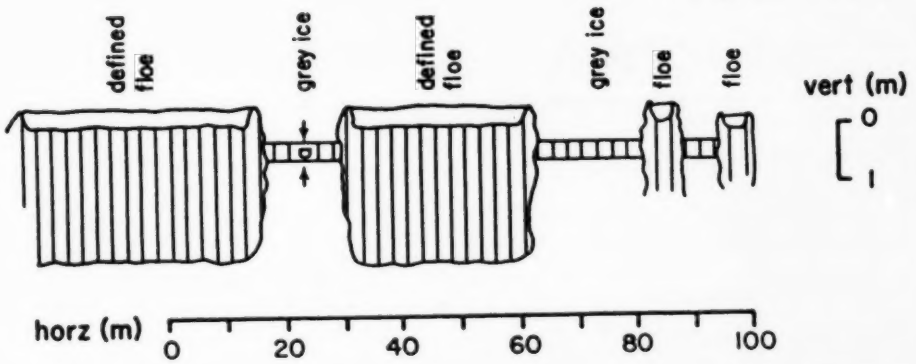

The letter represents thickness sample
a = 0·30 m
No core taken

(d)

LINE 5-0
Hopedale Area

date: 77 02 21
pos: lat; 55° 43'N
long; 57° 54'W

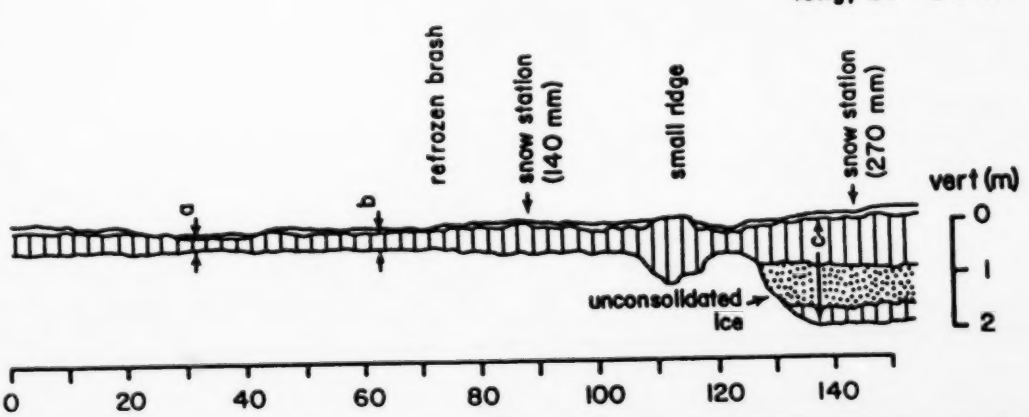

The letters represent thickness and core samples
a = 0·17 m
b = 0·27 m
c = 1·82 m
Core series, 4-1 to 4-3

(e)

LINE 6·0
Hopedale Area

date: 77 02 20
pos: lat; 55° 44' N
long; 57° 54' W

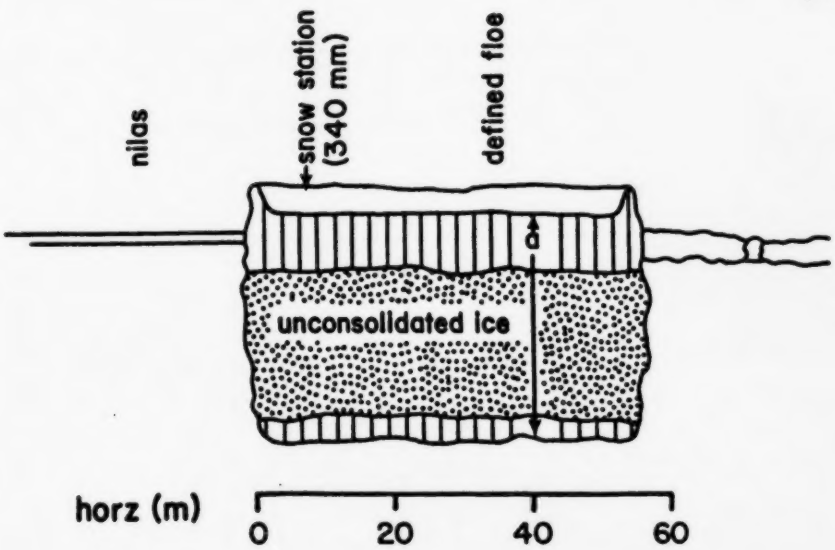

The letter represents thickness and core sample
a = 3·2m - 0·8 m solid ice
Core series, A-2

(f)

LINE 7·0
Hopedale Area

date: 77 02 23
pos: lat; 55° 29'N
long; 55° 50'W

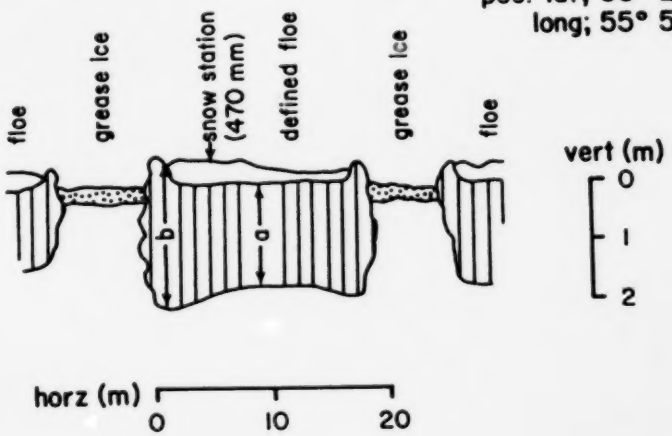

The letters represent thickness and core samples

a = 1·75m Core series, 5-0
b = 2·40

(g)

LINE 8·0
Hopedale Area

date: 77 02 24
pos: lat; 55° 05' N
long; 54° 39'W

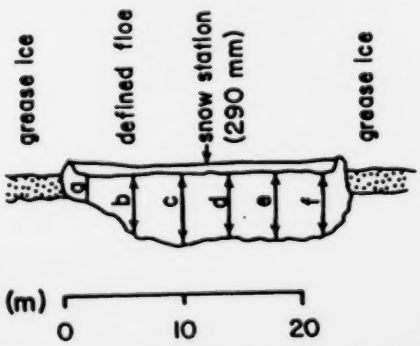

The letters represent thickness and core samples

a = 0·42 m d = 1·10 m
b = 1·03 m e = 1·15 m Core series, 6-1 to 6-6
c = 1·20 m f = 1·10 m

(h)